To be submitted to *The Astrophysical Journal*

A Sample of Very Young Field L Dwarfs and Implications for the Brown Dwarf "Lithium Test" at Early Ages[1]

J. Davy Kirkpatrick[2], Kelle L. Cruz[3], Travis S. Barman[4], Adam J. Burgasser[5], Dagny L. Looper[6], C. G. Tinney[7], Christopher R. Gelino[8], Patrick J. Lowrance[8], James Liebert[9], John M. Carpenter[3], Lynne A. Hillenbrand[3], John R. Stauffer[10]

ABSTRACT

Using a large sample of optical spectra of late-type dwarfs, we identify a subset of late-M through L field dwarfs that, because of the presence of low-gravity features in their spectra, are believed to be unusually young. From a combined sample of 303 field L dwarfs, we find observationally that 7.6±1.6% are younger than 100 Myr. This percentage is in agreement with theoretical predictions once observing biases are taken into account. We find that these young L dwarfs tend to fall in the southern hemisphere (Dec<0°) and may be previously unrecognized, low-mass members of nearby, young associations like Tucana-Horologium, TW

[1]Most of the spectroscopic data presented herein were obtained at the W.M. Keck Observatory, which is operated as a scientific partnership among the California Institute of Technology, the University of California and the National Aeronautics and Space Administration. The Observatory was made possible by the generous financial support of the W.M. Keck Foundation. Other spectroscopic data were collected at the Subaru Telescope, the twin telescopes of the Gemini Observatory, the Magellan-Clay Telescope, the Kitt Peak National Observatory Mayall Telescope, and the Cerro Tololo Interamerican Observatory Blanco Telescope.

[2]Infrared Processing and Analysis Center, MS 100-22, California Institute of Technology, Pasadena, CA 91125; davy@ipac.caltech.edu

[3]Department of Astronomy, MS 105-24, California Institute of Technology, Pasadena, CA 91125

[4]Lowell Observatory, Planetary Research Centre, 1400 West Mars Hill Road, Flagstaff, AZ 86001

[5]Massachusetts Institute of Technology, 77 Massachusetts Avenue, Building 37, Cambridge, MA 02139

[6]Institute for Astronomy, University of Hawai'i, 2680 Woodlawn Drive, Honolulu, HI 96822

[7]Department of Astrophysics, School of Physics, University of New South Wales, NSW 2052, Australia

[8]Spitzer Science Center, MS 220-6, California Institute of Technology, Pasadena, CA 91125

[9]Steward Observatory, 933 North Cherry Avenue, University of Arizona, Tucson, AZ 85721

[10]Spitzer Science Center, MS 314-6, California Institute of Technology, Pasadena, CA 91125

Hydrae, β Pictoris, and AB Doradus. We use a homogeneously observed sample of roughly one hundred and fifty 6300-10000 Å spectra of L and T dwarfs taken with the Low-Resolution Imaging Spectrometer at the W. M. Keck Observatory to examine the strength of the 6708-Å Li I line as a function of spectral type and further corroborate the trends noted by Kirkpatrick et al. (2000). We use our low-gravity spectra to investigate the strength of the Li I line as a function of age. The data weakly suggest that for early- to mid-L dwarfs the line strength reaches a maximum for a few×100 Myr, whereas for much older (few Gyr) and much younger (<100 Myr) L dwarfs the line is weaker or undetectable. We show that a weakening of lithium at lower gravities is predicted by model atmosphere calculations, an effect partially corroborated by existing observational data. Larger samples containing L dwarfs of well determined ages are needed to further test this empirically. If verified, this result would reinforce the caveat first cited in Kirkpatrick et al. (2006) that the lithium test should be used with caution when attempting to confirm the substellar nature of the youngest brown dwarfs.

Subject headings: binaries: general — stars: fundamental parameters — stars: late-type — stars: low-mass, brown dwarfs

1. Introduction

Determining the difference between an object stably burning hydrogen (a main sequence star) and an object of lower mass incapable of such stable fusion (a brown dwarf) is not always straightforward. Although objects with main sequence spectral types of O, B, A, F, G, or K are always stars and objects with a spectral type of T are always brown dwarfs, dwarfs of type M or L comprise a mixture of stellar and substellar objects.

By definition, distinguishing a brown dwarf from a star requires knowledge that the object is not burning hydrogen in its core. There is no direct way to probe the interiors of these objects, so other techniques are required. The most common indirect method used is the "lithium test" (Rebolo et al. 1992). This test recognizes the fact that the temperature ($T > 3{\times}10^6$K; Burrows et al. 1997; Nelson et al. 1993) needed to sustain core hydrogen fusion in the lowest mass stars is only slightly higher than that needed to burn lithium ($T \approx 2{\times}10^6$K; Pozio 1991). If lithium does not burn, that means hydrogen is also not being fused. Fortuitously lithium, once destroyed, is not easily manufactured again in stellar interiors, so stars and brown dwarfs will never have more than their natal abundance of this element. In principle, the presence or absence of lithium in the spectrum can thus provide

knowledge of inner temperatures.

In practice there are several drawbacks when applying the lithium test to M and L dwarfs:

(1) The ground-state resonance line of Li I is located at 6708 Å, a portion of the spectrum where the flux is quite low for late-M and L dwarfs. The low flux levels means that large telescopes are needed for observation of the line. Even then, very few late-type dwarfs are bright enough that they can be acquired at high resolution so to obtain a sizable sample of spectra, moderate resolution ($\Delta\lambda \approx 5 - 10$ Å) is required. Fortunately, this is sufficient for measuring Li I equivalent widths of a few Å or greater provided that the signal-to-noise ratio is high.

(2) As stated above, there is a $\sim 1 \times 10^6 K$ difference between the temperatures for lithium ignition and normal hydrogen ignition. In other words, some brown dwarfs are capable of burning lithium and for those the lithium test will fail. These higher mass brown dwarfs are unrecognizable as substellar based on this test alone.

(3) A sufficient amount of time needs to elapse for the natal supply of lithium to be extinguished. The Li I line may therefore still be present not because the object is substellar, but because it is a star too young to have fused its lithium store. In a very young, low-mass M star, lithium may still be present in the spectrum either because the core has not yet reached lithium-burning temperatures or because there has been insufficient time for convective recirculation to have destroyed all the lithium in the star and in particular all of the lithium in the photosphere (but this recirculation is expected to be rapid compared to the other two timescales considered here; Basri 1998). Despite these potential pitfalls, Basri (1998) has demonstrated that any object with lithium absorption and Teff $<$ 2670K is unambiguously a brown dwarf. Thus if we confine our focus to objects with temperatures cooler than this, the lithium test can be applied regardless of these considerations. Using the relation of optical dwarf spectral type to temperature from Kirkpatrick (2008b) – $T_{eff}(K) = 3759 - 135x$, where, e.g, x=0 for M0, 9 for M9, 10 for L0, and 18 for L8 – we find that an effective temperature of 2670K corresponds to a dwarf of optical type M8. For the remainder of this paper, we will therefore restrict our discussion of the lithium test to dwarfs with optical types of M8 and later.

(4) It is expected that the 6708-Å line will disappear at very cool temperatures as lithium forms molecular species. Lodders (1999) has shown that below $T_{eff} \approx 1500$K Li-bearing molecules like LiCl and LiOH begin to form. For brown dwarfs of solar age, this temperature corresponds to optical spectral types of late-L through mid-T (see Figure 7 of Kirkpatrick 2005). Stars of solar abundance do not exist at temperatures this low (see Figure

10 of Kirkpatrick 2005), so we can safely assume that objects in this range of spectral types are all brown dwarfs. For these the lithium test is not needed. This theoretical prediction of lithium disappearance at these types should nonetheless be tested with empirical data.

(5) Young (<100 Myr) brown dwarfs have radii larger than older stars and brown dwarfs of the same spectral type because they are still contracting to their final structural configuration (Burrows et al. 1997). These young brown dwarfs are also lower in mass than stars and older brown dwarfs of the same spectral type. Both the larger radius and the lower mass mean that these objects will have lower surface gravities, which should be detectable even with low-resolution spectroscopy. (See §4.1.) Lower gravity will weaken the Li I line due to the lower atmospheric pressure, making it much harder to detect. This has been observed by Kirkpatrick et al. (2006) in the low-gravity, early-L dwarf 2MASS J01415823−4633574, which shows no Li I line down to an equivalent width of 1 Å. Weak Li I is seen despite the fact that this object is believed to be a young (1-50 Myr), low-mass (6-25 $M_{Jupiter}$) brown dwarf and despite the fact that other brown dwarfs of similar spectral type are known that show prominent Li I lines – such as the L0 dwarf 2MASS J11544223−3400390 with a Li I equivalent width of 3 Å.

We can test points (4) and (5) using a unique set of spectroscopic data. Over the past several years we have amassed a library of optical spectra of L and T dwarfs primarily using the W. M. Keck Observatory. Data from Kirkpatrick et al. (1999a, 2000); Burgasser et al. (2000); Kirkpatrick et al. (2001); Wilson et al. (2001); Burgasser et al. (2003a,b); Thorstensen & Kirkpatric (2003); McGovern et al. (2004); Kirkpatrick et al. (2006) combined with new data presented in this paper now gives us a library of ∼150 spectra spanning the wavelength regime 6300-10000 Å and covering spectral types L0 through T8. With such a large set of homogeneous spectra, we can better characterize the behavior of the Li I line as a function of spectral type. Moreover, this large set of spectra enables us to identify peculiar objects, particularly those with unusual spectra indicative of low gravity. As stated above, low gravity in L and T dwarfs is an indicator of youth, so these spectra also enable us to characterize the Li I strength as a function of age.

In this paper we present the newest spectra in our optical spectral library (§2), analyze objects with detected Hα (§3), and identify objects with low-gravity (young) signatures (§4). We perform further analysis of the young objects (§5) and build statistics on the behavior of Li I line strengths as a function of both spectral type and age (§6). Conclusions are given in §7.

2. Object Selection, Observation, and Classification

2.1. The Two Samples

Over the past several years we have conducted Keck Low Resolution Imaging Spectrometer (LRIS, Oke et al. 1995) observations of two different samples. The first is a color-selected sample of southern hemisphere L dwarf candidates chosen from 2MASS. The second sample is a collection of late-L dwarfs, early-T dwarfs, and a few other interesting cases drawn from the literature. We present details on each sample below.

2.1.1. The Southern L Dwarf Sample from 2MASS

In July 2000, one of us (CGT) wished to begin a parallax program for ultra-cool dwarfs using facilities at the Anglo Australian Observatory (AAO). At this time, very few L dwarfs were recognized south of Dec=0°, so we performed a photometric search for L dwarf candidates using data from the Two Micron All Sky Survey (2MASS, Skrutskie et al. 2006). This search was performed in two steps. First, the 2MASS Second Incremental Data Release (IDR2) Point Source Catalog[1] was searched for objects meeting the following criteria: $-50° < \mathrm{Dec} < +5°$, $8.0 < K_s < 13.6$, $J - K_s > 1.30$, $R - K_s > 6.5$ (where optical magnitudes are available from the USNO-A), and $|b| > 25°$. In order to weed out fainter objects at early-L types, a further cut was employed to drop objects with $K_s > 13.0$ if $J - K_s < 1.6$. To supplement this data set, we also performed on the 2MASS Point Source Working Database a search for southern hemisphere data taken after 20 Feb 1999 (the cutoff date for the 2MASS IDR2) but before July 2000. Selection criteria on this set stipulated that the candidates have $-50° < \mathrm{Dec} < +5°$, $|b| > 25°$, $J - K_s > 1.30$, $R - K_s > 5.5$ (where optical magnitudes are available from the USNO-A), and $9.5 < K_s < 13.6$. Visual inspection of the DSS, XDSS, and 2MASS images was used to drop objects contaminated by bright stars or galaxies, lying in nebular regions such as the Lynds 134 cloud complexes, or having bright R-band counterparts on the optical plates. The latter objects are not always eliminated using the $R - K_s$ selection criterion because the USNO-A Catalog has as one of its constraints that any real object must be detected on both the blue and red plates; as some late-type giants will be R-band only sources on the optical sky plates, these will not be included in the USNO-A (Monet et al. 2003).

Our final candidate list of 68 objects is given in Table 1. Objects verified spectroscopi-

[1]Available at `http://irsa.ipac.caltech.edu`.

cally to be late-M or L dwarfs are given in the upper portion of the table; those objects known not to be late-M or L dwarfs are given in the lower portion. 2MASS source designations are listed in column 1, and photometric data from the final 2MASS All-Sky Release Point Source Catalog (Cutri et al. 2003), which postdates our selection, are given in columns 2-5. Using this later catalog as the data source, some of the objects we originally selected may no longer fall within our constraints (such as the $J-K_s$ color of 1.29 for 2MASS J04433761+0002051). Columns 6-7 give the optical spectral type and reference for the classification. For objects discovered previously by other surveys, alternate source designations are given in column 9.

As for the AAO L dwarf parallax program itself, observations of our confirmed candidates continue. Results from the program will be presented in a forthcoming paper.

2.1.2. Interesting Objects Pulled from the Literature

The goal of the second sample was to obtain optical spectra of late-M, L, and T dwarfs that either had no previous spectroscopic follow-up in the optical or that would benefit from an optical spectrum with higher signal-to-noise or covering a new epoch. These interesting objects[2] are listed in approximate order of RA below:

2MASS J0415−0935 is the latest optical T dwarf standard from Burgasser et al. (2003a).

2MASS J05185−2828 is a discovery from the ongoing 2MASS L dwarf search of Cruz et al. (2003) and because of a very unusual near-infrared spectrum was hypothesized to be a late-L + T dwarf double (Cruz et al. 2004). Its binary nature has been confirmed via HST imaging (Burgasser et al. 2006b).

SDSS J0830+4828, SDSS J0837−0000, SDSS J0857+5708, SDSS J1021−0304, and SDSS J1254−0122 are all classified in the near-infrared as late-L or early-T dwarfs (Leggett et al. 2000; Geballe et al. 2002), and we obtained LRIS spectra of these to explore the L/T transition at far optical wavelengths.

Gl 337CD adds to this sample near the L/T transition and is relatively bright ($K_s = 14.0$). Its optical type is L8 (Wilson et al. 2001) whereas its near-infrared type is T0 (Burgasser et al. 2006c).

2MASS J1209−1004 adds another data point to the L/T transition. This object is the T3

[2]In the text we abbreviate sources names with a prefix such as 2MASS, DENIS, or SDSS and a suffix of the form Jhhmm±ddmm, where hhmm is the truncated J2000 Right Ascension in hours and minutes and ±ddmm is the truncated J2000 Declination in degrees and minutes. Full designations are given in the tables.

near-infrared standard on the Burgasser et al. (2006c) scheme.

2MASS J1315−2649 is an L dwarf with abnormally strong and variable Hα emission (Hall 2002a; Gizis 2002; Hall 2002b; Riaz & Gizis 2007) and we chose to observe it again to check its Hα strength.

2MASS J2244+2043 is an extremely red ($J-K_s = 2.45\pm0.16$) late-L dwarf uncovered during a hunt for red QSOs in 2MASS. We chose to observe this object to see if the optical spectrum revealed any clues regarding its unusually red near-infrared photometry.

2.2. Spectroscopic Observations

Optical spectra were obtained with LRIS on the 10m Keck-I Observatory atop Mauna Kea, Hawaii. A 400 lines/mm grating blazed at 8500 Å was used with a 1″ slit and 2048×2048 CCD to produce 10-Å-resolution spectra covering the range 6300 – 10100 Å. The OG570 order-blocking filter was used to eliminate second-order light. The data were reduced and calibrated using standard IRAF routines. Flat-field exposures of the interior of the telescope dome were used to normalize the response of the detector.

Individual stellar spectra were extracted using the "apextract" routine in IRAF[3], allowing for the slight curvature of a point-source spectrum viewed through the LRIS optics and using a template where necessary. Wavelength calibration was achieved using neon+argon arc lamp exposures taken after each program object. Finally, the spectra were flux-calibrated using observations of standards from Hamuy et al. (1994). Most of the data have not been corrected for telluric absorption, so the atmospheric O_2 bands at 6867-7000, 7594-7685 Å and H_2O bands at 7186-7273, 8161-8282, ∼8950-9300, ∼9300-9650 Å are still present in the spectra. In the sections that follow, a few cases are noted where a correction for telluric absorption was applied by using the spectrum of a nearby field late-F/early-G star taken just before or after the spectrum of the program object.

Table 2 lists the UT dates of observation, program principal investigator, other observers assisting, and sky conditions for the sixteen different nights on which data were taken or attempted. The 3.5-year time span was a consequence of the fact that these L dwarf targets were used as filler targets during other programs and were thus observed only in twilight, during gaps in the main program, or during periods of cloud cover. As listed in the table,

[3]IRAF is distributed by the National Optical Astronomy Observatories, which are operated by the Association of Universities for Research in Astronomy, Inc., under cooperative agreement with the National Science Foundation.

three nights – 2000 Aug 23, 2001 Feb 20, and 2001 Nov 13 – had poor transparency that sometimes led, as in the spectrum of the L dwarf companion Gl 618.1B, to poor signal-to-noise. Two nights were completely lost to adverse weather conditions, but on the eleven other nights conditions were clear with good seeing for generally the entire night. The list of the southern L dwarf candidates observed with Keck-LRIS during these runs is given in Table 3. The discovery name is given in column 1, with the observing date and integration listed in columns 2-3. As for the sample from the literature, the list of targeted M and L dwarfs is given in Table 4, and the T dwarf target list is given in Table 5. The first four columns in both tables give the object name, the discovery reference, the UT observation date of our Keck-LRIS spectrum, and the integration time.

Finder charts are provided in Figure 1 for the twelve new late-M through late-L dwarfs identified in the southern sample. Charts are made from the J-band component of the 2MASS All-Sky Release Survey Images as served through the on-request mosaicking service available at the NASA/IPAC Infrared Science Archive[4].

2.3. Spectroscopic Classification

Sixty eight candidates met the criteria of the southern sample. Seventeen of these, as listed in the lower section of Table 1, were found not to be late-type dwarfs as judged by previously published spectra or our own LRIS observations. These consisted of 10 carbon stars, 4 M giants, 2 QSOs, and one reddened, early-type star. Of the remaining fifty-one objects, listed in the upper section of Table 1, we observed twenty-eight and took published optical classifications for the remaining twenty-three. The twenty-eight for which we obtained LRIS spectra are listed in Table 3 and are plotted on linear and logarithmic flux scales in Figure 2 and Figure 3. Spectra of objects from our literature sample, given in Table 4 and Table 5, are plotted on both linear and logarithmic scales in Figure 4 and Figure 5.

Classifications were assigned as follows. For late-M dwarfs, classifications were measured by eye using LRIS spectra of late-M dwarf secondary standards from Kirkpatrick et al. (1999a). For L dwarfs, the prescription for classification presented in Kirkpatrick et al. (1999a) and Kirkpatrick et al. (2000) was followed, using the indices[5] defined in those pa-

[4]Available at `http://irsa.ipac.caltech.edu/`

[5]A few typesetting errors appearing in Table 7 of Kirkpatrick et al. (1999a) should be noted. First, the numerator of the Na-b ratio should cover the 10-Å interval 8153.3-8163.3 Å (the same as the numerator for Na-a) instead of the 30-Å interval listed. Second, the numerator for Cs-b should be "Av. of 8918.5-8928.5 and 8958.5-8968.5" and the denominator should be "8938.5-8948.5". Third, the denominator of the TiO-b

pers. Measurements of each of the indices are given in columns 4-9 of Table 3 and columns 5-10 of Table 4, and the final types resulting from these indices are listed in column 10 of Table 3 and column 11 of Table 4. After index-based types were assigned, our LRIS spectra were compared by eye to LRIS spectra of the L dwarf standards to look for anomalies. Spectral types of objects having feature strengths uncharacteristic of field objects of like type were further given a "pec" (peculiar) suffix. These objects are discussed further in §4.

For the T dwarfs in Table 5, optical classifications were assigned using the index-based recipe outlined in Burgasser et al. (2003a). Measurements for the optical T dwarf indices are given in columns 5-9 of Table 5 and the resulting spectral types given in column 10. As with the L dwarfs these T dwarfs were compared by eye to LRIS spectra of the optical T dwarf standards to look for peculiarities and to check the final index-based types.

Because many of the objects in Table 3 are either new discoveries or now have optically derived spectral types for the first time, we provide distance estimates. As shown in Figure 9 of Kirkpatrick (2005), optical L dwarf spectral types correlate better with absolute J-band magnitude than do near-infrared L dwarf spectral types, so optical types can be used to derive more accurate spectrophotometric distances. Our distance estimates, listed in column 11 of Table 3, are derived using the 2MASS-measured J-band magnitudes of the objects, our measured optical spectral types, and the relation between absolute J-band magnitude and optical spectral type from Looper et al. (2008) for L dwarfs or the mean absolute J-band magnitudes computed by Kirkpatrick & McCarthy (1994) for M dwarfs.

Using our LRIS spectra, we have used the *splot* package in IRAF to compute the pseudo-equivalent widths[6] (or limits) for Hα emission at 6563 Å and Li I absorption at 6708 Å. In the case of limits, we measure the equivalent widths of positive and negative noise spikes in the same spectral region to ascertain the width of the largest real feature that could be masked at that signal-to-noise level. These are given in columns 12-13 of Table 3 and Table 4 and columns 11-12 of Table 5. (Note that we have expressed the equivalent width for both as positive.) We discuss those objects with measured Hα emission in §3; objects with measured lithium absorption are discussed later in §6.

---

ratio should cover the 15-Å interval 8455.0-8470.0 rather than the 35-Å interval given. Only this third index, TiO-b, is actually used in the spectral typing recipe.

[6]These pseudo-equivalent widths, measured relative to the local (not true) continuum, will be referred to simply as "equivalent widths" throughout the remainder of the paper.

3. Objects with Hα Emission

Unlike for warmer dwarfs, Hα is not a reliable indicator of youth in late-M and later dwarfs. Most late-M dwarfs show Hα emission as illustrated elsewhere (see Figure 6 of Gizis et al. 2000, Figure 1 of West et al. 2004, and Figure 3 of West et al. 2008). Indeed, four of our five late-M dwarfs from Table 3 exhibit Hα emission, as shown in the spectral zoom-ins of Figure 6.

Figure 6 also shows the L and T dwarfs from our sample that have Hα emission. (See Table 4 and Table 5.) Three early-L dwarfs, three mid- to late-L dwarfs, and one early-T dwarf show the feature. The emission lines in 2MASS J0141−4633 and 2MASS J1315−2649 vary but are persistent. In the case of 2MASS J0141−4633 this persistence has been measured over only a single night (Kirkpatrick et al. 2006). For 2MASS J1315−2649 our new spectrum shows an Hα equivalent width of 160 Å. Comparing this to the twelve separate epochs published earlier (Hall 2002a; Gizis 2002; Hall 2002b; Fuhrmeister et al. 2005; Barrado y Navascués 2006) we find that our observation places it squarely in its flaring state; the Hα equivalent width is ∼20 Å when the object is in quiescence (Riaz & Gizis 2007). In the case of 2MASS J2057−0252, there are two epochs of observation separated by nearly a year; our 2000 Aug 23 measurement of 11 Å equivalent width is consistent within the errors with the 2001 Jul 15 measurement of 8.44 Å from Schmidt et al. (2007), who have analyzed the emission properties of the Cruz et al. (2003) sample. Another object in common with the Cruz et al. (2003) sample, 2MASS J0144−0716, was caught in a flare during our observation, as chronicled in Liebert et al. (2003). Finally, Hα emission in the two latest objects, the L7.5 dwarf SDSS J0423−0414 and the T2 dwarf SDSS J1254−0122, has been described elsewhere (Burgasser et al. 2003a, Burgasser et al. 2005c).

4. Spectroscopic Effects of Low Gravity (Youth)

4.1. Introduction

Many published works on late-M dwarfs have discussed the utility of gravity-sensitive spectral features in discerning lower mass brown dwarfs from higher mass stars of the same temperature or spectral type. Since the early days of astronomical spectroscopy, the strengths of CaH, the Ca II triplet, and the neutral alkali lines have been identified as gravity sensitive and used to distinguish M giants from M dwarfs. In an M giant, the much more distended photosphere has much lower gravity and pressure than the photosphere of an M dwarf of equivalent temperature. A similar effect makes a young, low-mass brown dwarf distinguishable from an older, higher-mass brown dwarf (or star) of similar temperature.

Specifically, two effects are at work. First, a brown dwarf younger than ∼100 Myr will still be contracting to its final radius (see Fig. 10 of Burrows et al. 1997) and will have a more distended atmosphere than an older brown dwarf of the same spectral type. Second, a younger brown dwarf must necessarily have a lower mass than an older brown dwarf of the same temperature. Relative to the older object, the younger one is larger and less massive and thus has a relatively lower gravity and pressure.

One of the first papers to demonstrate these effects in low-mass stars and brown dwarfs, Steele & Jameson (1995), used a weakening of the Na I lines in Pleiades late-M brown dwarf candidates to argue that these objects were true members of the cluster. Martín et al. (1996) also noted that Pleiades brown dwarf candidates have slightly stronger VO bands than those of similarly classified field dwarfs. Luhman et al. (1997) found that an M8.5 brown dwarf candidate in the ρ Ophiuchi complex exhibited calcium hydride and K I strengths intermediate between an M8.5 V and an M8.5 III, whereas the Na I strengths were much more like the M8.5 III. Luhman et al. (1998) discussed how the optical spectrum of a brown dwarf candidate in the Taurus-Auriga complex had Na I and K I strengths and TiO/VO ratios more similar to those of a giant while the CaH strength was intermediate between an M dwarf and an M giant. Later studies have continued to use these gravity-sensitive diagnostics to argue for youth in other late-type dwarfs.

It is important to note here that the Pleiades cluster holds a special place in the study of low-gravity effects in brown dwarf spectra because of its nearness to the Sun and the extent to which its low-mass members have been scrutinized. As discussed above, not only has it been shown that substellar objects in the Pleiades show such effects empirically, but also (as we discuss below) the Pleiades cluster falls near the aforementioned upper age boundary of ∼100 Myr where theory predicts these effects will be just discernible. The Pleiades is one of the few clusters where it is possible to derive an age estimate from all three of the fundamental age indicators: the pre-main sequence turn-on, the upper main sequence turn-off, and the lithium depletion boundary (Bildsten et al. 1997). We discuss each in turn.

1) The pre-main sequence turn-on age for the Pleiades is the most difficult of these to measure because the Pleiades locus is only slightly different from the zero-age main sequence even for low-mass stars and because theoretical models do not match real cluster isochrones well at V-I > 2 (Stauffer et al. 2007), making it difficult to derive accurate pre- main sequence ages for clusters with ages $\geq$ 100 Myr. A reasonable pre- main sequence age estimate for the Pleiades is 100 Myr (Stauffer et al. 2007), but with considerable uncertainty.

2) Modern upper main sequence age estimates range from 77 Myr (Mermilliod 1981) for a minimal convective core overshoot parameter up to about 150 Myr (Mazzei & Pigatto 1989) for a relatively large convective core overshoot parameter. The most frequently quoted

upper-main sequence age is 100 Myr (Meynet et al. 1993).

3) It has been claimed that an age derived from the lithium depletion boundary should be more accurate than any other cluster age estimate (Bildsten et al. 1997) because there are relatively few adjustable parameters. Stauffer et al. (1998) derived a lithium depletion boundary age for the Pleiades of 125 Myr, with an estimated uncertainty of about 10 Myr. Burke et al. (2004) reanalyzed the Stauffer et al. (1998) data, and suggested a lithium depletion boundary age for the Pleiades of 126-148 Myr, dependent on how the bolometric correction is handled.

The following evidence from other clusters should be considered before adopting an age for the Pleiades. The α Persei cluster is another where it is possible to obtain age estimates from all three methods. If the eponymous star α Per, an F supergiant, is indeed a member of the cluster and is coeval with the other stars, its location in color-magnitude diagrams places an upper limit on the age of the cluster of $<$80 Myr (Ventura et al. 1998), as compared to the lithium depletion boundary age estimate of $\sim$90 Myr (Stauffer et al. 1999). A similar tendency for the lithium depletion boundary age to be significantly older than age estimates from other methods appears to be true for other open clusters (Jeffries & Naylor 2001). For that reason, we choose to treat the lithium depletion boundary age for the Pleiades as an upper limit, and to adopt a Pleiades age of 100-125 Myr for this paper.

Moving beyond the Pleiades and α Persei to slightly older ages, Bannister & Jameson (2007) suggest that the early-L dwarf 2MASP J0345432+254023 may be a member of the Ursa Major/Sirius Moving Group, which has an age of 400$\pm$100 Myr. This L0 dwarf does not look unusual relative to the majority of other early-L dwarfs, a reassuring fact because it was chosen as the L0 optical spectroscopic standard by Kirkpatrick et al. (1999a). Jameson et al. (2008) further identify the objects 2MASSW J0030438+313932 (optical L2), 2MASSI J1204303+321259 (optical L0), and 2MASS J15500845+1455180 (optical L2:) as being potential members of the Ursa Major Group, and none of these show spectral peculiarities (Kirkpatrick et al. 1999a; Cruz et al. 2003, 2007).

In summary, objects at ages $\sim$4$\times$ that of the Pleiades have spectra in which low gravity effects are no longer discernible at the $\sim$10 Å resolution of our classification spectra; conversely, objects of Pleiades age show spectral hallmarks of low gravity. Hence, we adopt $\sim$100 Myr as the oldest age at which the signatures of low gravity can reliably detected in our spectra.

4.2. Analysis of Low-Gravity (Young) Spectra

The spectra of a number of field ultra-cool (spectral types ≥M7) dwarfs from the literature have spectral morphologies that can be attibuted to low gravity. We identify another four low-gravity objects using new spectra presented in this paper. Table 6 gives this combined list of twenty low-gravity field dwarfs. For objects having optical spectral types >M8 we compare in the following subsections our spectra to fiducial spectra in order to estimate ages for the peculiar objects using *empirical* evidence only.

In these subsections, we provide qualitative analyses to aid in the recognition of low-gravity signatures. We feel that such "by-eye" assessments are, in fact, superior to classification via spectral indices because they tap the ability of the brain to consider the *totality* of information available in the spectra. This parallels the philosophy of William Morgan, one of the pioneers of the MKK classification system (Morgan et al. 1943), whose reasoning was described by Garrison (1995) as follows: "Morgan used the techniques of visual pattern recognition in a morphological approach to classification. In today's climate of the 'deification of quantification', it is sometimes difficult for people to see the power of such an approach, yet the human brain has evolved to be ideally suited to such a methodology. Morgan was fond of using the analogy of the brain's ability to recognize familiar human faces. With pattern recognition, the result is immediate; nothing is measured, but all of the pattern information is compared with experience."

This having been stated, in future papers we will outline quantitative spectroscopic classifications of our young objects. In Cruz et al. (in prep.) we will investigate spectral indices for the optical spectra of young L dwarfs, and in Kirkpatrick et al. (in prep.) we will establish spectral indices and a grid of spectral standards of known age to serve as comparisons to young, late-M dwarfs in both the optical and near-infrared regimes. A preview of the latter paper is shown in Figure 7, which demonstrates that optical spectra at our resolution can be distinguished at the level of ∼1 dex in log(age).

For some of our low-gravity objects we have obtained spectra at telescopes other than Keck or have obtained Keck data for comparison objects not included in the two samples discussed earlier. Details on these additional observations are given in Table 7. We also include in the following discussion two low-gravity L dwarfs, G 196-3B and Gl 417B, that are companions to main sequence stars and thus have independent measures of age via their association with a well studied primary star. These are discussed below in order of spectral type. To guide the eye in Figure 8 through Figure 13, old field objects (∼1 Gyr) are plotted in black, objects believed to have ages near that of the Pleiades (∼100 Myr) are shown in red, and those believed to be significantly younger than the Pleiades (∼10 Myr) are shown in magenta. Giant spectra, illustrating even lower gravities, are shown in blue.

4.2.1. 2MASS J0608−2753 (M8.5 pec) and SDSS J0443+0002 (M9 pec)

2MASS J0608−2753 was discovered by Cruz et al. (2003), who noted that its spectrum exhibited the hallmarks of low gravity. SDSS J0443+0002 was discovered by Hawley et al. (2002) but the spectrum in that paper was sufficiently noisy that the peculiarities went unnoticed. This object was recovered and reobserved as part of our southern L dwarf program. Figure 8 shows our new spectra of these objects. They are compared to spectra of a normal M9 field dwarf and the late-M dwarf Teide 1. The latter object, discovered by Rebolo et al. (1995), is a member of the Pleiades and is thus assumed to have the age of ∼100 Myr typically assigned to the cluster. Also noticeable in the spectra of 2MASS J0608−2753 and SDSS J0443+0002 is the Na I doublet, which is weaker than in both the normal field M9 and Teide 1, and the VO bands, which are stronger than these same two comparison spectra. The bands of CaH near 7050 Å and FeH at 9896 Å are somewhat weaker than in these same two comparison objects. (These same trends hold when comparing to the later Pleiad, Roque 4, in the left panel of Figure 9.) This evidence suggests that both 2MASS J0608−2753 and SDSS J0443+0002 have ages <100 Myr because they have gravities comparable to or lower than that of the Pleiad.

4.2.2. 2MASS J1022+0200, DENIS J0357−4417, 2MASS J0241−0326, 2MASS J0141−4633, and 2MASS J2213−2136 (L0 pec)

2MASS J1022+0200 was discovered by Reid et al. (2008) and that spectrum is shown in the left panel of Figure 9. DENIS J0357−4417 was first published by Bouy et al. (2003) who guessed a spectral type of "∼L3" based on its measured I-J color. Our spectrum is the first reported of this object, which comes from our southern L dwarf sample, and it shows DENIS J0357−4417[7] to have a considerably earlier type. Our spectrum is shown in the left panel of Figure 9.

Bouy et al. (2003) find DENIS J0357−4417 to be a binary with separation of 98±2.8 milliarcseconds and magnitude differences in the HST/WFPC2 filters of $\Delta m_{F675W} = 1.23\pm0.11$ mag and $\Delta m_{F814W} = 1.50\pm0.11$ mag. The latter difference means that at I-band the primary contributes four times more flux to the composite spectrum than the secondary does. This difference in I-band flux suggests that the L0 composite spectrum is comprised of spectra

[7]This object is referred to as DENIS-P J035726.9−441730 in Table 1 of Bouy et al. (2003) but as DENIS-P J035729.6−441730 throughout the text of that same paper. We assume the text is in error and retain the first designation because the entry in the DENIS 3rd Release clearly refers to this position, and it also coincides with the position of our independent discovery of this object in 2MASS (see Table 1).

differing by roughly three spectral subclasses (e.g., an L0 and an L3 or an M9.5 and an L2.5). We have tested this by adding a standard L0 spectrum to that of a standard L3 spectrum scaled down so that it has only one-fourth the flux of the L0 in the I-band and find that the composite spectrum is only slightly different from the L0 itself. Specifically, the TiO bands at 7053 and 8432 Å are somewhat shallower in the composite than in the L0 itself, but the strength of the alkali lines, the VO bands, and the hydrides are essentially unchanged. In other words, the composite spectrum is so little different than the single L0 dwarf that its spectrum would not be labelled unusual. Therefore, we can assume that the oddities seen in the composite spectrum of DENIS J0357−4417 are indicative of oddities in the primary spectrum itself and are not induced by the composite nature of the spectrum.

Also shown in the left panel of Figure 9 are spectra of a normal M9 dwarf (at top), a normal L0 dwarf (at bottom), and the late-M Pleiad known as Roque 4 (discovered by Zapatero Osorio et al. 1997). For both 2MASS J0608−2753 and DENIS J0357−4417 the K I and Na I lines along with the CaH bands are weaker than in a field early-L dwarf, and the VO bands are stronger than those seen in normal field late-M or early-L dwarfs. A similar spectral morphology to the Pleiad Roque 4 suggests an age estimate for 2MASS J1022+0200 and DENIS J0357−4417 of very roughly 100 Myr.

2MASS J0241−0326 was discovered by Cruz et al. (2007) and is a near duplicate of the canonical low-gravity L0 dwarf 2MASS J0141−4633. 2MASS J0141−4633 itself was discovered by Kirkpatrick et al. (2006), who studied the optical and near-infrared spectra of this object in detail. 2MASS J2213−2136 was discovered by Cruz et al. (2007) and is another near duplicate of 2MASS J0141−4633. All three of these are plotted in the right panel of Figure 9 along with the spectrum of the L0 Pleiad dwarf Roque 25 (top, discovered by Martín et al. 1998), and the late-M giant IRAS 14303−1042 (bottom).

The optical spectra of these objects reveal that the K I and Na I lines are weaker than normal as are the bands of CrH and FeH. Even weaker alkali lines and hydride bands, such as those seen in IRAS 14303−1042, are used as the gravity-dependent hallmarks of a giant spectrum. We interpret these spectral anomalies in 2MASS J0141−4633, 2MASS J0241−0326, and 2MASS J2213−2135 to be indicative of a surface gravity intermediate between that of a normal L dwarf and a late-M giant. Other peculiar features are the strengths of the VO bands, which are stronger than those seen in a normal M/L dwarf despite the fact that the TiO bandstrengths mimic those seen in an early-L dwarf. The oxides TiO and VO disappear from late-M and early-L dwarfs because of condensation. In the standard sequence (Kirkpatrick et al. 1999a), TiO disappears first and VO disappears at even later spectral types (i.e., cooler effective temperatures). Lower gravity leads to lower atmospheric pressure. This inhibits the formation of grains, pushing condensation to cooler

temperatures (Lodders 2002). The limiting cases of this phenomemon are the giant stars. At their very low gravities of log(g)≈0, late-M giants never reach temperatures low enough to trigger the formation of TiO and VO condensates, so gaseous TiO and VO still exist in their atmospheres and as absorbers in their optical spectra. (See spectrum of IRAS 14303−1042 in Figure 9.) 2MASS 0141−4633, 2MASS J0241−0326, and 2MASS J2213−2135 fall at values of T_{eff} where the formation of titanium-bearing condensates has already begun but where vanadium condensation has not yet been triggered. At these temperatures, low-gravity L dwarfs are very easy to spot via their weak TiO bands and overly strong VO bands.

Given that the spectra of 2MASS J0141−4633, 2MASS J0241−0326, and 2MASS J2213−2135 are clearly more unusual and point to a lower gravity than that of Roque 25, we can conclude that their ages are significantly younger than the 100 Myr age assigned to this Pleiades member. In fact, fits of the optical and near-infrared spectra of 2MASS J0141−4633 from Kirkpatrick et al. (2006) indicate 1 Myr < age < 50 Myr and log(g)≈4.0, implying a mass of 6 $M_{Jupiter}$ < M < 25 $M_{Jupiter}$.

4.2.3. 2MASS J1022+5825 (L1 pec)

This object was discovered by Reid et al. (2008). As seen in Figure 10, the best overall match is to a field L1 dwarf, but all of the alkali lines (K I, Na I, Rb I, and Cs I) are noticeably weaker in this object than in normal field L dwarfs, and the VO bands are more prominent than expected. In these respects its spectrum has a very strong resemblance to Roque 25, the L0 Pleiad, and suggests an age for 2MASS J1022+5825 of roughly 100 Myr.

Another unusual feature in the spectrum of 2MASS J1022+5825 is its strong Hα emission line with a measured equivalent width of 128 Å. As Schmidt et al. (2007) show, the emission strength just two nights later had dropped to 26 Å. Such variable emission has the potential to complicate interpretation of the gravity-sensitive features used in our analysis, especially when objects may have been spectroscopically observed on only one occasion. Such emission has two mechanisms that can alter the measured strengths of lines and bands. First, as noted in late-M and L dwarf flares (Liebert et al. 1999; Martín et al. 1999b; Schmidt et al. 2007), emission in the cores of resonance lines can partially or totally fill in the absorption lines causing them to appear weaker than they really are. Second, flux from the superheated material above the photosphere adds continuum flux, suppressing the contrast between absorption lines and bands and thereby making the lines and bands appear weaker than normal (i.e., it veils the features).

Fortunately such activity is not the cause of the features seen here. The first effect

would amplify the appearance of low gravity via anemic alkali linestrengths, but the second effect would contradict it because it would cause the VO bandstrengths to weaken, not strengthen. Hence, low gravity is still the most likely explanation for the peculiarities seen in this spectrum. In the case of 2MASS J1022+5825 we find that the emission appears to be confined to Hα because the strengths of the alkali lines do not change appreciably between the two nights. Veiling also appears not to be an issue because the VO bandstrengths are unaffected between the observations. In this case we are further reassured that the noted spectral peculiarities are caused by low gravity and not by other effects.

4.2.4. 2MASS J0033−1521, G 196-3B, and 2MASS J2208+2921 (L2 pec)

2MASS J0033−1521, discovered by Gizis et al. (2003) and rediscovered as part of the southern L dwarf sample, is shown in the left panel of Figure 11. Its alkali lines are weaker than those of a standard early-L dwarf, the most obvious manifestation being the shallowness of the cores of the K I doublet at 7665 and 7699 Å. Hydride bandstrengths are also weaker than normal, and this is particularly obvious in the CaH band near 6950 Å and the Wing-Ford FeH band at 9896 Å. Two bands noticeably weak or absent from the spectrum are TiO and VO, both of which are still evident in the spectra of normal early-L dwarfs in the field; the 8432 Å band of TiO and weak VO absorption near 7900 Å usually sculpt the continuum of an early-L dwarf but this is not seen in 2MASS J0033−1521.

We can interpret the peculiarities in this spectrum as the result of low gravity due to the weakness of the alkali lines and hydride bands. However, we note that this object does not have the strong VO bands seen in the low-gravity L0 and L1 dwarfs discussed above. If this object is truly low-gravity, then it falls at a temperature cool enough for VO condensation to have already taken place. Unfortunately for low-gravity classification, the loss of gaseous oxides robs the optical spectrum of some of its most telltale low-gravity signatures.

There is an additional problem at these temperatures: there are currently no firmly established, low-gravity cluster members with optical types later than L0 to use as age comparisons. In the case of 2MASS J0033−1521, its unusual features are not that anomalous when compared to a normal field L2 dwarf, and it is likely that a lower gravity object of the same class would still exhibit some VO absorption. We thus surmise that 2MASS J0033−1521 must lie at the old end of the predicted age range where low-gravity signatures are evident, and this gives it an age of $\sim$100 Myr.

G 196-3B was discovered by Rebolo et al. (1998) while performing a search for companions to young (X-ray active), nearby K and M dwarfs. The primary, G 196-3A, is an

M2.5 dwarf believed to have an age between 20 Myr and 300 Myr (Kirkpatrick et al. 2001). 2MASS J2208+2921 was discovered by Kirkpatrick et al. (2000) and labeled as one of only two peculiar L dwarfs known at that time. At the time of that paper, the causes for its peculiarity were not understood but an analysis of the feature strengths on a newly acquired Subaru spectrum reveals that this object is probably also a low-gravity L dwarf.

Spectra of G 196-3B and 2MASS J2208+2921 are shown in the right panel of Figure 11. In G 196-3B the cores of the K I doublet are noticeably weaker than field L dwarfs of similar type. Lines of Na I, Rb I, and Cs I over the 7500-9000 Å range are very weak but present at this resolution. The hydride bands of CaH, CrH, and FeH are weaker than normal. These features point to low gravity (youth) as the cause, and the independent age estimate from the primary confirms this. In the spectrum of 2MASS J2208+2921 the alkali lines are all weak, most notably the cores of the K I doublet. The hydride bands – CaH, CrH, and FeH – are all weak as well. Although the spectrum shows only very weak absorption by TiO at 8432 Å, the VO bands near 7400 Å and 7950 Å are obvious and slightly stronger than those seen in G 196-3B. Nevertheless, this spectrum is very similar to that of G 196-3B, so we suspect that 2MASS J2208+2921 has a similar age of ∼100 Myr.

4.2.5. 2MASS J1615+4953 (L4 pec) and Gl 417B (L4.5)

2MASS J1615+4953 was discovered by Cruz et al. (2007), who noted possible low-gravity signatures in its optical spectrum. Gl 417B was discovered by Kirkpatrick et al. (2001), who assigned an age of 80-300 Myr to it based on the activity, lithium abundance, and kinematics of its G dwarf primary, Gl 417A. Bouy et al. (2003) find that Gl 417B is a binary with separation of $0\farcs070\pm0\farcs0028$ and magnitude differences in the HST/WFPC2 filters of $\Delta m_{F814W} = 1.07\pm0.11$ mag and $\Delta m_{F1042M} = 1.04\pm0.11$ mag. It can be shown that the relation between M_I and optical spectral type suggests that the L4.5 composite spectrum is comprised of two spectra differing by roughly 2 or 2.5 spectral subclasses (e.g., an L4 + L6/L6.5 or an L4.5 + L6.5/L7). It can further be shown that such composite spectra differ little from that of the primary, so we can consider the peculiarities in the composite spectrum to be indicative of peculiarities in the primary spectrum alone.

The spectrum of 2MASS J1615+4953 in the left panel of Figure 12 has low signal-to-noise but the overall morphology best fits that of an L4 dwarf. A comparison to an even earlier, L3 dwarf shows that 2MASS J1615+4953 is too blue in its overall slope. We interpret this as an absence of absorption from the wings of the Na I "D" doublet at 5890 and 5896 Å. A more detailed examination also shows that the K I line cores are weaker along with all of the bands of CaH, CrH, and FeH. Low gravity is most likely the cause, and we tentatively

assign this object an age estimate of ∼100 Myr based on the fact that it is more peculiar than Gl 417B (∼80-300 Myr; see below). However, due to the poor signal-to-noise ratio of this spectrum we can not be completely certain that low gravity is the correct interpretation of its peculiarities. This object may prove to be an overly dusty L dwarf akin to those described in Looper et al. (2008).

The spectrum of Gl 417B in the right panel of Figure 12 shows some slight deviations from a normal, old, field mid-L dwarf. Lines of Rb I are somewhat weaker than in a field mid-L dwarf although other alkali lines of K I, Na I, and Cs I aren't noticeably different in strength. The TiO band at 8200 Å may also be somewhat weaker than normal. What is clear is that the spectrum of this fairly young object is not all that different from a much older field L4 or L5 dwarf. This supports the idea that peculiarities in the spectrum due to lower gravity are obvious only at ages <100-200 Myr, which is the age when these brown dwarfs are expected to have reached their final radius (Burrows et al. 1997).

4.2.6. 2MASS J2244+2043 (L6.5)

This is the final low-gravity spectrum illustrated here and it is the latest. The object was discovered as a byproduct of the 2MASS search for red Active Galactic Nuclei, led by B. O. Nelson and R. M. Cutri, and was first published in the trigonometric parallax paper of Dahn et al. (2002). The optical spectrum, typed as L6.5, is plotted in Figure 13 along with the optical L6 and L7 standards from Kirkpatrick et al. (1999a). The long-wavelength end of the spectrum is rather noisy, but it appears to show no Wing-Ford FeH band at 9896 Å, which does not match its spectral type or the fact that the 8692 Å band of FeH is clearly present. Other than that, however, there are no other obvious spectral oddities and no reason to label this spectrum as peculiar. The reason for discussing this object here is that its near-infrared spectrum is incredibly peculiar (McLean et al. 2003; Looper et al. 2008) and almost certainly the byproduct of much lower gravity. Not only is the H-band portion of the spectrum markedly triangular, an indicator of low gravity, but the $J - K_s$ color of 2.48±0.15 makes it one of the reddest L dwarfs known.

So why, then, is the optical spectrum so ordinary in appearance? Unlike the earlier L dwarfs discussed above, TiO and VO are no longer available to use as temperature or condensation bellwethers, the condensation of the oxides having completely stripped them from the photosphere. In mid- to late-L dwarf spectra, the main shapers of the emergent flux in the optical are the pressure broadened Na I and K I lines. In atmospheres of lower gravity and pressure, these alkali absorptions will be less pronounced, giving them strengths comparable to a much warmer field object. In late-L dwarfs, the hydrides begin to disappear

as well, but because this condensation will likely be inhibited in a lower gravity object just as it is for TiO and VO, these hydrides will appear in the spectrum at later types than normally seen. The combination of these two effects, then, conspire to create a spectrum which is virtually indistinguishable from an earlier type L dwarf of higher gravity. In other words, the lower gravity spectrum will have weaker alkalis and stronger hydrides than a high gravity L dwarf of comparable temperature. Hence there may be a degeneracy at mid- and late-L types whereby low-gravity objects are very difficult or impossible to distinguish in the optical. 2MASS J2244+2043 may be the first such object where this degeneracy is seen.

5. Analysis

5.1. Optical Spectral Type vs. Near-IR Color

As suggested in Kirkpatrick et al. (2006), near-infrared colors may provide an independent means of identifying low-gravity L dwarfs. In the case of 2MASS J0141−4633, the emergent flux at H- and K-bands is significantly higher, relative to the J-band flux, than that of a normal dwarf of the same optical spectral type. This is evident in its 2MASS measured near-infrared color of J-K_s=1.735±0.054, which is far redder than the J-K_s=1.29 color (see Figure 14) of a normal L0 dwarf. The unusually red color is believed to be caused by reduced collision-induced absorption by H_2 as expected at lower gravity (lower pressure). (See Borysow et al. 1997 for opacity plots of CIA H_2 demonstrating that H-band and especially K-band should be the most affected.) Another way of stating this is that low gravity dwarfs should tend to have redder J-K_s colors than higher gravity dwarfs of the same type. Optically determined spectral types should be independent of changes in the near-infrared CIA H_2 opacity, so plots of optical type vs. J-K_s color may be useful in ferreting out other young objects. We can check this by making the plot shown in Figure 14, which highlights objects already known to have the spectroscopic hallmarks of lower gravity.

To construct this plot we have built three samples spanning the ultra-cool dwarf regime from M7 to L8:

• M7-M9.5: Any published objects classified as M7 to M9.5 based on optical spectra were eligible for inclusion. However, objects selected photometrically from near-infrared surveys were excluded as this might bias the distribution of J-K_s colors. Primarily this sample is built from published spectroscopic follow-up of objects selected from proper motion studies or selected from optical photometric surveys. To ensure adequate statistics we built this list at random until the number of objects in each integral subtype bin (M7-7.5, M8-8.5, and M9-9.5) was roughly twenty-five.

• L0-L5.5: Finding L dwarfs free of near-infrared photometric selection bias would result in very small or null lists of objects, so we simply drew our sample from the lists given at http://www.DwarfArchives.org. Objects had to have well measured optical types (i.e., no uncertain types were included) and errors in the 2MASS J-K_s color had to be <0.10 mag.

• L6-L8: The selection criteria were the same as for the L0-L5.5 sample except that the restriction on J-K_s color error was dropped to increase the sample size.

These three samples are graphically presented in Figure 14. Each bin along the y-axis represents a full integral subtype: "M7" includes M7 and M7.5 dwarfs, "M8" includes M8 and M8.5 dwarfs, etc. "L8" includes only type L8 because optical types of L8.5, L9, and L9.5 are not currently defined. In order to show more information than a standard histogram would allow, we have plotted the distributions as follows. For each bin, the median color in the group is plotted highest in the bin; colors falling further from the median are plotted progressively lower down the y-axis. This gives each bin a patterning of points that look approximately like an inverted "V". As each individual point contributing to the distribution is plotted on such a diagram, the error bars on each of the individual color measurements can also be shown.

With these samples in hand, we then checked objects comprising these lists and marked those displaying signatures of low-gravity in their spectra. These low-gravity objects are labeled on Figure 14. As predicted, the low-gravity objects tend to have redder J-K_s colors, sometimes dramatically redder, than the median color for their optical spectral class. However, there are also low-gravity dwarfs with J-K_s colors that aren't unusually red.

Moreover, there appear to be some objects having very red J-K_s colors for their type but no indication of lower gravity in their optical spectra. Two examples are the M9.5 dwarf SSSPM J2310−1759 (Lodieu et al. 2005; J-K_s=1.407±0.041) and the L4.5 dwarf 2MASS J0512−2949 (J-K_s=2.178±0.071) from the southern L dwarf sample of Table 1 and Table 3. Two other examples are noted by Looper et al. (2008), who study two particularly red L dwarfs – the optical L4.5 2MASS J18212815+1414010 (J-K_s=1.78±0.03) and the optical L6 2MASS J21481628+4003593 (J-K_s=2.38±0.04) – the unusually red colors for which appear to be the result of an overabundance of atmospheric dust and are perhaps unrelated to low gravity. (On the blue side of the distribution, unusually blue objects are sometimes low-metallicity dwarfs [Kirkpatrick 2008a] in which collision induced absorption by H_2 is the dominant absorption mechanism in the near-infrared, whereas other blue objects may have atypically thin and/or large-grained clouds decks that may be unrelated or only partly the result of lower metallicity [Burgasser et al. 2008].) Therefore, unusually red near-infrared colors alone can not be used to identify low-gravity dwarfs because higher metallicity and/or dustier L dwarfs can also exhibit redder colors for their optical type.

5.2. Are We Finding Too Many Young L Dwarfs?

As the number of low-gravity ultra-cool dwarfs in the published literature continues to grow (see Table 6), we must ask whether their frequency of occurrence is consistent with expectations. If the frequency is much higher than predictions, then this would suggest that we may have assigned the wrong physical cause to peculiarities observed in the optical spectra above. There are also clear indications that these low-gravity dwarfs tend to be found in the southern hemisphere, where known, nearby (<100 pc) young stellar associations are concentrated. Because non-neglible color selection biases exist for late-M dwarfs in the studies discussed below, we restrict the subsequent discussion to L dwarfs alone.

The first two peculiar L dwarfs were noted by Kirkpatrick et al. (2000) and we now believe that one of these, 2MASS J2208+2921, can be explained via low-gravity (youth). That original sample contained 92 L dwarfs with optical spectra and spectral type determinations. Three of these – GD 165B, Gl 417B, and Gl 584C – are not strictly "field" L dwarfs since they are companions to stars. As a result the percentage of low-gravity field L dwarfs in this sample is thus 1/89, or 1.1±1.1%. It should be noted that this sample is comprised of 73 objects north of Dec=0° and 16 objects south of Dec=0°. Of the latter group, only one is south of Dec=−30°.

The southern L dwarf sample in the current paper is comprised of 24 L dwarfs, of which one (Gl 618.1B) is a companion object, and all have optical spectra and spectral classifications. The identification of three of these (2MASS J0033−1521, 2MASS J0141−4633, and DENIS-P J0357−4417) as young objects gives a low-gravity percentage of 3/23, or 13.0±7.5%, for field L dwarfs. Despite its large error bar, this result appears at odds with the frequency found in the earlier Kirkpatrick sample. It is important to note, however, that this newer sample contains only objects located south of Dec=0°.

The on-going sample of Cruz and collaborators expands markedly on the Kirkpatrick samples. All objects were photometrically selected using the same prescription regardless of hemisphere (Cruz et al. 2003; Reid et al. 2008), so the sample is uniform. In that collection there are 241 field L dwarfs with optical spectra and spectral classifications, 22 of which show low-gravity features[8]. That sample, comprised of a nearly equal split of objects at northern vs. southern declinations (116 in the north, 125 in the south), gives a low-gravity fraction of 22/241, or 9.1±1.9%.

Combining all of these samples and removing duplicates gives a total fraction of 23/303,

[8]Some of these low-gravity L dwarfs remain unpublished but will be discussed in a future paper by Cruz and collaborators.

or 7.6±1.6%, for low-gravity field L dwarfs. Broken down by hemisphere, we find low-gravity fractions of 7/172 (4.1±1.5%) for Dec> 0° and 16/131 (12.2±3.1%) for Dec< 0°, confirming the north/south dichotomy seen in the smaller Kirkpatrick samples alone.

Are these empirical numbers in agreement with expectations? Both Allen et al. (2005) and Burgasser (2004c) provide predictions for the makeup of the low-mass star and brown dwarf populations in the Solar Neighborhood. The former paper uses Bayesian statistical methods to compute the mass and age distribution that best constructs the observed field luminosity function, using the evolutionary models of Burrows et al. (2001). The latter work uses Monte Carlo simulations on a range of plausible star formation rates and initial mass functions along with theoretical evolutinary models from Burrows et al. (1997) and Baraffe et al. (2003) to predict an array of possible outcomes for the makeup of the Solar Neighorhood. Both works demonstrated that L dwarfs are expected to be, on average, younger than M dwarfs or T dwarfs. Kinematic evidence supports this claim. Zapatero Osorio et al. (2007) measure U, V, W space motions and deduce that nearby L and T dwarfs appear to comprise a kinematically younger population, with ages in the likely interval 0.5-4 Gyr, than that of stars with types G through early-M.

The underlying reason for the relative youth of L dwarfs is the fact that they are comprised of two distinct populations. Some L dwarfs are actually low-mass stars, but theory predicts that the only "stellar" L dwarfs are those falling in a very restrictive mass range (∼0.072-0.085 $M_{\odot}$ according to the Baraffe et al. 1998, 2003 models; see figure 9.20 of Kirkpatrick 2008b). The rest of the L dwarfs are brown dwarfs that never settle onto a main sequence and continue to cool with time. Hence, the transitory nature of the "substellar" L dwarfs means that the only brown dwarfs seen at these spectral types are those that have not yet had sufficient time to cool into the T dwarf class.

To compare our observational data to predictions, we use evidence from previous sections that our ability to label an L dwarf spectrum as low gravity is indicative of the fact that the object has an age of ∼100 Myr or younger. The Allen et al. (2005) results predict that within a given volume of space there is a 3.1% probability of a field M6 dwarf being younger than 100 Myr. At type L0 this probability increases to 5.6%. At mid- to late-L this probability drops to 3.7% and plummets further to 2.1% for early-T and 1.6% for late-T. Burgasser (2004c) plots the median age as a function of effective temperature and shows that the median age is substantially lower in the early-L through mid-T dwarf regime than it is for late-M dwarfs or late-T dwarfs.

Such numbers are applicable to a complete volume-limited sample. Unfortunately, the Kirkpatrick samples are primarily limited by the depths of 2MASS, and the Cruz samples, which were designed to provide a complete census of L dwarfs within 20 pc of the Sun

using 2MASS data, used a sliding magnitude limit depending upon the J-K_s color of the object in 2MASS. In both the Cruz and Kirkpatrick et al. (2000) samples, late-L dwarfs were specifically targetted by using fainter magnitude limits for candidates with redder colors. As we have seen in §4.3, this biases our searches in favor of young, earlier L dwarfs at fainter magnitudes (and presumably larger distances) since these low-gravity objects tend to have redder J-K_s colors (see Figure 14).

Very young objects are not expected to be well mixed with older constituents of the Milky Way, so our all-sky total is the best metric to use for comparison. Our overall rate of 7.6±1.6% for L dwarfs with ages less than ∼100 Myr is in rough agreement with the Allen et al. (2005) predicted rate of 3.7-5.6% once the J-K_s color selection bias is considered. The difference between hemispheres is likely attributable to the fact that the southern sky has a preponderance of young, nearby associations, and our selection technique is particularly well tuned to find examples beyond the intended distance cutoff. We discuss more about these associations in the following section.

5.3. Are These Low-gravity Field Dwarfs Members of Known Young Associations?

Table 6 lists the low-gravity field dwarfs discussed above along with other low-gravity ultracool field dwarfs from other published work. This list contains 20 objects total. (Several other new, low-gravity discoveries not listed here will be discussed in Cruz et al. 2008.) The table gives the object name in column 1, the optical and near-infrared spectral type along with their references in columns 2-5, the 2MASS $J - K_s$ color and error in column 6, the discovery reference and reference pointing out the low-gravity nature of the object in columns 7-8, and notes on the diagnostics used for establishing low gravity in column 9. Given their implied youth and relative proximity to the Sun, could these objects be members of previously identified young stellar associations?

Figure 15 shows the locations of these 20 sources plotted on the celestial sphere. Plotted for comparison are the locations of members of the four young (<100 Myr), nearby (<60 pc) stellar associations currently recognized (Zuckerman & Song 2004) – the TW Hydrae Association (∼8 Myr), the β Pictoris Moving Group (∼12 Myr), the Tucana-Horologium Association (∼30 Myr), and the AB Doradus Moving Group (∼50 Myr). We have coded the symbols for each of the 20 sources so that those believed to have ages near 100 Myr are shown as solid stars and those believed to be substantially younger (∼10 Myr, as determined in §4.2 or from references in the literature) are shown as open stars.

This figure shows that some of these young, ultracool objects have sky locations and estimated ages similar to these known groups. The four known/suspected members of the TW Hydrae Association – SSSPM J1102−3431, 2MASS J1139−3159, 2MASS J1207−3932, and DENIS J1245−4429 – are obvious in the lower left portion of the figure. As noted in Kirkpatrick et al. (2006), 2MASS J0141−4633 has a sky location coincident with both the β Pictoris Moving Group and the Tucana/Horologium Association along with an estimated age range in agreement with both groups. Other very young candiates – 2MASS J0241−0326 and 2MASS 2213−2136 – have sky locations and assumed ages consistent with known members of the β Pictoris Moving Group.

Others appear to have sky locations and young ages inconsistent with membership in any of these known groups. Three northern hemisphere objects lying along an almost constant line of RA=10^h23^m fall in a part of the sky well separated from the other groups. All five of the young candidates with 16^h <RA< 24^h also lie in a part of the sky sparsely populated by known association members. Nonetheless, given the closeness of some of these nearby groups, our Solar System may fall near an edge or even within the true spatial volume of the association. In this case, members can fall almost anywhere on the sky and locations provide only weak constraints for individual objects. Kinematic and distance information is required to establish membership with certainty.

At the moment we have proper motions for only a few of these 20 objects. Trigonometric parallaxes and radial velocities are also needed so that distances and UVW space motions can be measured. Only then we can test for membership in known groups and see if there may be objects, particularly the northern ones, that may be hinting at the presence of heretofore unrecognized, young associations. Most intriguing is the possibility of uncovering young associations solely of low-mass stars, assuming such a mode of star formation can actually occur. We have begun some of this follow-up work and will report progress in forthcoming papers.

6. Analyzing the Lithium Results

A number of the newly acquired Keck-LRIS spectra from Figure 2 and Figure 4 show the 6708-Å line in absorption. Zooms of the 6300-7100 Å region of these eight spectra are shown in Figure 16. Equivalent width measurements or limits for all of the LRIS spectra are given in Table 3 through Table 5. As has been true in previous summaries, we do not detect the Li I line in any the late-M or T dwarfs at the ∼10 Å resolution we employ.

6.1. Lithium Absorption Strength as a Function of Spectral Type

Using the list of lithium detections along with the non-detections in Table 3 and Table 4, we can update the lithium statistics plot first presented as Figure 7 of Kirkpatrick et al. (2000). This update is shown in Figure 17. In the upper panel we show the measured Li I equivalent widths as a function of optical spectral type for all L dwarfs for which we have obtained LRIS spectra, now numbering 123 objects. The two panels below this encapsulate the statistical analysis of this distribution. In the middle panel is shown the percentage of L dwarfs with Li I detections of 3 Å or more as a function of optical type. Due to the increased sample of late-L dwarfs now available, we can now state confidently that there is a slight turnover at late-L in the fraction of objects with strong Li I lines. In fact, none of the T dwarfs for which we have optical spectra in Table 5 or those included in Burgasser et al. (2003a) show Li I, although their detection limits are generally worse than 3 Å equivalent width. This weakening of the Li I line is further demonstrated in the bottom panel of Figure 17, which shows as a function of type the equivalent width of those lines which are detected. After growing steadily from early-L through mid-L, these Li I strengths peak around L5.5-L6.5 then weaken for later types.

The peak in Li I strength at ∼L6 corresponds roughly to the temperatures where monatomic lithium is expected to disappear into molecular form (Lodders 1999). It should be kept in mind, however, that our Li I measurements are made against a relative continuum heavily influenced by wings of the strong Na I "D" doublet to the blue and strong K I doublet to the red. That having been said, Lodders (1999) shows that both Na and K are expected to disappear into molecular species (solid Na_2S and gaseous KCl) at temperatures much lower than this, so the abrupt change in Li I strength is probably not caused by modulations in the continuum opacity. Hence, the Li weakening can safely be attributed to the disappearance of monatomic lithium from the atmosphere. Lodders (1999) predicts that the culprit is the formation of LiCl gas. It should also be noted that lithium is expected to disappear in monatomic form before either cesium or rubidium does, again in agreement with our observations.

6.2. Lithium Absorption Strength as a Function of Age

We now have in hand a sufficiently large sample of L dwarfs spanning ranges in temperature and age that we can examine in detail the "second order" effect of Li I line strength versus age. To quantify this, we select four optical spectral types – L0, L2, L4, and L6.5 – where we have a good sampling across a wide span of ages. Objects in each of those bins can be divided into two sets: those with normal spectra and those with spectra that appear

peculiar because of low-gravity effects, as discussed in §4.2. Table 8 lists objects by spectral type (column 1), name (columns 2, 4, 6, and 8) and their Li I equivalent width measurements (columns 3, 5, 7, and 9). Dwarfs with normal, non-peculiar spectra are given in columns 2-5, with those showing no lithium in columns 2-3, and those with lithium in columns 4-5. Dwarfs exhibiting peculiar, low-gravity spectra are listed in columns 6-7, and those with very peculiar, low-gravity spectra are listed in columns 8-9. By dividing the columns in this way we are subdividing the spectra into empirical age bins. Normal spectra without detected Li I are expected to be high mass and old. Normal spectra with Li I are expected to be somewhat lower in mass, and because they have the same spectral type as the non-lithium dwarfs, must therefore be younger. Spectra exhibiting low-gravity features are expected to be younger still, and those showing the most peculiar features are expected to be of even lower gravity and the youngest of all.

We analyze each grouping in the table:

L0: We have optical spectra of six objects with normal L0 spectral types. There are five where no lithium line was detected, and two of these had no detection down to 0.5 Å equivalent width (EW). These are presumably the older, higher-mass L0's. The fifth normal L0 exhibits a Li I line with 3 Å EW. Presumably this object is younger and lower in mass than the others. We have optical spectra of an additional six L0's with unusual spectra. The three less peculiar ones, which we believe have an age near 100 Myr (in fact, one is a member of the Pleiades), show no Li I line. Two of these show no line down to at least 3 Å EW. The other objects, which we believe to have ages substantially less than 100 Myr based on discussion in §4.2, show no lines down to 2 Å EW or better. Figure 18 plots the highest-SNR spectrum from each of the four age bins. The inset is a zoom around the location of the 6708-Å Li I line to demonstrate how the Li strength varies as a function of age. Notice that the line when detectable is still very weak.

L2: We have optical spectra of twelve objects with normal L2 spectral types. There are nine with no Li I detection, with all but one of these having no measurable line down to 1 Å EW. The three other normal L2s have Li I detections of 1.7, 6, and 8 Å EW and are presumably younger and lower mass than the first nine. The object with the 1.7 Å EW detection is the binary Kelu-1 AB, for which Liu & Leggett (2005) estimate an age of 300-800 Myr. This object may be somewhat older than the other objects in its age bin because the detected lithium is presumed to come from the lower mass secondary, not from the primary itself. We also note three L2s whose spectra appear peculiar due to low gravity. All of these are believed to be ∼100 Myr old, and they have Li I EWs of 4 and 6 Å. No L2 dwarfs have yet been identified in the "Very Peculiar Dwarfs" category of Table 8. Figure 19 shows an example spectrum from each age bin. Appreciable Li I detections are seen in the two bins

of lowest age.

L4: We have optical spectra of six objects with normal L4 spectral types. Of these, five have no measurable Li I line, the most stringent limits being the 0.5 and 0.7 Å measures in the two objects with the highest signal-to-noise. One of these, GD 165B, is believed to have an age of 1.2-5.5 Gyr based on age estimates of its white dwarf primary (Kirkpatrick et al. 1999b). The other two normal L4s have measured EWs of 3.3 and 10.5 Å and presumably are younger and lower mass than the others. Additionally we have optical spectra of one peculiar L4 and one peculiar L4.5, which are assumed to be lower gravity than the normal L4s. The slightly peculiar L4.5, Gl 417B, is believed to have an age of 80-300 Myr based on age indicators from its G dwarf primary (Kirkpatrick et al. 2001), and it shows a Li I EW of 11.5 Å. Further complicating the interpretation of this spectrum is the fact that imaging by the Hubble Space Telescope hints that the B component itself is a double (Bouy et al. 2003). The other peculiar L4, 2MASS J1615+4953, has no Li I detection down to 8 Å EW but the SNR is poor and this object may be unusual because of excess dust and not because of low gravity, as stated in §4.2. No extremely peculiar L4 dwarfs are yet known, so the rightmost column in Table 8 is again blank. Figure 20 shows a spectrum for each of the other three age bins.

L6.5: We have optical spectra of six objects with normal L6.5 spectral types. Three of these do not show Li I, and two of these have stringent limits of at least <2 Å EW. The three other L6.5 spectra all show Li I. Two of these show a strong line of at least ∼12 Å EW. Although both appear to have normal spectra in the optical, 2MASS J2148+4003 has a strikingly unusual near-infrared spectrum whose oddities are likely due to excessive atmospheric dust (Looper et al. 2008). The final L6.5 spectrum, 2MASS J2244+2043, shows a weaker Li I line of only ∼5 Å EW. Although its optical spectrum appears normal, we place it in the "peculiar" bin only because its near-infrared spectrum show odd features that are best attributed to low gravity (McLean et al. 2003). No L6.5 objects are known that might occupy the rightmost columns of the table. Figure 21 depicts these results graphically, with insets showing the range in Li I EW.

To summarize, the true strength of Li I line as a function of age is difficult to interpret from the extant data for several reasons: (1) Many of the age bins in Table 8 are sparsely populated so conclusions are based on poor statistics; (2) both known and unrecognized binarity makes the interpretation of even well measured lines difficult as it is not known *a priori* what the relative contributions to the line strength are from the primary and the secondary; (3) some of these spectra have SNR levels that are too low at 6708 Å to obtain accurate EW measurements. For now, we see evidence indicating that the Li I line weakens markedly for the youngest ages, but the most important tests of this – the very peculiar

L dwarfs of lowest gravity – have not yet been identified for types later than ∼L0. High signal-to-noise spectra of additional low-gravity field L dwarfs, such as those to be discussed in Cruz et al. 2008, and confirmed L dwarf members of young clusters are needed to bolster the statistics.

6.3. Comparison to Theory

Theory stipulates that objects below ∼60 M_{Jup} will never reach the lithium fusion temperature of ∼2×10^6K, so they will always retain their primordial complement of lithium. Objects of higher mass easily destroy their lithium, which is not produced as a byproduct of normal thermonuclear reactions in the cores of stars and brown dwarfs. Therefore, the absence of lithium can be used as a direct test of substellarity, as first proposed by Rebolo et al. (1992). Chabrier et al. (1996) calculated that brown dwarfs with masses of 60 M_{Jup} will have depleted their stores of lithium by a factor of two in 250 Myr and by a factor of one hundred in 1 Gyr. Higher mass objects burn up the lithium more quickly, a 70 M_{Jup} object reducing its store by a factor of two in 130 Myr and by a factor of one hundred in 220 Myr. An 80 M_{Jup} object accomplishes these same feats in 90 and 140 Myr, respectively.

Complete lithium destruction occurs because these objects spend the first portion of their lives as M dwarfs, where they are fully convective and fully mixed. Therefore, material in the upper atmosphere of the object eventually circulates to the core where lithium burning can take place. All brown dwarfs with masses above 60 M_{Jup} are expected to go through the fully convective mid- to late-M dwarf regime (see evolutionary tracks in Figures 8 and 9 of Burrows et al. 1997), residing there for at least the first ∼400 Myr of their lives, then they evolve to lower temperatures where they may no longer be convective. This allows plenty of time for the depletion to have occurred, according to the models.

However, retaining a primordial abundance of lithium and being able to detect that lithium observationally in the spectrum are two different issues. There are two regimes where the lithium test may have to be amended. The first concerns objects of very cool temperature. We have already observed that the equivalent width of the Li I line at 6708 Å diminishes on average at types later than ∼L6, presumably due to the formation of lithium-bearing molecules at colder temperatures. The second concerns objects of very low gravity. As first mentioned in Kirkpatrick et al. (2006) the lithium test should also be carefully considered before being applied to brown dwarfs of very young age. The reason for this is the expected (and observed) weakening of the other alkali lines as gravity is diminished; the Li I line is expected to weaken too, thus making the lithium test more difficult to use in this regime. We derived a test of this using empirical data in §5.2, but results were inconclusive.

Do atmospheric models of L dwarfs predict a weakening of the Li I line? Figure 22 shows the behavior of models[9] at three different temperatures as gravity is lowered. It should be noted that interior physics, such as the destruction of lithium by convection toward the core, is not included in these simulations; the total lithium abundance is held fixed so that the behavior of the line is due solely to atmospheric chemistry and physics. In the 2400K models, corresponding roughly to an optical type of L0 (see §9.4.1 of Kirkpatrick 2008b), the Li I line is seen only at the highest gravities and disappears entirely by log(g)=5.0 at the resolution (10 Å) shown here. At 2100K, corresponding to an optical type of L2, the Li I line weakens and then vanishes around log(g)=4.0. At 1800K, corresponding to types L4-4.5, the line weakens throughout the gravity sequence and vanishes only at log(g)=2.5.

In conclusion, we find that theory predicts the weakening of the Li I line at lower gravities, an effect supported (albeit weakly) by current observational data. Although additional optical spectra of L dwarfs covering a wide range of gravities/ages are needed to bolster the empirical evidence, predictions nonetheless bear out the caveat addressed by Kirkpatrick et al. (2006) in their study of 2MASS J0141−4633. Namely, they suggested that researchers apply the lithium test with caution for very young brown dwarfs because the Li I line is expected to be considerably weaker and may, in fact, be undetectable at moderate resolution in those objects.

7. Summary

Using a large set of optical specta, we have shown that a subset of objects with peculiar spectra can be identified as low-gravity brown dwarfs. Low gravity is a hallmark of youth, as these objects have lower masses and more extended atmospheres than higher mass, older field dwarfs. We find that the observed percentage of young (<100 Myr old) L dwarfs in our sample – 7.6±1.6% – is consistent with theoretical predictions once selection biases are considered. Even though low gravity enables these young objects to be identified readily via spectroscopy, it complicates the brown dwarf "lithium test" because it weakens the observable Li I line for a given lithium abundance and spectral type. Our sample of young brown dwarfs

[9]These synthetic spectra, which are updated versions of those from Allard et al. (2001), have been computed with version 15 of the `PHOENIX` model atmosphere code. These models incorporate numerous updates including but not limited to the use of the new Barber et al. (2006) water line list and the hydride line lists from Dulick et al. (2003) and Burrows et al. (2002). The lithium abundance was set to the Lodders (2003) recommended value of A(Li) = 3.28 (where A(H) = 12.0); all other elemental abundances where set to those of Asplund et al. (2005). Cloud and cloud-free scenarios were modeled in the standard "Cond" and "Dusty" approaches of Allard et al. 2003.

is found to lie primarily in the southern hemisphere, which (probably not coincidentally) is the location of known, nearby young associations. Further work on these young objects is needed to establish or refute membership in these groups.

We would like to thank Peter Allen for useful discussions on his 2005 paper. We would like to thank the staff at the W. M. Keck Observatory for their help in acquiring the LRIS data: observing assistants Joel Aycock, Gary Puniwai, Julie Rivera, Gabrelle Saurage, and Cynthia Wilburn as well as instrument specialists Paola Amico, Randy Campbell, Bob Goodrich, Grant Hill, Marc Kassis, and Greg Wirth. We would also like to thank the staff at the Subaru Telescope for their guidance in taking and reducing the FOCAS spectra: telescope operators Alan Hatakeyama and Robert Potter along with FOCAS support astronomer Takashi Hattori. We further wish to recognize and acknowledge the very significant cultural role and reverence that the summit of Mauna Kea has always had within the indigenous Hawaiian community. We are most fortunate to have the opportunity to conduct observations from this mountain. This publication makes use of data products from the Two Micron All Sky Survey, which is a joint project of the University of Massachusetts and the Infrared Processing and Analysis Center/California Institute of Technology, funded by the National Aeronautics and Space Administration and the National Science Foundation. This research has made use of the NASA/IPAC Infrared Science Archive, which is operated by the Jet Propulsion Laboratory, California Institute of Technology, under contract with the National Aeronautics and Space Administration. The finder charts in Figure 1 were generating using the mosaicking service available at http://hachi.ipac.caltech.edu:8080/montage/. Our research has benefitted from the M, L, and T dwarf compendium housed at DwarfArchives.org whose server was funded by a NASA Small Research Grant, administered by the American Astronomical Society.

REFERENCES

Allard, F., Guillot, T., Ludwig, H.-G., Hauschildt, P. H., Schweitzer, A., Alexander, D. R., & Ferguson, J. W. 2003, Brown Dwarfs, 211, 325.

Allard, F., Hauschildt, P. H., Alexander, D. R., Tamanai, A., & Schweitzer, A. 2001, ApJ, 556, 357.

Allen, P. R., Koerner, D. W., Reid, I. N., & Trilling, D. E. 2005, ApJ, 625, 385.

Asplund, M., Grevesse, N., & Sauval, A. J. 2005, Cosmic Abundances as Records of Stellar Evolution and Nucleosynthesis, 336, 25.

Bannister, N. P., & Jameson, R. F. 2007, MNRAS, 378, L24.

Barrado y Navascués, D. 2006, A&A, 459, 511.

Barrado y Navascués, D., Béjar, V. J. S., Mundt, R., Martín, E. L., Rebolo, R., Zapatero Osorio, M. R., & Bailer-Jones, C. A. L. 2003, A&A, 404, 171.

Barrado y Navascués, D., Zapatero Osorio, M. R., Béjar, V. J. S., Rebolo, R., Martín, E. L., Mundt, R., & Bailer-Jones, C. A. L. 2001, A&A, 377, L9.

Baraffe, I., Chabrier, G., Barman, T. S., Allard, F., & Hauschildt, P. H. 2003, A&A, 402, 701.

Baraffe, I., Chabrier, G., Allard, F., & Hauschildt, P. H. 1998, A&A, 337, 403.

Barber, R. J., Tennyson, J., Harris, G. J., & Tolchenov, R. N. 2006, MNRAS, 368, 1087/

Basri, G. 1998, Brown Dwarfs and Extrasolar Planets, 134, 394.

Bildsten, L., Brown, E. F., Matzner, C. D., & Ushomirsky, G. 1997, ApJ, 482, 442.

Borysow, A., Jorgensen, U. G., & Zheng, C. 1997, A&A, 324, 185.

Bouy, H., Brandner, W., Martín, E. L., Delfosse, X., Allard, F., & Basri, G. 2003, AJ, 126, 1526.

Burgasser, A. J., Looper, D. L., Kirkpatrick, J. D., Cruz, K. L., & Swift, B. J. 2008, ApJ, 674, 451.

Burgasser, A. J., Geballe, T. R., Leggett, S. K., Kirkpatrick, J. D., & Golimowski, D. A. 2006c, ApJ, 637, 1067.

Burgasser, A. J., Kirkpatrick, J. D., Cruz, K. L., Reid, I. N., Leggett, S. K., Liebert, J., Burrows, A., Brown, M. E. 2006, ApJS, 166, 585.

Burgasser, A. J., Burrows, A., & Kirkpatrick, J. D. 2006, ApJ, 639, 1095.

Burgasser, A. J., Reid, I. N., Leggett, S. K., Kirkpatrick, J. D., Liebert, J., & Burrows, A. 2005, ApJ, 634, L177.

Burgasser, A. J., Kirkpatrick, J. D., & Lowrance, P. J. 2005, AJ, 129, 2849.

Burgasser, A. J., McElwain, M. W., Kirkpatrick, J. D., Cruz, K. L., Tinney, C. G., & Reid, I. N. 2004, AJ, 127, 2856.

Burgasser, A. J. 2004, ApJS, 155, 191.

Burgasser, A. J., Kirkpatrick, J. D., Liebert, J., & Burrows, A. 2003a, ApJ, 594, 510.

Burgasser, A. J., et al. 2003b, ApJ, 592, 1186.

Burgasser, A. J., et al. 2002, ApJ, 564, 421.

Burgasser, A. J., Kirkpatrick, J. D., Reid, I. N., Liebert, J., Gizis, J. E., & Brown, M. E. 2000, AJ, 120, 473.

Burke, C. J., Pinsonneault, M. H., & Sills, A. 2004, ApJ, 604, 272.

Burrows, A., Ram, R. S., Bernath, P., Sharp, C. M., & Milsom, J. A. 2002, ApJ, 577, 986.

Burrows, A., et al. 1997, ApJ, 491, 856.

Burrows, A., Hubbard, W. B., Lunine, J. I., & Liebert, J. 2001, Reviews of Modern Physics, 73, 719.

Chabrier, G., Baraffe, I., & Plez, B. 1996, ApJ, 459, L91.

Chauvin, G., et al. 2005, A&A, 438, L29.

Chauvin, G., Lagrange, A.-M., Dumas, C., Zuckerman, B., Mouillet, D., Song, I., Beuzit, J.-L., & Lowrance, P. 2004, A&A, 425, L29.

Chiu, K., Fan, X., Leggett, S. K., Golimowski, D. A., Zheng, W., Geballe, T. R., Schneider, D. P., & Brinkmann, J. 2006, ArXiv Astrophysics e-prints, arXiv:astro-ph/0601089.

Cruz, K. L., Kirkpatrick, J. D., & Burgassser, A. J. 2008, in prep.

Cruz, K. L., et al. 2007, AJ, 133, 439.

Cruz, K. L., Burgasser, A. J., Reid, I. N., & Liebert, J. 2004, ApJ, 604, L61.

Cruz, K. L., Reid, I. N., Liebert, J., Kirkpatrick, J. D., & Lowrance, P. J. 2003, AJ, 126, 2421.

Cutri, R. M., et al. 2003, The IRSA 2MASS All-Sky Point Source Catalog, NASA/IPAC Infrared Science Archive. http://irsa.ipac.caltech.edu/applications/Gator/.

Dahn, C. C., et al. 2002, AJ, 124, 1170.

Deacon, N. R., Hambly, N. C., & Cooke, J. A. 2005, A&A, 435, 363.

Delfosse, X., et al. 1997, A&A, 327, L25.

Delfosse, X., Tinney, C. G., Forveille, T., Epchtein, N., Borsenberger, J., Fouqué, P., Kimeswenger, S., & Tiphène, D. 1999, A&AS, 135, 41.

Dulick, M., Bauschlicher, C. W., Jr., Burrows, A., Sharp, C. M., Ram, R. S., & Bernath, P. 2003, ApJ, 594, 651.

Fuhrmeister, B., Schmitt, J. H. M. M., & Hauschildt, P. H. 2005, A&A, 439, 1137.

Garrison, R. F. 1995, PASP, 107, 507.

Geballe, T. R., et al. 2002, ApJ, 564, 466.

Gizis, J. E., Reid, I. N., Knapp, G. R., Liebert, J., Kirkpatrick, J. D., Koerner, D. W., & Burgasser, A. J. 2003, AJ, 125, 3302.

Gizis, J. E. 2002, ApJ, 575, 484.

Gizis, J. E., Monet, D. G., Reid, I. N., Kirkpatrick, J. D., Liebert, J., & Williams, R. J. 2000, AJ, 120, 1085.

Hall, P. B. 2002, ApJ, 580, L77.

Hall, P. B. 2002, ApJ, 564, L89.

Hamuy, M., Suntzeff, N. B., Heathcote, S. R., Walker, A. R., Gigoux, P., & Phillips, M. M. 1994, PASP, 106, 566.

Hawley, S. L., et al. 2002, AJ, 123, 3409.

Irwin, M., McMahon, R. G., & Reid, N. 1991, MNRAS, 252, 61P.

Jameson, R. F., Casewell, S. L., Bannister, N. P., Lodieu, N., Keresztes, K., Dobbie, P. D., & Hodgkin, S. T. 2008, ArXiv e-prints, 710, arXiv:0710.4786.

Jeffries, R. D., & Naylor, T. 2001, From Darkness to Light: Origin and Evolution of Young Stellar Clusters, 243, 633.

Kendall, T. R., Mauron, N., Azzopardi, M., & Gigoyan, K. 2003, A&A, 403, 929.

Kendall, T. R., Delfosse, X., Martín, E. L., & Forveille, T. 2004, A&A, 416, L17.

Kirkpatrick, J. D., & McCarthy, D. W. 1994, AJ, 107, 333.

Kirkpatrick, J. D., et al. 1999a, ApJ, 519, 802.

Kirkpatrick, J. D., Allard, F., Bida, T., Zuckerman, B., Becklin, E. E., Chabrier, G., & Baraffe, I. 1999, ApJ, 519, 834.

Kirkpatrick, J. D., et al. 2000, AJ, 120, 447.

Kirkpatrick, J. D., Dahn, C. C., Monet, D. G., Reid, I. N., Gizis, J. E., Liebert, J., & Burgasser, A. J. 2001, AJ, 121, 3235.

Kirkpatrick, J. D. 2005, ARA&A, 43, 195.

Kirkpatrick, J. D., Barman, T. S., Burgasser, A. J., McGovern, M. R., McLean, I. S., Tinney, C. G., & Lowrance, P. J. 2006, ApJ, 639, 1120.

Kirkpatrick, J. D. 2008, 14th Cambridge Workshop on Cool Stars, Stellar Systems, and the Sun, 384, 85.

Kirkpatrick, J. D. 2008b, *M Dwarfs and L Dwarfs*, Chapter 9 of *Stellar Spectral Classification* by Richard Gray & Christopher Corbally, Princeton University Press, in press.

Knapp, G. R., et al. 2004, AJ, 127, 3553.

Leggett, S. K., et al. 2000, ApJ, 536, L35.

Liebert, J., Kirkpatrick, J. D., Cruz, K. L., Reid, I. N., Burgasser, A., Tinney, C. G., & Gizis, J. E. 2003, AJ, 125, 343.

Liebert, J., Kirkpatrick, J. D., Reid, I. N., & Fisher, M. D. 1999, ApJ, 519, 345.

Liu, M. C., & Leggett, S. K. 2005, ApJ, 634, 616.

Lodders, K. 2003, ApJ, 591, 1220.

Lodders, K. 2002, ApJ, 577, 974.

Lodders, K. 1999, ApJ, 519, 793.

Lodieu, N., Scholz, R.-D., McCaughrean, M. J., Ibata, R., Irwin, M., & Zinnecker, H. 2005, A&A, 440, 1061.

Looper, D. L., Burgasser, A. J., Kirkpatrick, J. D., & Swift, B. J. 2007, ApJ, 669, L97.

Looper, D. L., Kirkpatrick, J. D., et al., 2008, soon to be submitted.

Lucas, P. W., Roche, P. F., Allard, F., & Hauschildt, P. H. 2001, MNRAS, 326, 695.

Luhman, K. L., Liebert, J., & Rieke, G. H. 1997, ApJ, 489, L165.

Luhman, K. L., Briceno, C., Rieke, G. H., & Hartmann, L. 1998, ApJ, 493, 909.

Luyten, W. 1980, Minneapolis: University of Minnesota, 1980, NLTT Catalog, Vol. III-IV.

Martín, E. L., Delfosse, X., Basri, G., Goldman, B., Forveille, T., & Zapatero Osorio, M. R. 1999, AJ, 118, 2466.

Martín, E. L., Basri, G., & Zapatero Osorio, M. R. 1999, AJ, 118, 1005.

Martín, E. L., Basri, G., Zapatero-Osorio, M. R., Rebolo, R., & López, R. J. G. 1998, ApJ, 507, L41.

Martín, E. L., Rebolo, R., & Zapatero-Osorio, M. R. 1996, ApJ, 469, 706.

Mazzei, P., & Pigatto, L. 1989, A&A, 213, L1.

McCaughrean, M. J., Close, L. M., Scholz, R.-D., Lenzen, R., Biller, B., Brandner, W., Hartung, M., & Lodieu, N. 2004, A&A, 413, 1029.

McGovern, M. R., Kirkpatrick, J. D., McLean, I. S., Burgasser, A. J., Prato, L., & Lowrance, P. J. 2004, ApJ, 600, 1020.

McLean, I. S., McGovern, M. R., Burgasser, A. J., Kirkpatrick, J. D., Prato, L., & Kim, S. S. 2003, ApJ, 596, 561.

Mermilliod, J. C. 1981, A&A, 97, 235.

Meynet, G., Mermilliod, J.-C., & Maeder, A. 1993, A&AS, 98, 477.

Monet, D. G., et al. 2003, AJ, 125, 984.

Morgan, W. W., Keenan, P. C., & Kellman, E. 1943, Chicago, Ill., The University of Chicago press [1943].

Nakajima, T., Tsuji, T., & Yanagisawa, K. 2004, ApJ, 607, 499.

Nelson, L. A., Rappaport, S., & Chiang, E. 1993, ApJ, 413, 364.

Neuhäuser, R., Guenther, E. W., Wuchterl, G., Mugrauer, M., Bedalov, A., & Hauschildt, P. H. 2005, A&A, 435, L13.

Oke, J. B., et al. 1995, PASP, 107, 375.

Perryman, M. A. C., et al. 1997, A&A, 323, L49.

Phan-Bao, N., et al. 2003, A&A, 401, 959.

Pozio, F. 1991, Memorie della Societa Astronomica Italiana, 62, 171.

Rebolo, R., Zapatero Osorio, M. R., Madruga, S., Bejar, V. J. S., Arribas, S., & Licandro, J. 1998, Science, 282, 1309.

Rebolo, R., Zapatero-Osorio, M. R., & Martin, E. L. 1995, Nature, 377, 129.

Rebolo, R., Martin, E. L., & Magazzu, A. 1992, ApJ, 389, L83.

Reid, I. N., Cruz, K. L., Kirkpatrick, J. D., Allen, P. R., Mungall, F., Liebert, J., Lowrance, P., & Sweet, A. 2008, ArXiv e-prints, 806, arXiv:0806.3413.

Reid, I. N., Kirkpatrick, J. D., Gizis, J. E., Dahn, C. C., Monet, D. G., Williams, R. J., Liebert, J., & Burgasser, A. J. 2000, AJ, 119, 369.

Riaz, B., & Gizis, J. E. 2007, ApJ, 659, 675.

Ruiz, M. T., Leggett, S. K., & Allard, F. 1997, ApJ, 491, L107.

Savage, A., Bolton, J. G., & Wright, A. E. 1976, MNRAS, 175, 517.

Schmidt, S. J., Cruz, K. L., Bongiorno, B. J., Liebert, J., & Reid, I. N. 2007, AJ, 133, 2258.

Schneider, D. P., et al. 2002, AJ, 123, 458.

Scholz, R.-D., McCaughrean, M. J., Zinnecker, H., & Lodieu, N. 2005, A&A, 430, L49.

Seifahrt, A., Guenther, E., & Neuhäuser, R. 2005, A&A, 440, 967.

Skrutskie, M. F., et al. 2006, AJ, 131, 1163.

Stauffer, J. R., Schultz, G., & Kirkpatrick, J. D. 1998, ApJ, 499, L199.

Stauffer, J. R., et al. 1999, ApJ, 527, 219.

Stauffer, J. R., et al. 2007, ApJS, 172, 663.

Steele, I. A., & Jameson, R. F. 1995, MNRAS, 272, 630.

Thorstensen, J. R., & Kirkpatrick, J. D. 2003, PASP, 115, 1207.

Totten, E. J., & Irwin, M. J. 1998, MNRAS, 294, 1.

Ventura, P., Zeppieri, A., Mazzitelli, I., & D'Antona, F. 1998, A&A, 334, 953.

Vrba, F. J., et al. 2004, AJ, 127, 2948.

West, A. A., et al. 2004, AJ, 128, 426.

West, A. A., Hawley, S. L., Bochanski, J. J., Covey, K. R., Reid, I. N., Dhital, S., Hilton, E. J., & Masuda, M. 2008, AJ, 135, 785

Wilson, J. C., Kirkpatrick, J. D., Gizis, J. E., Skrutskie, M. F., Monet, D. G., & Houck, J. R. 2001, AJ, 122, 1989.

Wilson, J. C., Miller, N. A., Gizis, J. E., Skrutskie, M. F., Houck, J. R., Kirkpatrick, J. D., Burgasser, A. J., & Monet, D. G. 2003, IAU Symposium, 211, 197.

Zapatero Osorio, M. R., Martín, E. L., Béjar, V. J. S., Bouy, H., Deshpande, R., & Wainscoat, R. J. 2007, ApJ, 666, 1205

Zapatero Osorio, M. R., Béjar, V. J. S., Martín, E. L., Rebolo, R., Barrado y Navascués, D., Bailer-Jones, C. A. L., & Mundt, R. 2000, Science, 290, 103.

Zapatero Osorio, M. R., Béjar, V. J. S., Rebolo, R., Martín, E. L., & Basri, G. 1999, ApJ, 524, L115.

Zapatero Osorio, M. R., Rebolo, R., Martin, E. L., Basri, G., Magazzu, A., Hodgkin, S. T., Jameson, R. F., & Cossburn, M. R. 1997, ApJ, 491, L81.

Zuckerman, B., & Song, I. 2004, ARA&A, 42, 685

Table 1. List of L Dwarf Candidates

2MASS designation[c] (1)	J mag (2)	H mag (3)	K_s mag (4)	$J-K_s$ color (5)	Opt. Sp. Type (6)	Type Ref. (7)	Discovery Ref. (8)	Other designation (9)
Confirmed Late-M and L Dwarfs								
2MASS J00145575−4844171	14.050±0.035	13.107±0.036	12.723±0.030	1.327±0.046	L2.5 pec	1	1	
2MASS J00165953−4056541	15.316±0.061	14.206±0.048	13.432±0.038	1.884±0.072	L3.5	1	1	
2MASS J00242463−0158201	11.992±0.035	11.084±0.022	10.539±0.023	1.453±0.042	M9.5	2	20, 21	BRI 0021−0214
2MASS J00332386−1521309	15.286±0.056	14.208±0.051	13.410±0.039	1.876±0.068	L2 pec	1	3	
2MASS J00511078−1544169	15.277±0.050	14.164±0.048	13.466±0.039	1.811±0.063	L3.5	4	4	
2MASS J00531899−3631102	14.445±0.026	13.480±0.031	12.937±0.029	1.508±0.039	L3.5	1	1	
2MASS J00584253−0651239	14.311±0.026	13.444±0.030	12.904±0.033	1.407±0.042	L0	4	4	
2MASS J01174748−3403258	15.178±0.036	14.209±0.039	13.489±0.037	1.689±0.052	L2:	5	5	
2MASS J01415823−4633574	14.832±0.043	13.875±0.026	13.097±0.032	1.735±0.054	L0 pec	24	24	
2MASS J01443536−0716142	14.191±0.026	13.008±0.029	12.268±0.023	1.923±0.035	L5	1	6	
2MASS J02052940−1159296	14.587±0.030	13.568±0.037	12.998±0.030	1.589±0.042	L7	2	7	DENIS−P J0205.4−1159
2MASS J02511490−0352459	13.059±0.027	12.254±0.024	11.662±0.019	1.397±0.033	L3	5	5	
2MASS J02550357−4700509	13.246±0.027	12.204±0.024	11.558±0.024	1.688±0.036	L8	1	8	DENIS−P J0255−4700
2MASS J02572581−3105523	14.672±0.039	13.518±0.032	12.876±0.032	1.796±0.050	L8	1	1	
2MASS J03185403−3421292	15.569±0.055	14.346±0.044	13.507±0.039	2.062±0.067	L7	1	1	
2MASS J03370359−1758079	15.621±0.058	14.412±0.050	13.581±0.041	2.040±0.071	L4.5	4	4	
2MASS J03572695−4417305	14.367±0.032	13.531±0.026	12.907±0.027	1.460±0.042	L0 pec	1	9	DENIS-P J035726.9−441730
2MASS J04082905−1450334	14.222±0.030	13.337±0.030	12.817±0.023	1.405±0.038	L2	5	26	
2MASS J04234858−0414035	14.465±0.027	13.463±0.035	12.929±0.034	1.536±0.043	L7.5	1	10, 23	SDSSp J042348.57−041403.5
2MASS J04285096−2253227	13.507±0.023	12.668±0.027	12.118±0.026	1.389±0.035	L0.5	11	11	
2MASS J04390101−2353083	14.408±0.029	13.409±0.029	12.816±0.023	1.592±0.037	L6.5	5	5	
2MASS J04433761+0002051	12.507±0.026	11.804±0.024	11.216±0.021	1.291±0.033	M9 pec	1	25	SDSS J044337.61+000205.1
2MASS J04455387−3048204	13.393±0.026	12.580±0.024	11.975±0.021	1.418±0.033	L2	5	5	
2MASS J04532647−1751543	15.142±0.035	14.060±0.035	13.466±0.035	1.676±0.049	L3:	5	5	
2MASS J05120636−2949540	15.463±0.057	14.156±0.048	13.285±0.042	2.178±0.071	L4.5	1	5	
2MASS J05233822−1403022	13.084±0.024	12.220±0.021	11.638±0.027	1.446±0.036	L2.5	5	5	
2MASS J05264348−4455455	14.082±0.033	13.307±0.028	12.705±0.027	1.377±0.043	M9.5	1	1	
2MASS J09095749−0658186	13.890±0.024	13.090±0.021	12.539±0.026	1.351±0.035	L0	1	12	DENIS−P J0909−0658
2MASS J09532126−1014205	13.469±0.028	12.644±0.027	12.142±0.022	1.327±0.036	L0:	13	13	
2MASS J10101480−0406499	15.508±0.059	14.385±0.037	13.619±0.046	1.889±0.075	L6	5	5	
2MASS J10452400−0149576	13.160±0.024	12.352±0.025	11.780±0.023	1.380±0.033	L1	14	14	

Table 1—Continued

2MASS designation[c] (1)	J mag (2)	H mag (3)	K_s mag (4)	$J-K_s$ color (5)	Opt. Sp. Type (6)	Type Ref. (7)	Discovery Ref. (8)	Other designation (9)
2MASS J10584787−1548172	14.155±0.035	13.226±0.025	12.532±0.029	1.623±0.045	L3	2	7	DENIS−P J1058.7−1548
2MASS J11544223−3400390	14.195±0.033	13.331±0.028	12.851±0.033	1.344±0.047	L0	1	1	
2MASS J12130336−0432437	14.683±0.035	13.648±0.025	13.014±0.030	1.669±0.046	L5	5	5	
2MASS J12185957−0550282	14.050±0.027	13.327±0.024	12.780±0.030	1.270±0.040	M8	1	5	
2MASS J12281523−1547342	14.378±0.030	13.347±0.032	12.767±0.030	1.611±0.042	L5	2	7	DENIS−P J1228.2−1547
2MASS J13054019−2541059	13.414±0.026	12.392±0.025	11.747±0.023	1.667±0.035	L2	2	15	Kelu−1
2MASS J14090310−3357565	14.248±0.026	13.424±0.033	12.865±0.029	1.383±0.039	L2	1	1	
2MASS J14413716−0945590	14.020±0.029	13.190±0.031	12.661±0.030	1.359±0.042	L0.5	1	8	DENIS-P J1441−0945; G 124-62B[a]
2MASS J15074769−1627386	12.830±0.027	11.895±0.024	11.312±0.026	1.518±0.037	L5	16	16	
2MASS J15394189−0520428	13.922±0.029	13.060±0.026	12.575±0.029	1.347±0.041	L4:[b]	1	22	DENIS-P J153941.96−052042.4
2MASS J16184503−1321297	14.247±0.024	13.402±0.026	12.920±0.026	1.327±0.035	L0:	1	1	
2MASS J16202614−0416315	15.283±0.049	14.348±0.040	13.598±0.038	1.685±0.062	L2.5	17	17	Gl 618.1B
2MASS J20575409−0252302	13.121±0.024	12.268±0.024	11.724±0.025	1.397±0.035	L1.5	1	5	
2MASS J21041491−1037369	13.841±0.029	12.975±0.025	12.369±0.024	1.472±0.038	L2.5	1	5	
2MASS J21073169−0307337	14.200±0.032	13.443±0.031	12.878±0.030	1.322±0.044	sd:M9	1	5	
2MASS J21304464−0845205	14.137±0.032	13.334±0.032	12.815±0.033	1.322±0.046	L1.5	1	1	
2MASS J21580457−1550098	15.040±0.040	13.867±0.033	13.185±0.036	1.855±0.054	L4:	1	1	
2MASS J22064498−4217208	15.555±0.066	14.447±0.061	13.609±0.055	1.946±0.086	L2	4	4	
2MASS J22244381−0158521	14.073±0.027	12.818±0.026	12.022±0.023	2.051±0.035	L4.5	4	4	
2MASS J23440624−0733282	14.802±0.037	13.846±0.035	13.232±0.033	1.570±0.050	L4.5	1	1	
			Objects Confirmed as Other Types					
2MASS J01241236−4537057	13.410±0.029	12.493±0.026	12.076±0.026	1.334±0.039	M giant	1	-	
2MASS J01343566−0931030	16.187±0.131	14.793±0.074	13.579±0.055	2.608±0.142	carbon star	1	-	
2MASS J04475750−0553241	13.789±0.029	12.441±0.032	11.734±0.019	2.055±0.035	reddened	1	-	(early type, reddened star)
2MASS J10152592−0204318	14.050±0.027	12.866±0.025	11.946±0.026	2.104±0.037	carbon star	1	-	
2MASS J12274004−0027506	12.757±0.024	11.513±0.021	10.545±0.023	2.212±0.033	carbon star	18	-	FASTT 542
2MASS J12562145−0811144	11.317±0.024	10.426±0.024	9.994±0.021	1.323±0.032	M giant	1	-	
2MASS J13414737−0813470	12.872±0.024	11.813±0.021	11.444±0.026	1.428±0.035	M giant	1	-	
2MASS J13451789−0829573	15.622±0.068	14.165±0.039	12.822±0.027	2.800±0.073	QSO	1	1	(redshift z=0.57)
2MASS J13592063−3023395	14.613±0.033	13.081±0.028	11.820±0.025	2.793±0.041	carbon star	14	-	
2MASS J14322874−0531178	13.989±0.028	12.531±0.023	11.240±0.021	2.749±0.035	carbon star	18	-	

Table 1—Continued

2MASS designation[c] (1)	J mag (2)	H mag (3)	K_s mag (4)	$J-K_s$ color (5)	Opt. Sp. Type (6)	Type Ref. (7)	Discovery Ref. (8)	Other designation (9)
2MASS J15010693−0531388	13.588±0.026	12.391±0.021	11.498±0.021	2.090±0.033	carbon star	5	-	
2MASS J15151106−1332278	12.599±0.026	11.511±0.023	10.795±0.021	1.804±0.033	carbon star	14	-	
2MASS J15514921−0750489	16.867±0.181	15.080±0.072	13.533±0.042	3.334±0.186	carbon star	1	-	
2MASS J16014265−1249447	14.416±0.029	13.105±0.029	12.382±0.029	2.034±0.041	carbon star	1	-	
2MASS J20135152−2806020	14.242±0.030	13.461±0.028	12.944±0.027	1.298±0.040	M8-9 III	1	-	
2MASS J21001879−0606550	15.306±0.045	13.557±0.025	12.073±0.021	3.233±0.050	carbon star	1	-	
2MASS J22351322−4835588	13.809±0.029	12.949±0.029	12.124±0.026	1.685±0.039	QSO	-	19	

Note. — Spectral type and discovery references are (1) this paper, (2) Kirkpatrick et al. 1999a, (3) Gizis et al. 2003, (4) Kirkpatrick et al. 2000, (5) Cruz et al. 2003, (6) Liebert et al. 2003, (7) Delfosse et al. 1997, (8) Martín et al. 1999a, (9) Bouy et al. 2003, (10) Geballe et al. 2002, (11) Kendall et al. 2003, (12) Delfosse et al. 1999, (13) Cruz et al. 2007, (14) Gizis 2002, (15) Ruiz et al. 1997, (16) Reid et al. 2000, (17) Wilson et al. 2001, (18) Totten & Irwin 1998, (19) Savage et al. 1976, (20) Luyten 1980, (21) Irwin et al. 1991, (22) Kendall et al. 2004, (23) Schneider et al. 2002, (24) Kirkpatrick et al. 2006, (25) Hawley et al. 2002, (26) Wilson et al. 2003.

[a]Common proper motion for DENIS-P J1441−0945 and G 124-62A confirmed by Seifahrt et al. (2005).

[b]DENIS J1539−0520 is typed in the optical as L3.5 by Reid et al. (2008).

[c]Source designations for 2MASS discoveries are given as "2MASx Jhhmmss[.]ss±ddmmss[.]s". The "x" in the prefix will vary depending upon the catalog from which the object was discovered: "S" is used for objects from the 2MASS All-Sky Point Source Catalog, "SW" is used for objects taken from the Survey Point Source Working Database, "Ss" is used for objects taken from the 2MASS Sampler Point Source Catalog, "P" is used for objects discovered in the prototype data. The suffix is the sexigesimal Right Ascension and Declination at J2000 equinox.

Table 2. Nights of Observation at Keck

Obs. Date (UT) (1)	Principal Investigator (2)	Other Observer Assisting (3)	Sky Conditions (4)
2000 Aug 23	Kirkpatrick	(none)	cirrus throughout night
2000 Dec 26	Kirkpatrick	Liebert	clear
2000 Dec 27	Carpenter	Hillenbrand	clear
2000 Dec 28	Carpenter	Hillenbrand	clear, seeing poorer than average
2001 Feb 20	Kirkpatrick	Liebert	mostly clear, light clouds late in night
2001 Nov 13	Stauffer	Kirkpatrick	spotty clouds
2002 Jan 01	Carpenter	(none)	clear
2002 Jan 02	Carpenter	(none)	clear
2002 Jan 03	Carpenter	(none)	clear first half, then fog forced closure
2002 Feb 19	Kirkpatrick	Lowrance	never opened (fog and snow)
2002 Feb 20	Kirkpatrick	Lowrance	never opened (fog)
2003 Jan 02	Kirkpatrick	Lowrance	clear
2003 Jan 03	Kirkpatrick	Lowrance	clear
2003 Dec 22	Kirkpatrick	Lowrance	clear
2003 Dec 23	Kirkpatrick	Lowrance	clear
2003 Dec 24	Kirkpatrick	Lowrance	clear

Table 3. New Spectroscopic Observations of Objects from Table 1

Object name (1)	Obs. Date (UT) (2)	Int. (s) (3)	CrH-a (4)	Rb-b/ TiO-b (5)	Cs-a/ VO-b (6)	Color-d (7)	KI fit (8)	Oxide fit (9)	Final opt. type (10)	Dist.[d] (pc) (11)	Hα EW (Å) (12)	Li I EW (Å) (13)
2MASS J00145575−4844171	2003 Dec 23	600	1.57(2)	—	—	8.97(-)	(3-4)	(2-3)	L2.5[e]	20:	<1	<0.5
2MASS J00165953−4056541	2003 Jan 02	1200	1.73(3-4)	1.30(4)	1.22(3-4)	7.83(-)	(3)	—	L3.5	29	<1	6.5
2MASS J00332386−1521309	2003 Dec 24	1200	1.50(2)	—	—	7.25(-)	(2)	(4)	L2 pec	39:	<3	<2
2MASS J00531899−3631102	2003 Dec 23	600	1.69(3)	1.31(4)	1.16(3)	9.17(-)	(4)	—	L3.5	20	<1	≤1
2MASS J01415823−4633574	2003 Dec 23	2400	0.97(<0)	0.68(0)	0.69(<0)	8.28(-)	(pec)	—	L0 pec	39:	10.5	≤1
2MASS J01443536−0716142	2001 Feb 20	960	2.20(5)	1.75(6)	1.31(4)	11.40(5)	(4-5)	—	L5	13	13[b]	<0.5
DENIS-P J0255−4700	2000 Dec 26	2400	1.29(8)	2.14(7)	1.67(8)	36.54(>8)	—	(8)	L8	*5*	<1	<0.2
2MASS J02572581−3105523	2003 Dec 24	1200	1.32(8)	—	—	29.63(8)	—	(8)	L8	9	<2	<0.5
2MASS J03185403−3421292	2003 Dec 24	1800	1.49(7)	—	—	21.90(7)	—	(7)	L7	16	<10[c]	9:
DENIS-P J035729.6−441730	2003 Dec 24	1200	1.02(<0)	0.69(0)	0.73(<0)	7.74(-)	(0)	—	L0 pec	32:	<2	≤2
SDSSp J042348.57−041403.5	multi dates[a]	5100	1.56(7)	2.07(7)	1.72(8+)	26.81(7-8)	—	—	L7.5	*15*	3	11
SDSS J044337.61+000205.1	2003 Dec 24	600	0.97(<0)	0.49(<0)	0.68(<0)	6.53(-)	(∼0)	—	M9 pec	15:	2.5	<2
2MASS J05120636−2949540	2003 Dec 24	1200	1.78(3-4)	—	—	11.29(5)	(4)	(5)	L4.5	26	≤2	11
2MASS J05264348−4455455	2003 Dec 24	600	1.15(0)	0.63(<0)	0.80(0)	6.42(-)	(∼0)	—	M9.5	30	4	<1
DENIS-P J0909−0658	2003 Dec 22	600	1.21(0)	0.79(1)	0.79(0)	6.45(-)	(0)	—	L0	25	≤1	<0.5
2MASS J11544223−3400390	2003 Jan 02	600	1.17(0)	0.72(0)	0.78(0)	7.20(-)	(0)	—	L0	29	4	3
2MASS J12185957−0550282	2003 Dec 22	300	1.03(<0)	0.56(<0)	0.79(0)	4.25(-)	(<0)	—	M8	38	6	<2
2MASS J14090310−3357565	2001 Feb 20	1200	1.37 (1)	1.10(2-3)	1.00(2)	6.63(-)	(2)	—	L2	24	<2	<1
DENIS-P J1441−0945	2003 Jan 03	600	1.29(0-1)	0.84(1)	0.86(1)	6.54(-)	(0)	—	L0.5	26	<1	<0.5
DENIS-P J153941.96−052042.4	2000 Aug 23	1200	1.48(2)	—	—	10.93(5)	(3-4)	(4)	L4:	14:	<10	<10
2MASS J16184503−1321297	2000 Aug 23	1200	1.44(1-2)	—	—	5.89(-)	(0)	(∼0)	L0:	30:	<5	<5
Gl 618.1B	2000 Aug 23	2400	1.86(4)	—	—	4.97(-)	(2-3)	(2-3)	L2.5	*30*	≤2	<2
2MASS J20575409−0252302	2000 Aug 23	1200	1.33(1)	0.94(1-2)	0.88(1)	6.61(-)	(2)	—	L1.5	15	11	5
2MASS J21041491−1037369	2000 Aug 23	1200	1.46(1-2)	1.21(3-4)	0.98(2)	6.39(-)	(2-3)	—	L2.5	18	<1	<1
2MASS J21073169−0307337	2000 Aug 23	1200	1.25(0-1)	0.59(<0)	0.91(1-2)	5.24(-)	(<0)	—	d/sdM9	32:	2	<1
2MASS J21304464−0845205	2000 Aug 23	768	1.60(2-3)	—	—	6.54(-)	(1-2)	(1)	L1.5	25	<4	<4
2MASS J21580457−1550098	2000 Aug 23	1200	1.69(3)	—	—	8.52(-)	(4)	(4)	L4:	23	<5	≤11
2MASS J23440624−0733282	2003 Jan 03	420	2.01(4-5)	1.55(4-5)	1.38(4-5)	11.42(5)	(4-5)	—	L4.5	19	<1	<0.5

[a]SDSSp J0423−0414 was observed on four separate dates: 2001 Nov 13 (900s integration), 2002 Jan 01 (1200s), 2002 Jan 02 (1200s), and 2002 Jan 03 (1800s). All analysis was performed on a coadded spectrum combining all 5100s of integration.

[b]2MASS J0144−0716 shows variable Hα emission when spectra from different epochs are compared. See Liebert et al. (2003) for further discussion.

[c]2MASS J0318−3421 shows a possible *absorption* trough of ∼10 Å EW at the location of Hα, but this is likely a data artifact since it is aphysically broad.

[d]Entries in italics are distances as measured through trignonometric parallax. All other entries are distances derived from spectrophotometric parallaxes. For SDSSp J0423−0414, the trigonometric parallax is from Vrba et al. (2004); for Gl 618.1B the distance is from its association with the primary, Gl 618.1A, whose trigonometric parallax was measured by Hipparcos (Perryman et al. 1997).

[e]The optical spectrum of 2MASS J0014−4844 is slightly peculiar, perhaps indicative of lower metallicity.

Table 4. Supporting Observations of L Dwarfs

Object name (1)	Disc. ref. (2)	Obs. Date (UT) (3)	Int. (s) (4)	CrH-a (5)	Rb-b/ TiO-b (6)	Cs-a/ VO-b (7)	Color-d (8)	KI fit (9)	Oxide fit (10)	Final opt. type (11)	Hα EW (Å) (12)	Li I EW (Å) (13)
2MASS J05185995−2828372	1	2003 Dec 24	1200	1.63(7)	—	—	26.58(7-8)	—	(7)	L7	<7	<5
SDSSp J083008.12+482847.4	2	multidate[a]	2400	1.14(8+)	—	—	35.07(8+)	—	(8+)	L8	<6	<2
SDSSp J085758.45+570851.4	2	2002 Jan 02	1200	1.35(8)	—	—	26.83(7-8)	—	(8)	L8	<8	14:
Gl 337CD[b]	3	2000 Dec 26	2400	1.24(8)	2.54(8)	1.80(8+)	44.67(8+)	—	(8)	L8	<2	<2
2MASSI J1315309−264951	4	2003 Jan 02	1200	2.01(5-6)	1.83(6)	1.47(5)	15.42(6)	(∼5)	(5-6)	L5.5	160	<2
2MASSW J2244316+204343	5	2000 Dec 26	2400	1.44(7-8)	1.85(6)	1.57(6-7)	15.23(6)	—	(6-7)	L6.5	<5	≤5

Note. — Discovery references are (1) Cruz et al. 2004, (2) Geballe et al. 2002, (3) Wilson et al. 2001, (4) Gizis 2002, (5) Dahn et al. 2002.

[a]SDSS J0830+4828 was observed on two separate dates: 2002 Jan 01 (1200s integration) and 2002 Jan 02 (1200s). All analysis was performed on a coadded spectrum combining all 2400s of integration.

[b]Gl 337CD is also known as 2MASS J0912146+145940 and was identified as a close double by Burgasser et al. (2005a).

Table 5. Supporting Observations of T Dwarfs

Object name (1)	Disc ref. (2)	Obs. Date (UT) (3)	Int. (s) (4)	Cs I (A) (5)	CrH(A)/ H_2O (6)	FeH(B) (7)	Color-e (8)	By-eye type (9)	Final opt. type (10)	Hα EW (Å) (11)	Li I EW (Å) (12)
2MASS J04151954−0935066	1	2000 Dec 26	3600	1.18	0.24	0.89	4.59(-)	(8 std)	T8 std	—[c]	—[c]
SDSSp J083717.22−000018.3	2	multidate[a]	14400	1.84(<2)	0.89(<2)	0.89(-)	3.35(<2)	(0)	T0	<6	<6
SDSSp J102109.6−030419	2	2000 Dec 26	2400	1.88(2-5)	0.67(2-5)	1.37(5)	3.85(2)	(2(-5))	T3.5	<13	<5
2MASS J12095613−1004008	3	multidate[b]	9600	1.86(2-5)	0.63(5)	1.24(∼5)	4.22(-)	(2-5)	T3.5	<8	<4
SDSSp J125453.9−012247	2	2000 Dec 26	2400	1.96	0.77	1.09	4.20	(2 std)	T2 std	28	<5

Note. — Discovery references are (1) Burgasser et al. 2002, (2) Leggett et al. 2000, (3) Burgasser et al. 2004a.

[a]SDSS J0837−0000 was observed on three separate dates: 2000 Dec 26 (7200s integration), 2000 Dec 27 (3600s), and 2000 Dec 28 (3600s). All analysis was performed on a coadded spectrum combining all 14400s of integration.

[b]2MASS J1209−1004 was observed on three separate dates: 2003 Dec 22 (2400s integration), 2003 Dec 23 (3600s), and 2003 Dec 24 (3600s). All analysis was performed on a coadded spectrum combining all 9600s of integration.

[c]2MASS J0415−0935 has a flux measurement at or very close to zero at these wavelengths, so meaningful equivalent width measures are not possible.

Table 6. Ultra-cool Field[e] Dwarfs (≥M7) with Spectroscopic Signatures of Low Gravity (Youth)[a]

Object Name (1)	Optical Sp. Type (2)	Opt. Ref. (3)	Near-IR Sp. Type (4)	Near-IR Ref. (5)	2MASS J-K_s (6)	Disc. Ref. (7)	Youth Ref. (8)	Diagnostics (9)
2MASS J00332386−1521309	L2 pec	1	—	—	1.88±0.07	18	1	(see Figure 11)
2MASS J01415823−4633574	L0 pec	2	L0 pec	2	1.74±0.05	2	2	(see Figure 9)
2MASSI J0241115−032658	L1 pec	8	—	—	1.76±0.08	8	8	(see Figure 9)
2MASSI J0253597+320637	M7 pec?	14	—	—	1.07±0.03	14	14	marginally weak CaH, possibly weak Na I
DENIS J035726.9−441730	L0 pec	1	—	—	1.46±0.04	3	1	(see Figure 9)
DENIS J0436278−411446	M8 pec?	8	—	—	1.04±0.04	17	8	slightly weak Na I, slightly strong VO?
SDSS J044337.61+000205.1	M9 pec	1	—	—	1.29±0.03	4	1,8	(see Figure 8)
2MASSI J0608528−275358	M9 pec	14	—	—	1.22±0.04	14	14	(see Figure 8)
2MASS J10220489+0200477	L0 pec?	1	—	—	1.20±0.04	5	1	(see Figure 9)
2MASS J10224821+5825453	L1 pec	1	—	—	1.34±0.04	5	1	(see Figure 10)
SDSS J102552.43+321234.0	—	—	L7.5±2.5	13	—[c]	13	1	weak near-IR K I, weak H_2O
SSSPM J1102−3431[b]	M8.5 pec	16	—	—	1.15±0.03	16	16	weak Na I, strong VO, weak CaH
2MASSW J1139511−315921	M8 pec	15	M9 pec	19	1.18±0.03	15	15	weak CaH, weak Na I doublet, strong VO
2MASSW J1207334−393254	M8 pec	15	M8 pec	19	1.05±0.04	15	15	weak CaH, weak Na I doublet, strong VO
DENIS J124514.1−442907	M9.5 pec	19	M9 pec	19	1.15±0.05	19	19	weak CaH, weak Na I doublet, strong VO, etc.
2MASSI J1615425+495321	L4 pec[d]	8	—	—	2.48±0.15	8	8	(see Figure 12)
2MASSW J2208136+292121	L2 pec	6	—	—	1.65±0.11	6	1	(see Figure 11)
2MASS J22134491−2136079	L0 pec	1	—	—	1.62±0.05	8	1	(see Figure 9)
2MASSW J2244316+204343	L6.5	1	???	7	2.45±0.16	9	7	(see Figure 13)
SDSSp J224953.45+004404.2	L3	4	L5±1.5	10	2.23±0.14	11	12	peaky H-band, weak 1.1 μm H_2O, weak near-IR K I

Note. — Key to references: (1) this paper, (2) Kirkpatrick et al. 2006, (3) Bouy et al. 2003, (4) Hawley et al. 2002, (5) Reid et al. 2008, (6) Kirkpatrick et al. 2000, (7) Looper et al. 2008, (8) Cruz et al. 2007, (9) Dahn et al. 2002, (10) Knapp et al. 2004, (11) Geballe et al. 2002, (12) Nakajima et al. 2004, (13) Chiu et al. 2006, (14) Cruz et al. 2003, (15) Gizis 2002, (16) Scholz et al. 2005, (17) Phan-Bao et al. 2003, (18) Gizis et al. 2003, (19) Looper et al. 2007.

[a]Other possible low-g dwarfs have been noted due to color anomalies only, e.g., SDSS 0107+0041 in Knapp et al. (2004). For T dwarfs Knapp et al. (2004) and Burgasser et al. (2006a) have found that for fixed T_{eff} the H-K color is diagnostic of gravity because it measures the importance of gravity- (pressure-) sensitive CIA H_2. Based on the combined work of these two groups, the lowest gravities probed by the currently known set of T dwarfs is $4.5 < log(g) < 5.0$.

[b]SSSPM J1102−3431: Also known as 2MASS J11020983−3430355.

[c]SDSS J1025+3212: Not detected at 2MASS J-band.

[d]2MASS J1615+4953: Spectrum has poor signal-to-noise and may prove to be dusty rather than low gravity.

[e]Includes any field objects not known to be companions to other stars.

Table 7. Log of Spectroscopic Observations for Objects Shown in Figure 7 - Figure 13

2MASS Name (1)	Other Name (2)	Obs. Date (UT) (3)	Teles. (4)	Inst. (5)	Int.(s) (6)	Spec. Ref. (7)	Sp. Type (8)	Tell. Corr.?[e] (9)
2MASS J00332386−1521309		2003 Dec 24	Keck	LRIS	1200	8	L2 pec	no
2MASS J01415823−4633574		2003 Dec 23	Keck	LRIS	2400	4	L0 pec	no
2MASS J02052940−1159296	DENIS-P J0205.4−1159	1997 Nov 09	Keck	LRIS	1200	1	L7 (std)	no
2MASS J02411151−0326587		2005 Oct 10	Gemini-S	GMOS	1187	5	L0 pec	no
2MASS J03435353+2431115	Roque 4	2003 Jan 03	Keck	LRIS	2400	8	late-M Pleiad	yes
2MASS J03454316+2540233		1997 Nov 09	Keck	LRIS	1200	1	L0 (std)	no
2MASS J03471791+2422317	Teide 1	2003 Jan 02	Keck	LRIS	1800	8	late-M Pleiad	yes
—– J0348306 +224450	Roque 25	2003 Jan 02	Keck	LRIS	6000	8	L0 Pleiad	yes
2MASS J03572695−4417305	DENIS-P J035729.6−441730	2003 Dec 24	Keck	LRIS	1200	8	L0 pec	no
2MASS J04300724+2608207	KPNO-Tau6	2003 Jan 02	Keck	LRIS	1200	8	M8.5	yes
2MASS J04433761+0002051	SDSS J044337.61+000205.1	2003 Dec 24	Keck	LRIS	600	8	M9 pec	no
2MASS J06085283−2753583		2003 Dec 23	Keck	LRIS	1200	6	M8.5 pec	yes
2MASS J07065882+0852370	V CMi	2003 Dec 23	Keck	LRIS	1	8	late-M giant	yes
2MASS J08503593+1057156		multidate[a]	Keck	LRIS	10800	1	L6 (std)	no
2MASS J10042066+5022596	G 196-3B	multidate[b]	Keck	LRIS	3600/6000	3	L2 pec	both[b]
2MASS J10220489+0200477		multidate[c]	CTIO-4m	RC-Spec	1200	7	L0 pec	no
2MASS J10224821+5825453		2004 Feb 10	KPNO-4m	RC-Spec	600	7	L1 pec	no
2MASS J11122567+3548131	Gl 417B	multidate[d]	Keck	LRIS	6000	2	L4.5 pec	no
2MASS J11463449+2230527		1997 Dec 07	Keck	LRIS	1200	1	L3 (std)	no
2MASS J11550087+2307058		1998 Jan 22	Keck	LRIS	2400	1	L4 (std)	no
2MASS J12073346−3932539		2003 Jan 02	Keck	LRIS	600	8	M8	yes
2MASS J12281523−1547342	DENIS-P J1228.2−1547	1997 Dec 09	Keck	LRIS	1200	1	L5 (std)	no
2MASS J12391934+2029519		1997 Dec 08	Keck	LRIS	1200	1	M9	no
2MASS J13054019−2541059	Kelu-1AB	1998 Jan 22	Keck	LRIS	1200	1	L2 (std)	no
2MASS J14325988−1056035	IRAS 14303−1042	2003 Jan 03	Keck	LRIS	10(or 15)	8	late-M giant	yes
2MASS J14392836+1929149		1997 Dec 08	Keck	LRIS	1200	1	L1 (std)	no
2MASS J16154255+4953211		2004 Sep 12	Gemini-N	GMOS	960	5	L4 pec	no
2MASS J19165762+0509021	vB 10	2004 Jul 15	Keck	LRIS	300	8	M8 (std)	yes
2MASS J22081363+2921215		2007 Aug 21	Subaru[f]	FOCAS	1200	8	L2 pec	no
2MASS J22134491−2136079		2007 Aug 21	Subaru[f]	FOCAS	1200	8	L0 pec	no
2MASS J22443167+2043433		2000 Dec 26	Keck	LRIS	2400	8	L6.5	no

Note. — Key to reference for spectral acquisition: (1) Kirkpatrick et al. 1999a, (2) Kirkpatrick et al. 2000, (3) Kirkpatrick et al. 2001, (4) Kirkpatrick et al. 2006, (5) Cruz et al. 2007, (6) Cruz et al. 2003, (7) Reid et al. 2008 and DwarfArchives.org, (8) this paper.

[a]2MASS J0850+1057 was observed on five different dates; the plotted spectrum is a sun of all five. Exposure times were 2400s on 1997 Nov 09 (UT), 1200s on 1997 Dec 07 (UT), 1200s on 1997 Dec 08 (UT), 1200s on 1997 Dec 09 (UT), and 4800s on 1998 Jan 24 (UT).

[b]G 196-3B was observed using a blue (3900-8700Å) on one night and our standard red setup (6300-10100 Å) on two other nights. Observations for the blue setup were done in superior conditions, so the plotted spectrum shortward of 8500 Å is from this set, and data longward of 8500 Å come from the poorer data taken with the red setup. Data taken with the blue setup were corrected for telluric absorption; data with the red setup were not telluric corrected. The exposure time for the blue setup was 3600s on 2001 Feb 19 (UT). Exposure times for the red setup were 2400s on 1999 Mar 04 (UT) and 3600s on 1999 Mar 05 (UT).

[c]2MASS J1022+0200 was observed for 600s on two different dates, 2003 Apr 04 (UT) and 2006 Jan 15 (UT). The plotted spectrum is the sum of these two observations.

[d]Gl 417B was observed on three different dates; the plotted spectrum is a sum of all three. Exposure times were 1200s on 1998 Dec 14 (UT), 1200s on 1999 Mar 04 (UT), and 3600s on 1999 Mar 05 (UT).

[e]Indicates whether or not the spectrum was telluric corrected using a G dwarf spectrum acquired near in time and near on sky to the program object.

[f]Observation and reduction procedures for Subaru-FOCAS data are discussed in Looper et al. (2008).

Table 8. Lithium Equivalent Width Measurements for L0, L2, L4, and L6.5 Dwarfs

	Normal Dwarfs (without Lithium)		Normal Dwarfs (with Lithium)		Peculiar Dwarfs (Low-g)		Very Peculiar Dwarfs (Very Low-g)	
Sp. Ty.	Name	EW (Å)	Name	EW (Å)	Name	EW (Å)	Name	EW (Å)
(1)	(2)	(3)	(4)	(5)	(6)	(7)	(8)	(9)
L0	2MASSW J0058425−065123	<1	2MASS J11544223−3400390	2.9±0.7	DENIS-P J035729.6−441730	≤2	2MASS J01415823−4633574[e]	≤1
	2MASP J0345432+254023	<0.5			Roque 25	<3	2MASS J02411151−0326587	<2
	DENIS-P J0909−0658	<0.5			2MASS J10220489+0200477	<10	2MASS J22134491−2136079	<1
	2MASSW J1449378+235537	<10						
	2MASS J16184503−1321297	<5						
L2	2MASSW J0015447+351603	<0.5	Kelu-1[b]	1.7±0.5	2MASS J00332386−1521309	<2		
	2MASSW J0030438+313932	<1.0	2MASSI J1726000+153819	6±2	G 196-3B[c]	6.0±0.7		
	2MASSI J0224367+253704	<1	2MASSW J2206540−421721	8±2	2MASSW J2208136+292121	4±1		
	2MASSI J0753321+291711	<1						
	2MASSW J0829066+145622	<0.5						
	2MASSW J0928397−160312	<1						
	2MASSW J0944027+313132	<1						
	2MASSI J1332286+263508	<2						
	2MASS J14090310−3357565	<1						
L4	2MASSW J1155009+230706	<0.5	2MASSW J0129122+351758	3.3±1.2	Gl 417B[d]	9.4±0.5		
	GD 165B[a]	<0.7	2MASSW J1246467+402715	10.5±1.5	2MASS 16154255+4953211	≤8		
	DENIS-P J153941.96−052042.4	<10						
	2MASS J21580457−1550098	≤11						
L6.5	2MASSW J0801405+462850	<2	2MASSW J0829570+265510	18±5	2MASS J22443167+2043433[f]	5±3		
	2MASSW J0920122+351742	<0.5	2MASS J21481628+4003593[g]	12.6±0.2				
	2MASSI J1711457+223204	≤7						

[a]GD 165B: Age estimate using the white dwarf primary is 1.2-5.5 Gyr (Kirkpatrick et al. 1999b).

[b]Kelu-1: Age estimate from model fits is 300-800 Myr (Liu & Leggett 2005).

[c]G 196-3B: Age estimates from the presence of the lithium in G 196-3B itself as well as activity diagnostics in the primary is 20-300 Myr (Rebolo et al. 1998); an age estimate using indicators from the early-M primary alone is 60-300 Myr (Kirkpatrick et al. 2001).

[d]Gl 417B: Age estimate from the G dwarf primary is 80-300 Myr (Kirkpatrick et al. 2001). Gl 417B is actually typed as L4.5 but is included here as an L4 so that this bin of peculiar, low-gravity L4 dwarfs could be populated.

[e]2MASS J0141−4633: Age estimate from fitting of theoretical models to spectra is 1-50 Myr (Kirkpatrick et al. 2006).

[f]2MASS J2244+2043: This object has a normal L6.5 optical spectrum, but its near-infrared spectrum is extremely peculiar. In this case, the peculiarity may be attributable to low gravity (McLean et al. 2003).

[f]2MASS J2148+4003: This object has a normal L6.5 optical spectrum, but its near-infrared spectrum is extremely peculiar. In this case, the peculiarity is best explained by excessive atmospheric dust (Looper et al. 2008).

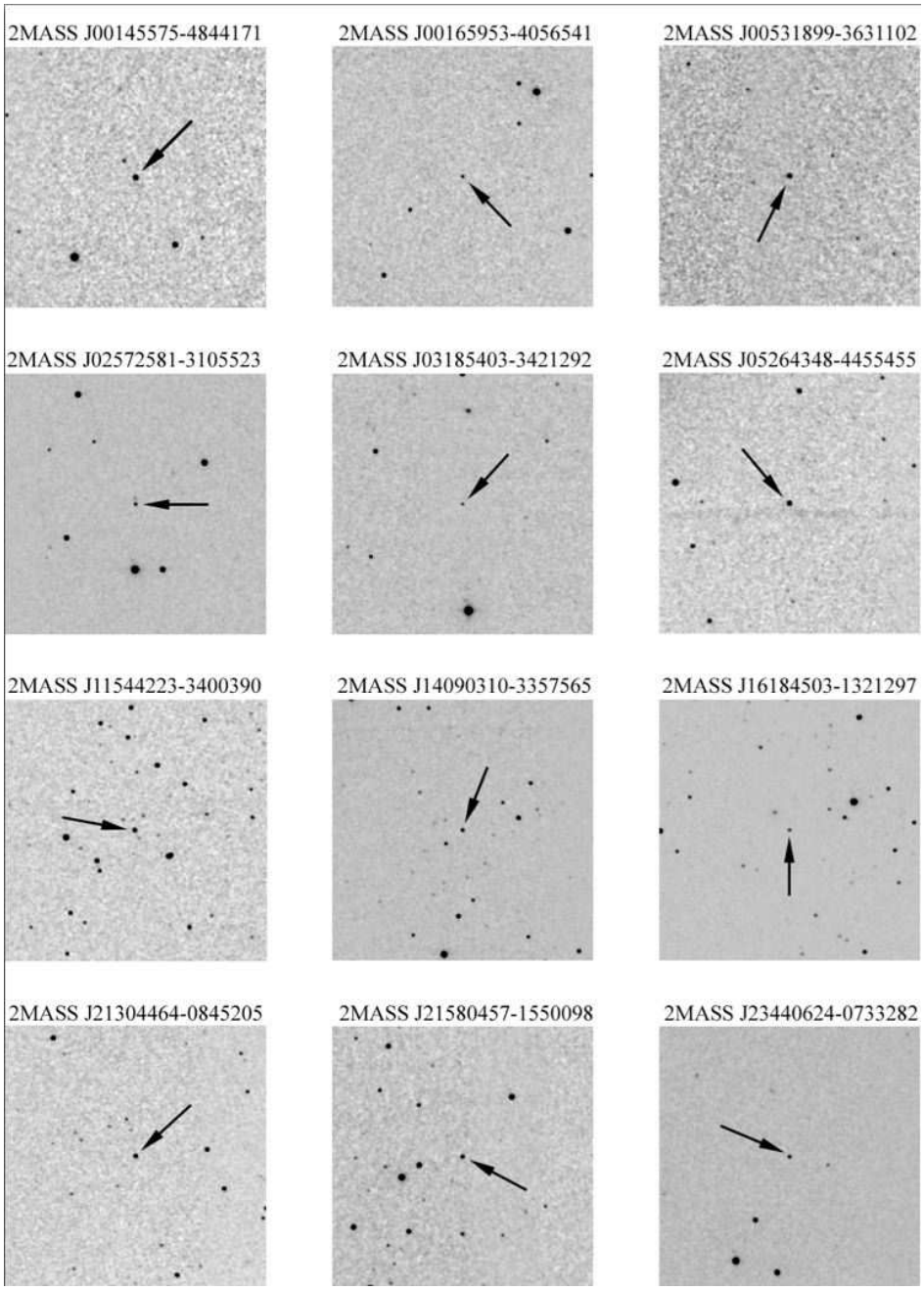

Fig. 1.— 2MASS *J*-band finder charts for the new objects identified in Table 1. All images are five arcminutes square with north up and east to the left. The positions of the new L and late-M dwarfs are marked with arrows. Note that the fainter object a few arcseconds north of 2MASS J02572581−3105523 is merely an artifact – a latent image persisting from the previous 2MASS frame and caused by the brighter star due south.

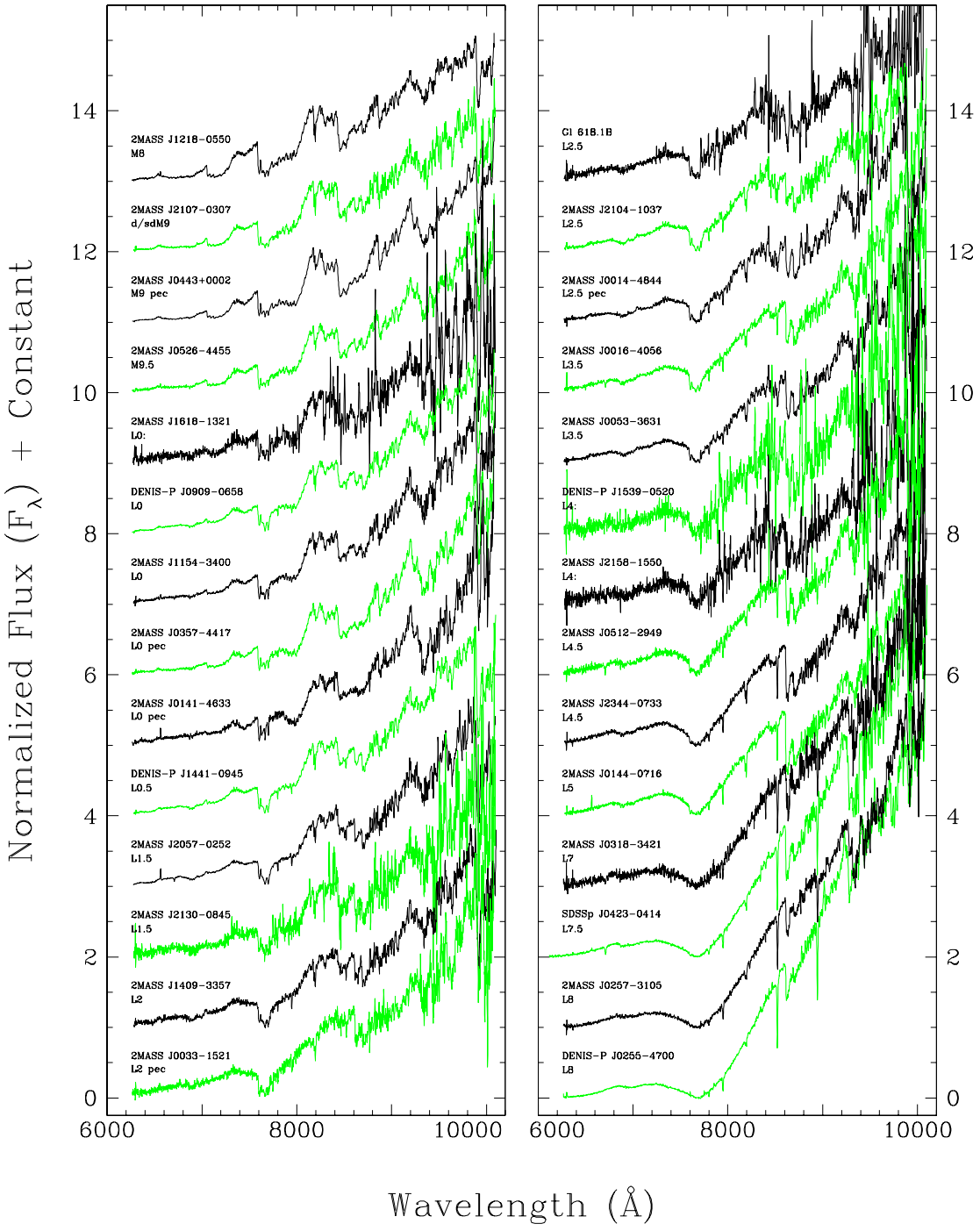

Fig. 2.— Keck/LRIS spectra of the twenty-eight objects listed in Table 3. Each spectrum is normalized to one at 8250 Å and an integral offset is added to this normalized flux so that the spectra are clearly separated along the y-axis. Spectra are ordered from earliest to latest with M8 through L2 shown in the left panel and L2.5 through L8 shown in the right. The spectra shown here are not corrected for telluric absorption. Colors of the spectra in Figure 2 through Figure 5 alternate between black and green to aid in presentation.

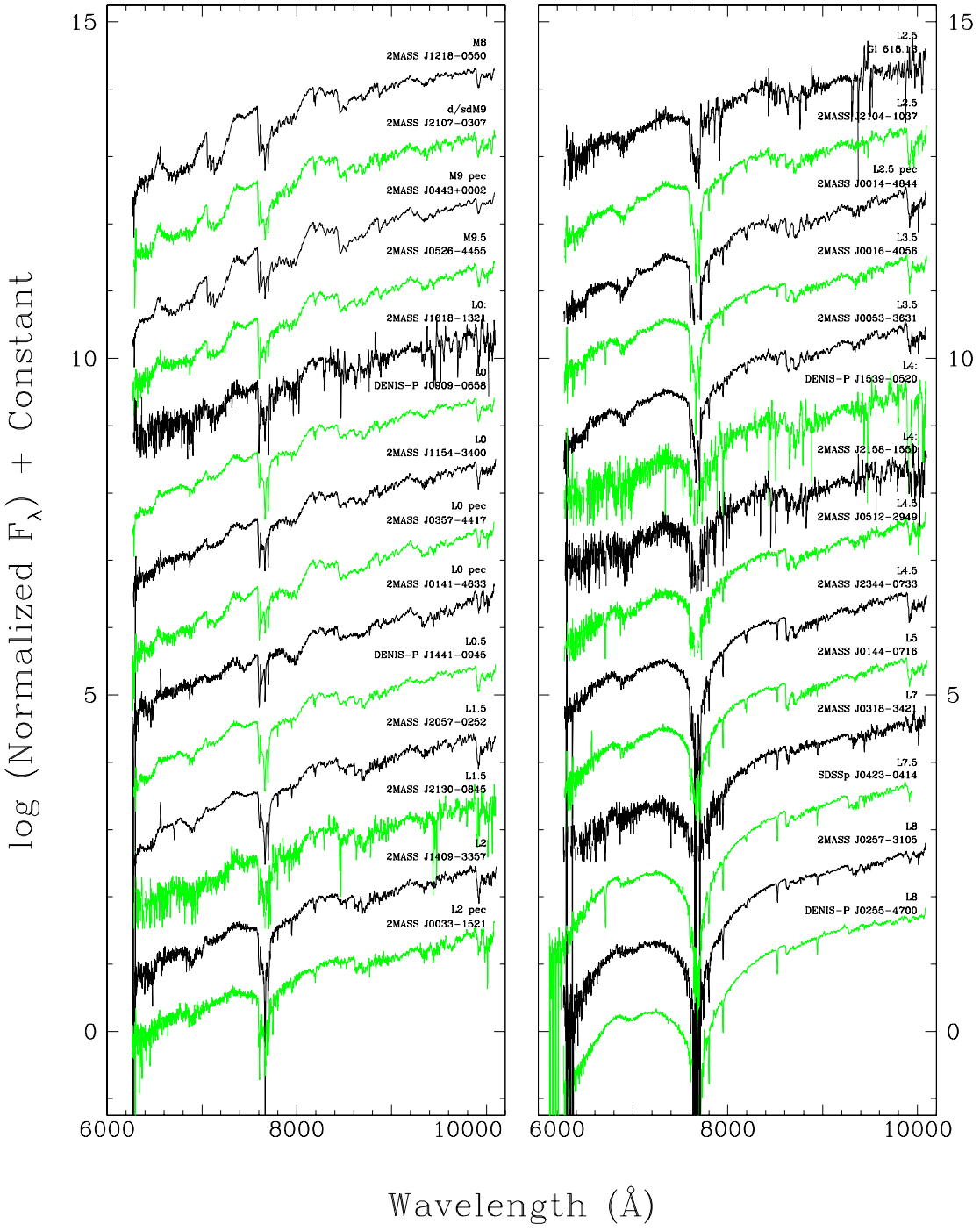

Fig. 3.— The same data shown in Fig. 2 except that the y-axis is scaled logarithmically to emphasize features at shorter wavelengths.

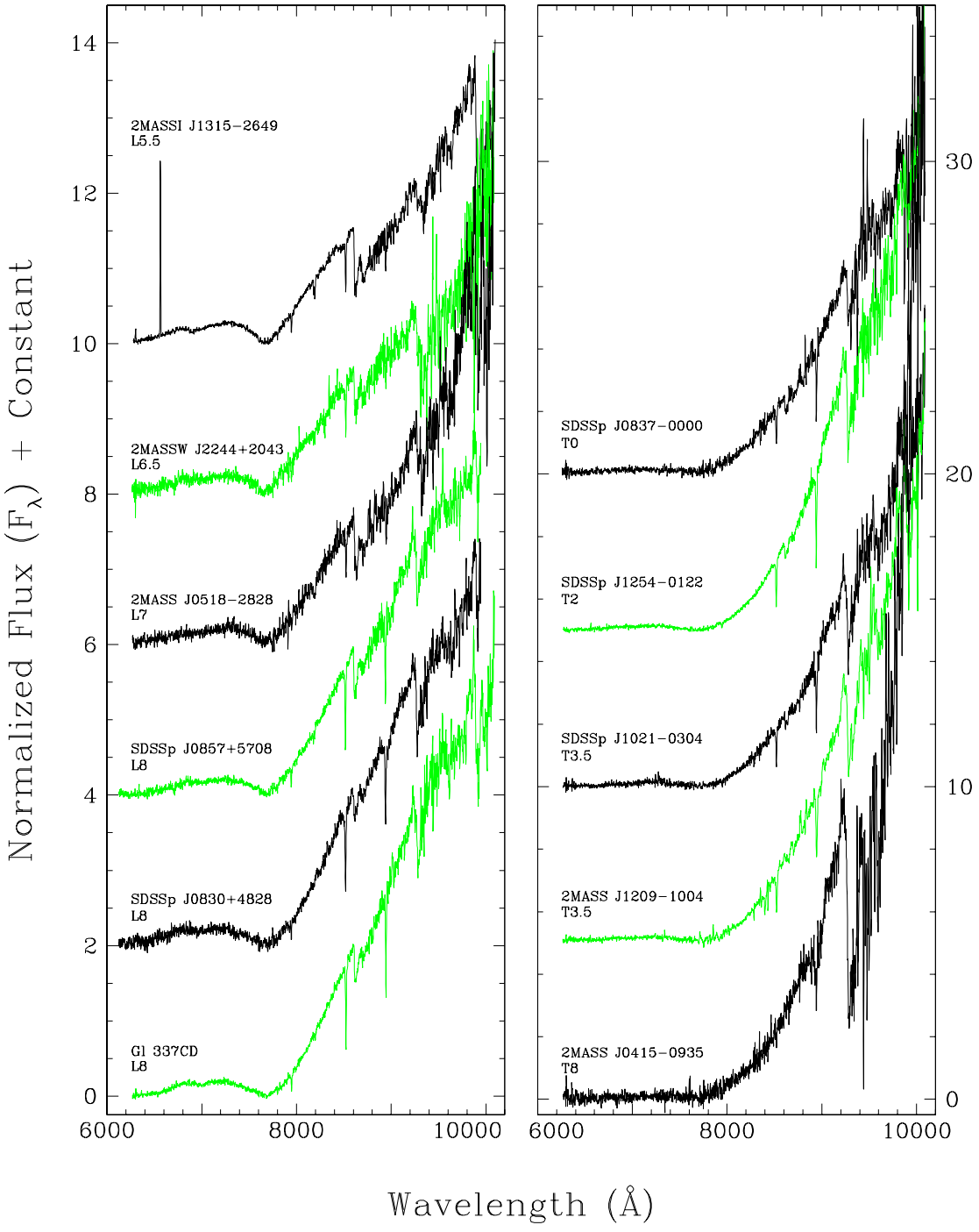

Fig. 4.— Keck/LRIS spectra of the eleven objects in Table 4 and Table 5. All spectra have been normalized to unity at 8250 Å. Integral offsets have been added along the y-axis to separate the spectra vertically – offsets are 2, 4, 6, 8, and 10 for the left panel and 5, 10, 15, and 20 for the right. All of these spectra have been corrected for telluric absorption except for 2MASS J2244+2043 and 2MASS J0518−2828.

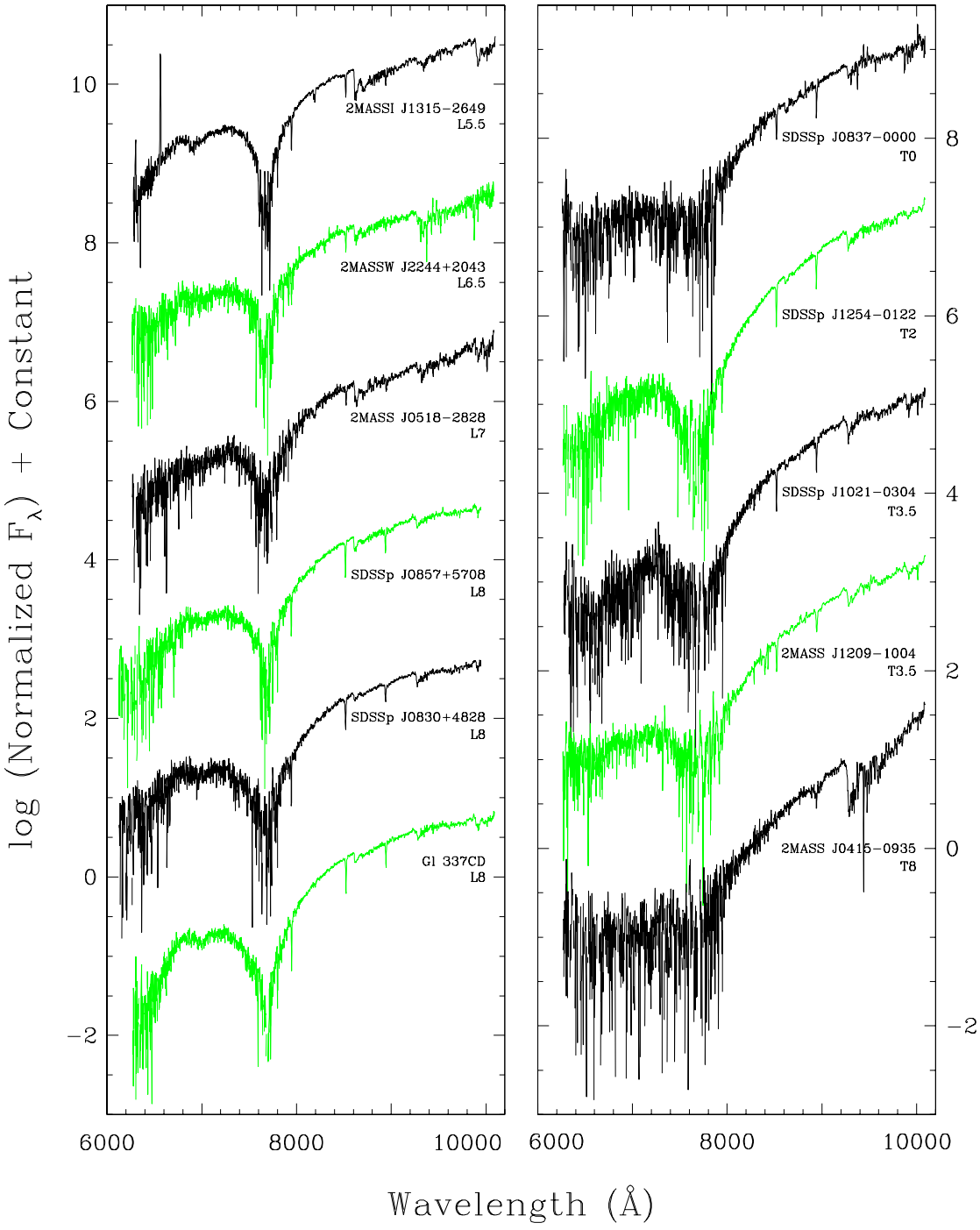

Fig. 5.— The same as Figure 4 except that the objects are plotted on a logarithmic, rather than a linear, scale to emphasize features at the shortest wavelengths and to avoid overlap at the red end of the spectra. Vertical offsets are integral multiples of two in both panels.

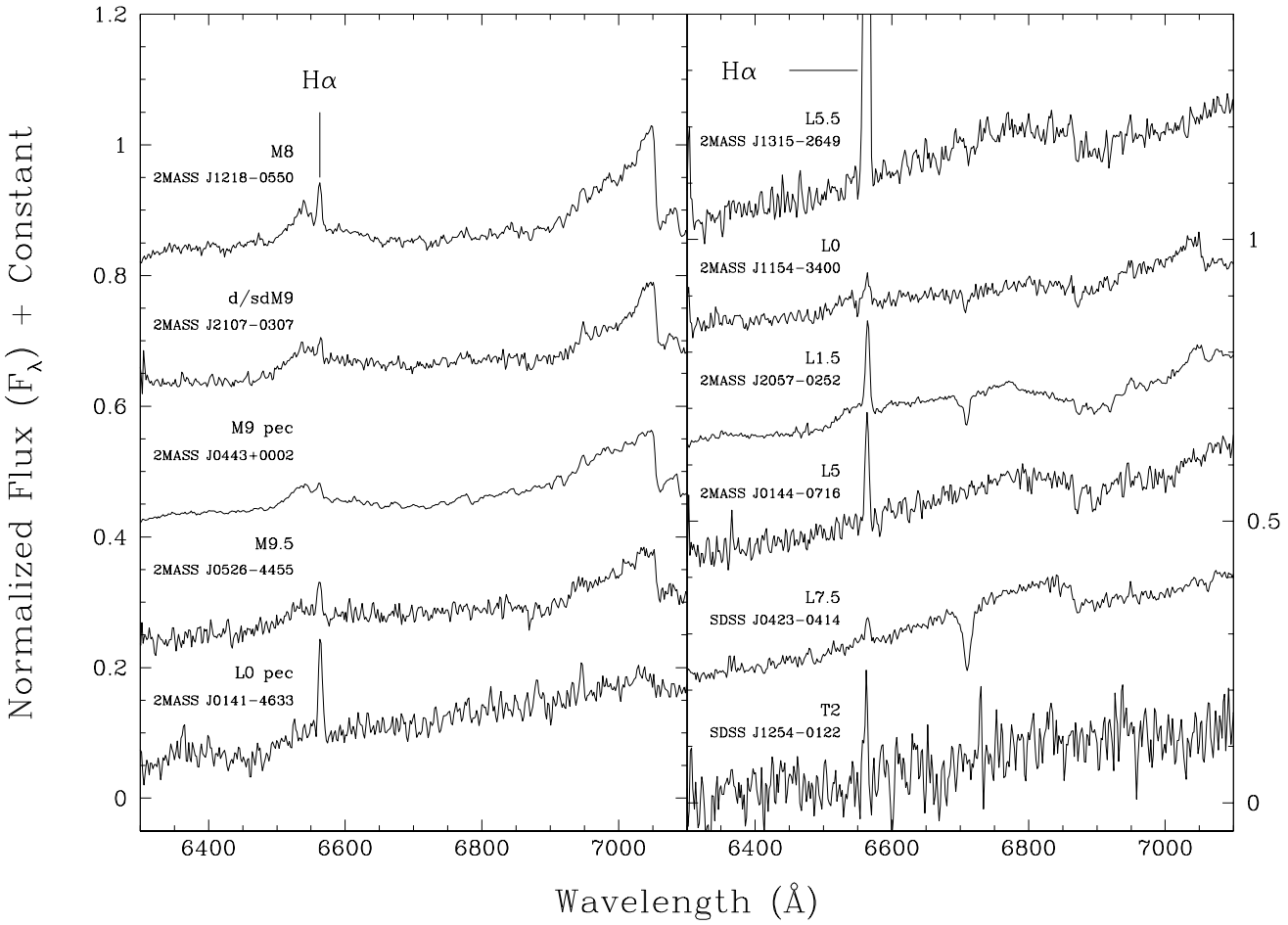

Fig. 6.— Zooms of the Keck/LRIS spectra in the 6300-7100 Å region for those objects in Table 3 exhibiting Hα emission. Note that three of the objects (2MASS J1154−3400, 2MASS J2057−0252, and SDSS J0423−0414) exhibit both Li I absorption at 6708 Å and Hα emission.

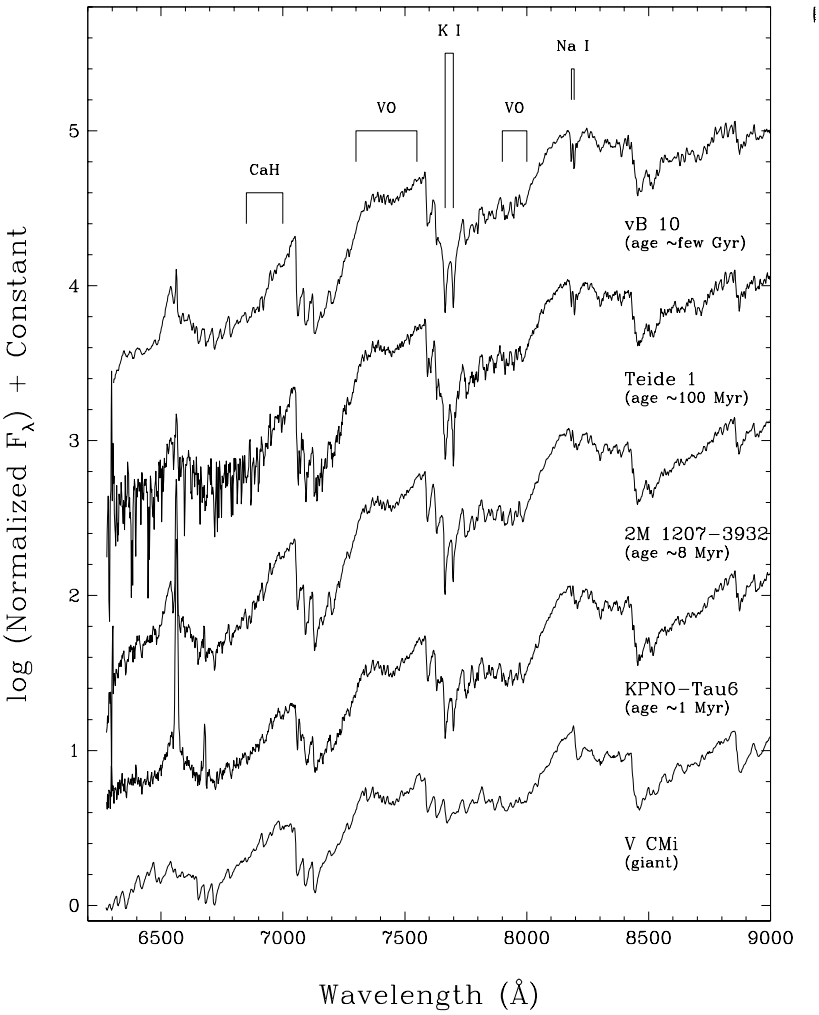

Fig. 7.— An optical spectral sequence showing feature changes as a function of age (gravity) at M8-M8.5. Each object is labeled with its age as deduced from membership in a cluster (either the Pleiades at ∼100 Myr, the TW Hydrae Association at ∼8 Myr, or the Taurus Molecular Cloud at ∼1 Myr) or from association with a higher mass primary (in the case of vB 10). Note the weakening of alkali lines (K I and Na I) and the CaH band as well as the strengthening of the VO bands from oldest (vB 10) to youngest (KPNO-Tau6). Although the change in spectral morphology is subtle from object to object, the plot demonstrates that gravity differences can be discerned at the ∼1 dex level in log(age). The spectrum of a late-M giant with log(g)≈0 is shown at the bottom to illustrate the behavior of these features at even lower gravities. All spectra have been corrected for telluric absorption.

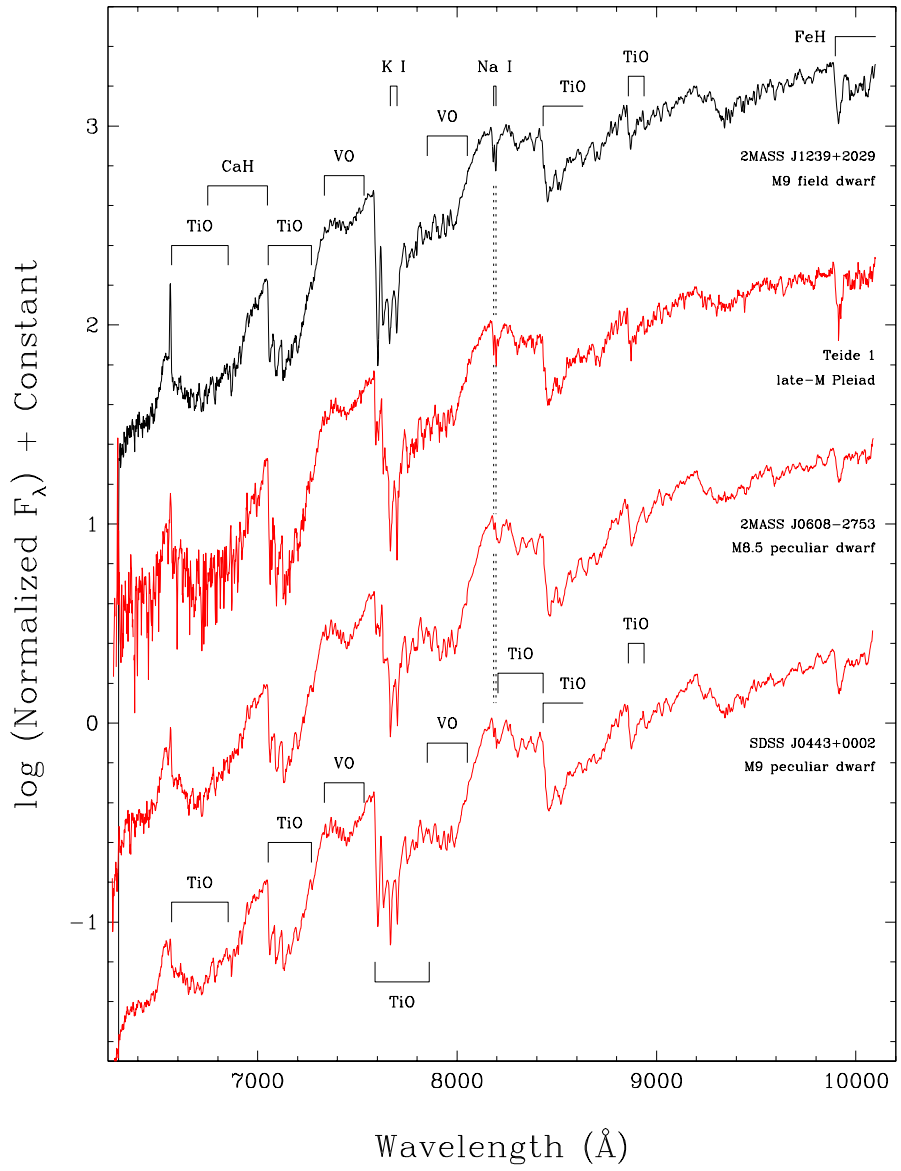

Fig. 8.— The peculiar M8.5 dwarf 2MASS J0608−2753 and the peculiar M9 dwarf SDSS J0443+0002 compared to an M9 field dwarf (2MASS J1239+2029) and a late-M member of the Pleiades (Teide 1). Prominent spectral features are marked. Spectra have been normalized to unity at 8250 Å and offset along the y-axis to separate them vertically.

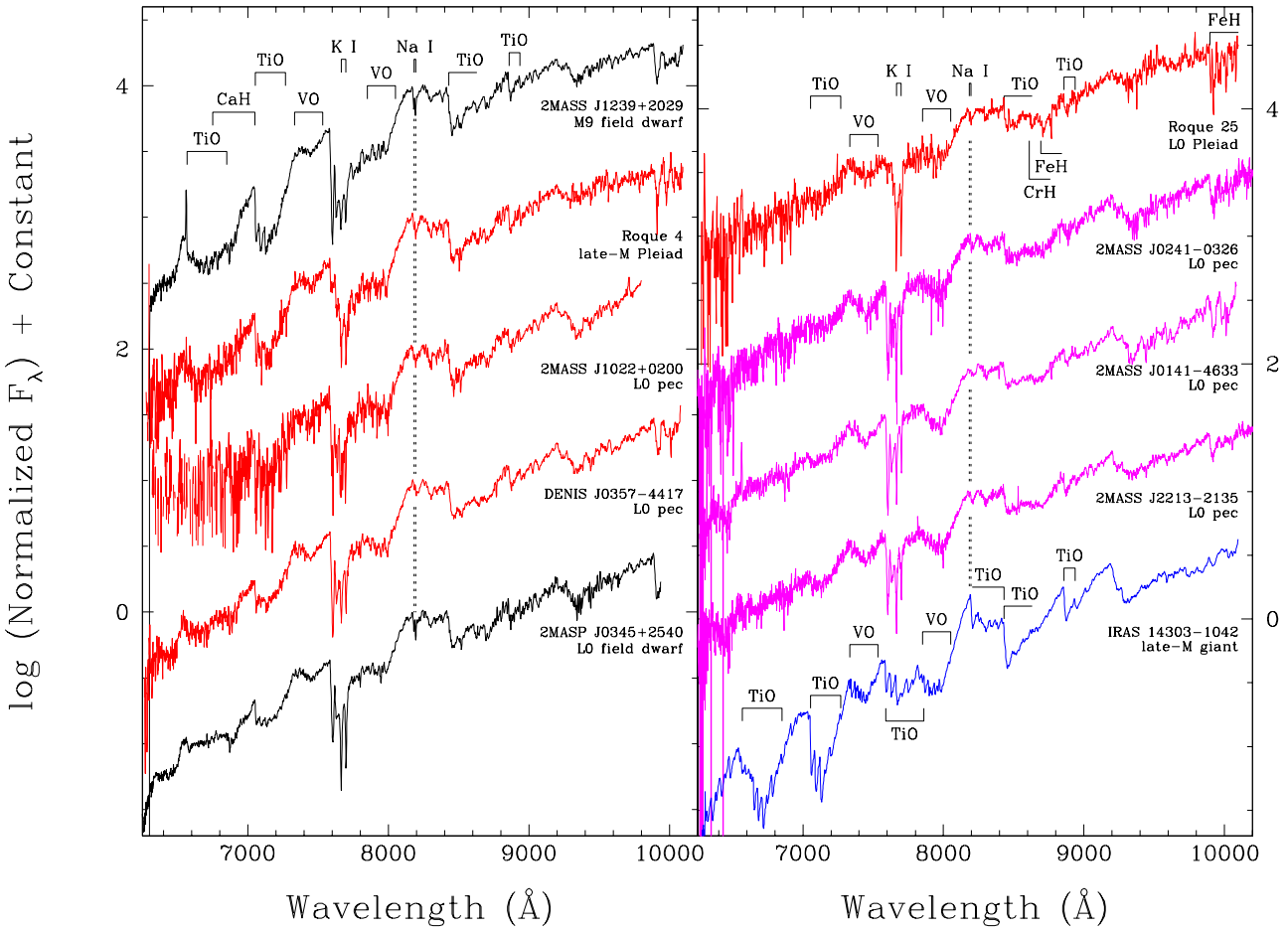

Fig. 9.— (Left) The slightly peculiar L0 dwarfs 2MASS J1022+0200 and SDSS J0357−4417 compared to a normal field M9 (2MASS J1239+2029), an M9 dwarf in the Pleiades (Roque 4), and the standard L0 dwarf 2MASP J0345+2540 from Kirkpatrick et al. (1999a). Prominent features are marked. (Right) The more peculiar L0 dwarfs 2MASS J0241−0326, 2MASS J0141−4633, and 2MASS J2213−2135 compared to an L0 member of the Pleiades (Roque 25) and a late-M giant (IRAS 14303−1042). In both panels spectra have been normalized to unity at 8250 Å and offset along the y-axis to separate them vertically.

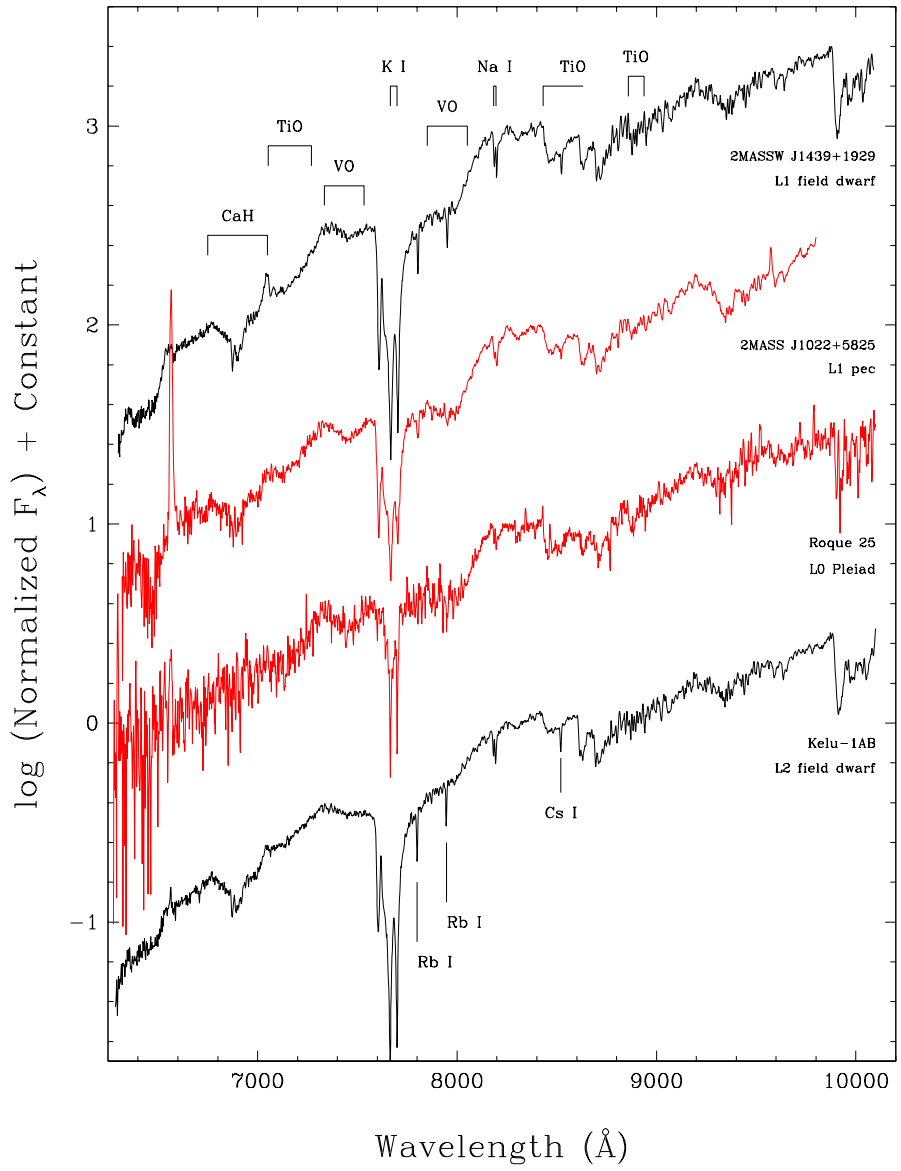

Fig. 10.— The peculiar L1 dwarf 2MASS J1022+5828 compared to the standard L1 dwarf 2MASSW J1439+1929 and an L0 dwarf (Roque 25) in the Pleiades. Prominent features are marked. Spectra have been normalized to unity at 8250 Å and have been offset along the y-axis to separate the spectra vertically.

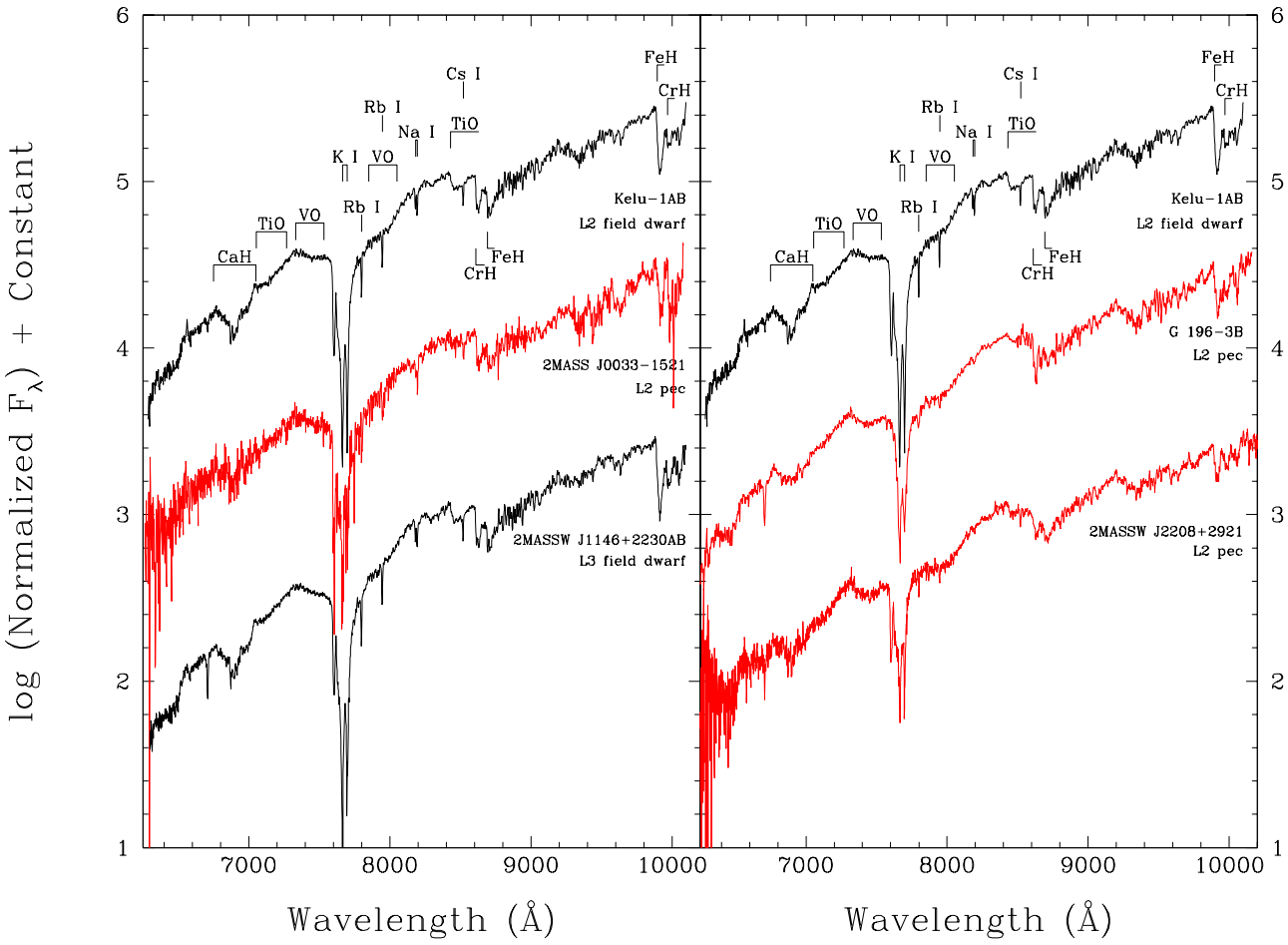

Fig. 11.— (Left) The peculiar L2 dwarf 2MASS J0033−1521 compared to the standard L2 dwarf Kelu-1 and the standard L3 dwarf 2MASS J1146+2230. (Right) The peculiar L2 dwarfs G 196-3B and 2MASS J2208+2921 compared to the same L2 standard shown in the left panel. In both panels the spectra have been normalized to unity at 8250 Å and a constant offset added to separate the spectra vertically.

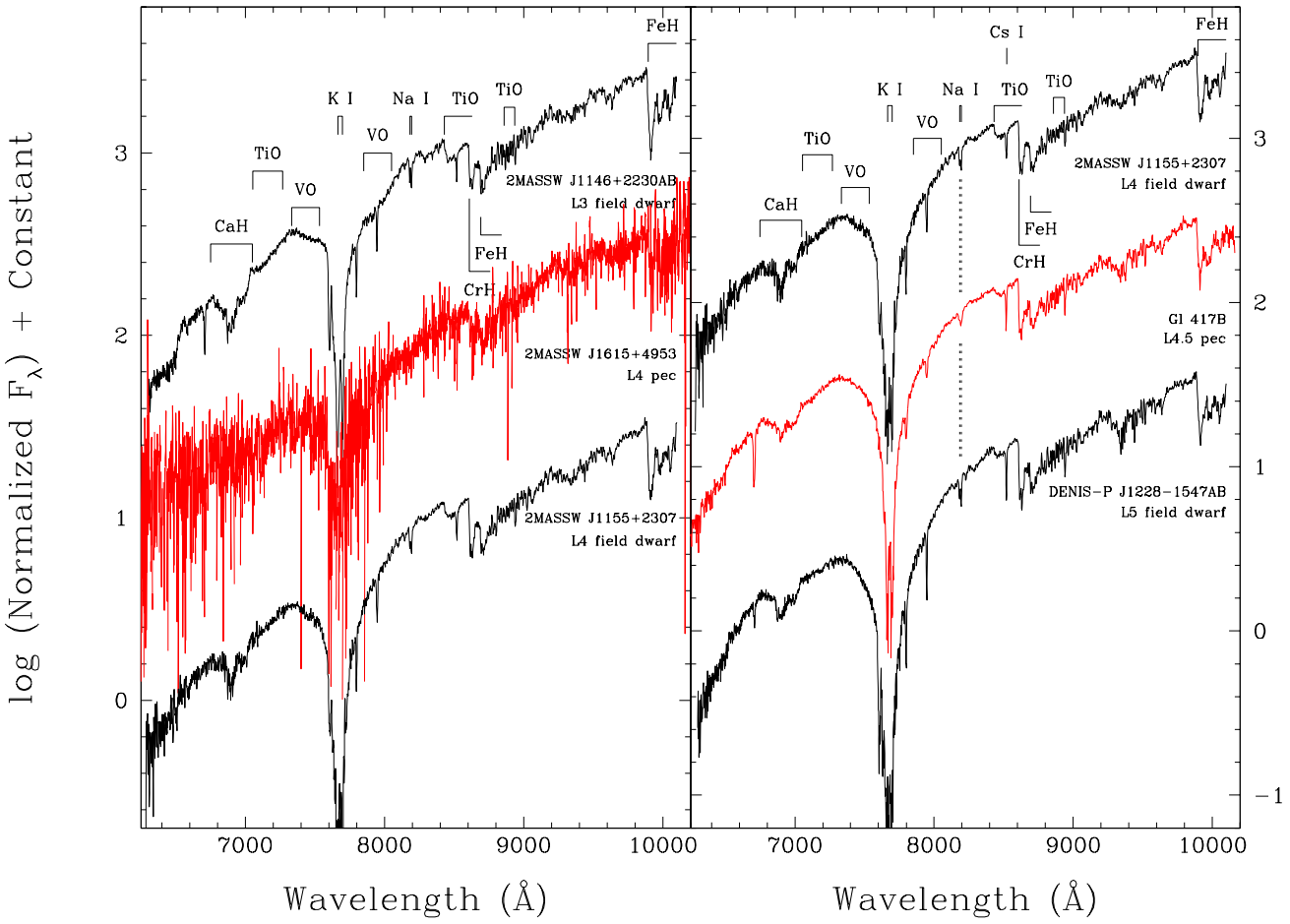

Fig. 12.— (Left) The peculiar L4 dwarf 2MASS J1615+4953 compared to the standard L3 dwarf 2MASS J1146+2230 and the standard L4 dwarf 2MASS J1155+2307. (Right) The peculiar L4.5 dwarf Gl 417B compared to the same L4 standard shown in the left panel and the L5 standard DENIS J1228-1547. In both panels the spectra have been normalized to unity at 8250 Å and a constant offset added to separate the spectra vertically.

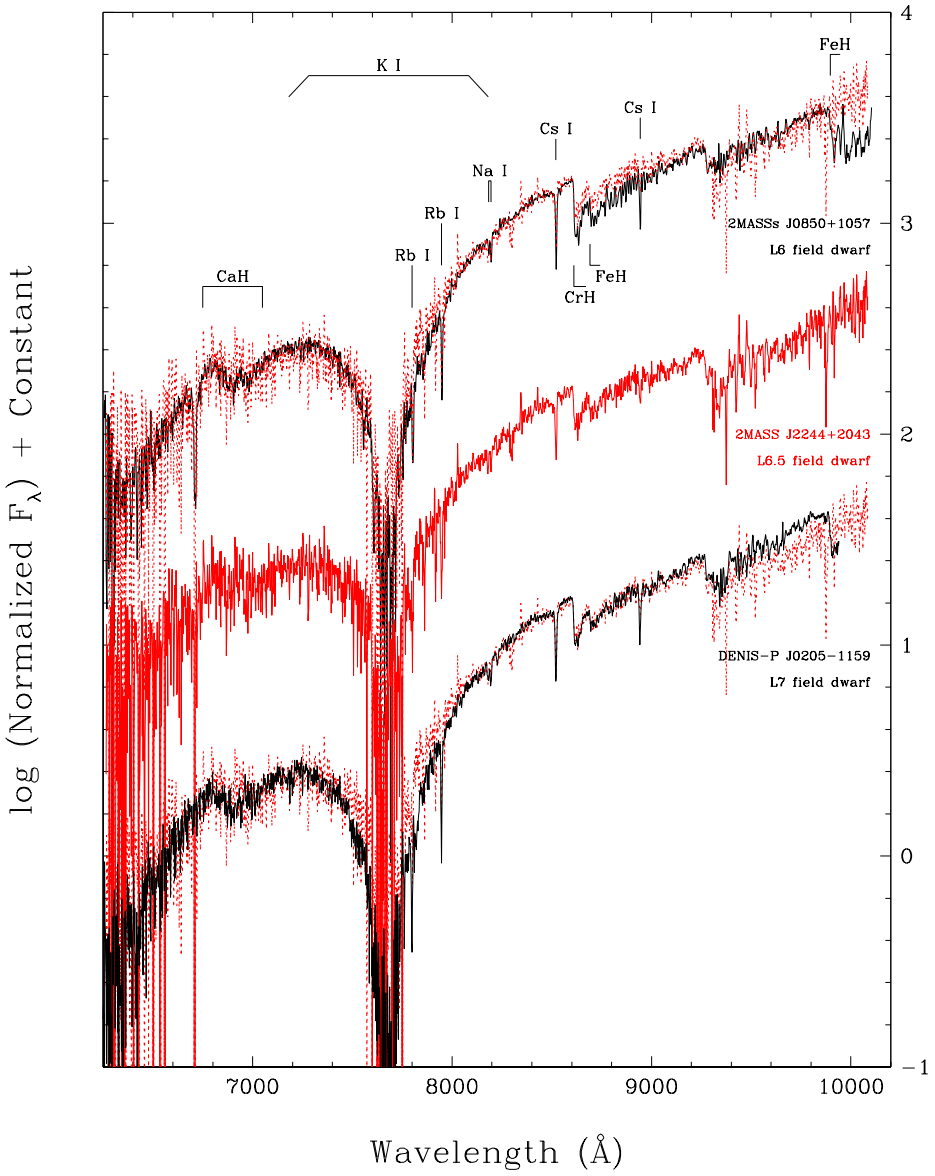

Fig. 13.— 2MASS J2244+2043 (red) compared to the L6 and L7 optical standards (black) 2MASS J0850+1057 and DENIS J0205−1159. Even though the near-infrared spectrum of this object is extremely peculiar with respect to normal late-L dwarfs, the optical spectrum differs only subtly from a normal L6.5 dwarf. In both panels the spectra have been normalized to unity at 8250 Å and a constant offset added to separate the spectra vertically. Flux is plotted in logarithmic units so that features across all wavelengths can be more easily distinguished.

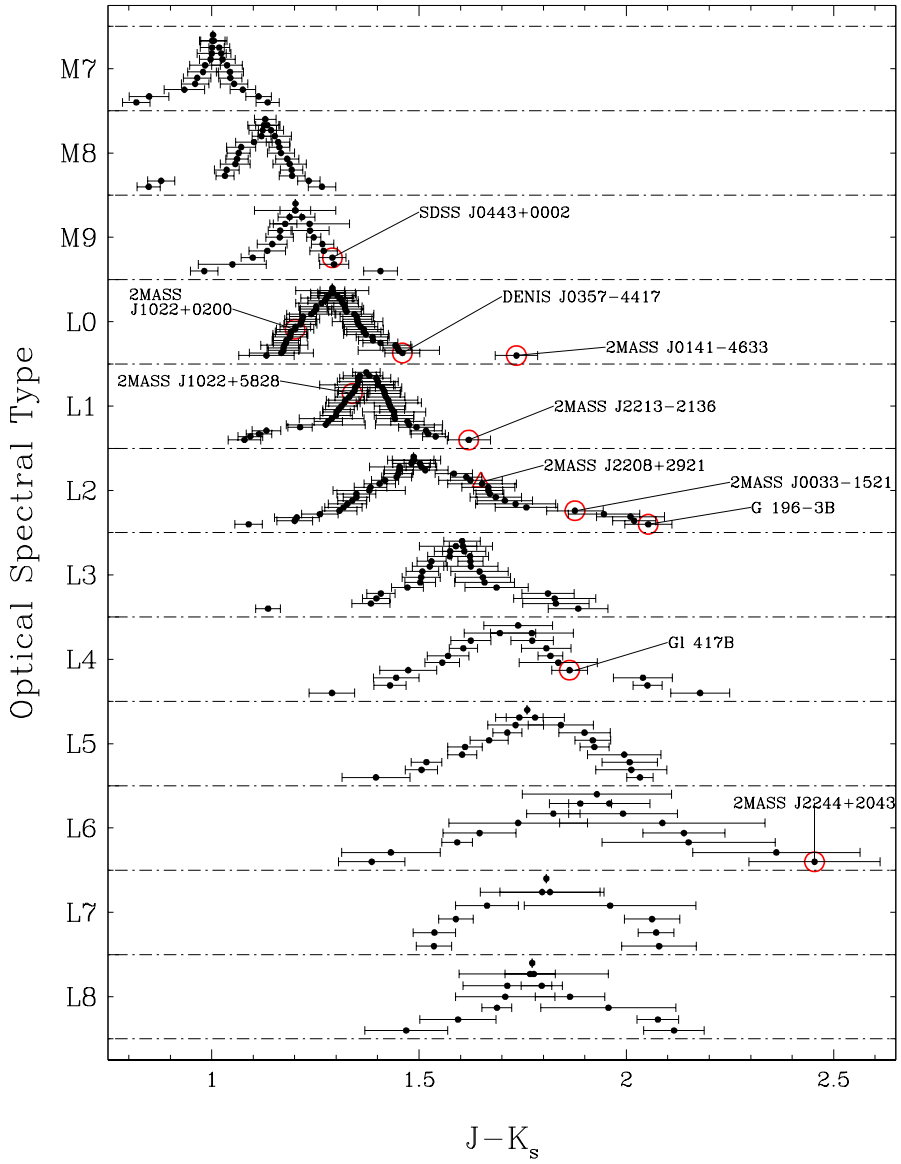

Fig. 14.— J-K$_s$ colors for a collection of M7-L8 dwarfs with optically determined spectral types. Each bin represents a full integral subtype: "M7" includes M7 and M7.5 dwarfs, "M8" includes M8 and M8.5 dwarfs, etc. For each group of objects, the median color in the group is plotted highest in the bin; colors falling farther from the median are plotted progressively farther down the y-axis. Sample selections are described in the text. We use red circles to mark eleven objects we spectroscopically identify as low-gravity. We also mark with a red triangle the color location of a peculiar L dwarf, 2MASS J2208+2921, from Kirkpatrick et al. (2000) that did not meet the selection criteria for the plot.

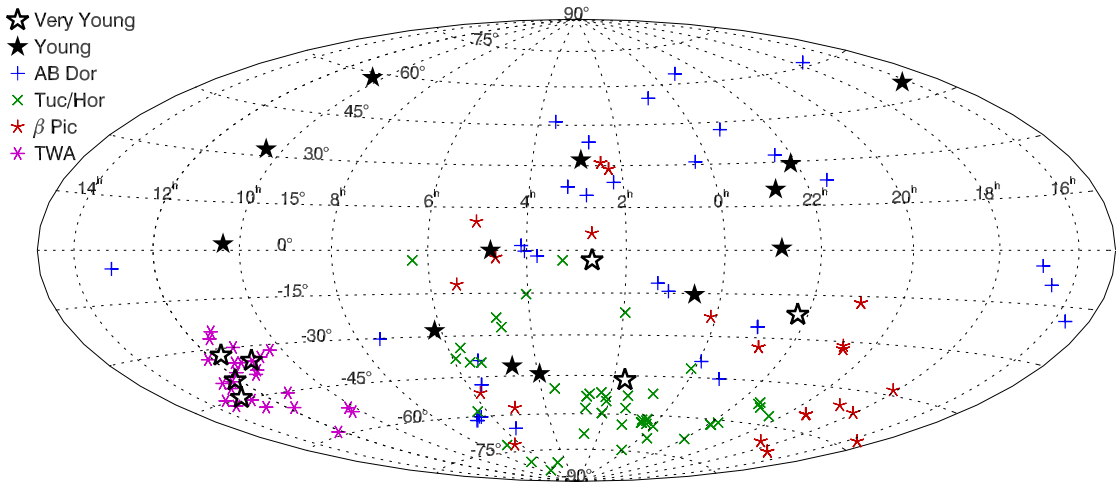

Fig. 15.— Hammer (equal-area) projection of the sky in J2000 equatorial coordinates showing members of the AB Doradus Moving Group (blue plus signs), the Tucana-Horologium Association (green x's), β Pictoris Moving Group (red asterisks), and the TW Hydrae Association (magenta snowflakes) as listed in Zuckerman & Song (2004). Locations of the 20 low-gravity field dwarfs of Table 6 are shown by solid stars for objects with age estimates $\sim$100 Myr and by open stars for objects with age estimates $\sim$10 Myr.

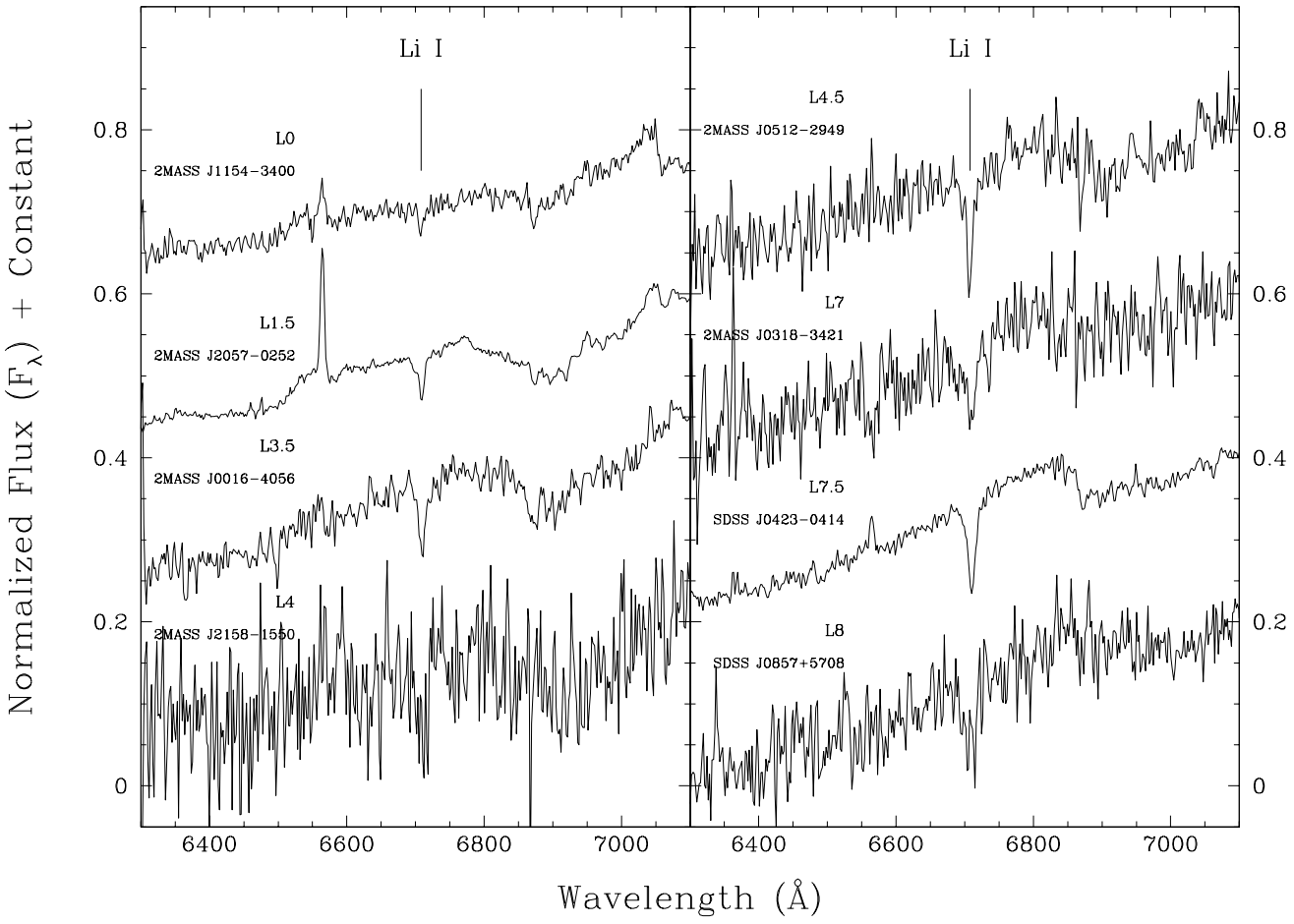

Fig. 16.— Zooms of the Keck/LRIS spectra in the 6300-7100 Å region for those objects from the southern L dwarf sample and literature sample exhibiting Li I absorption.

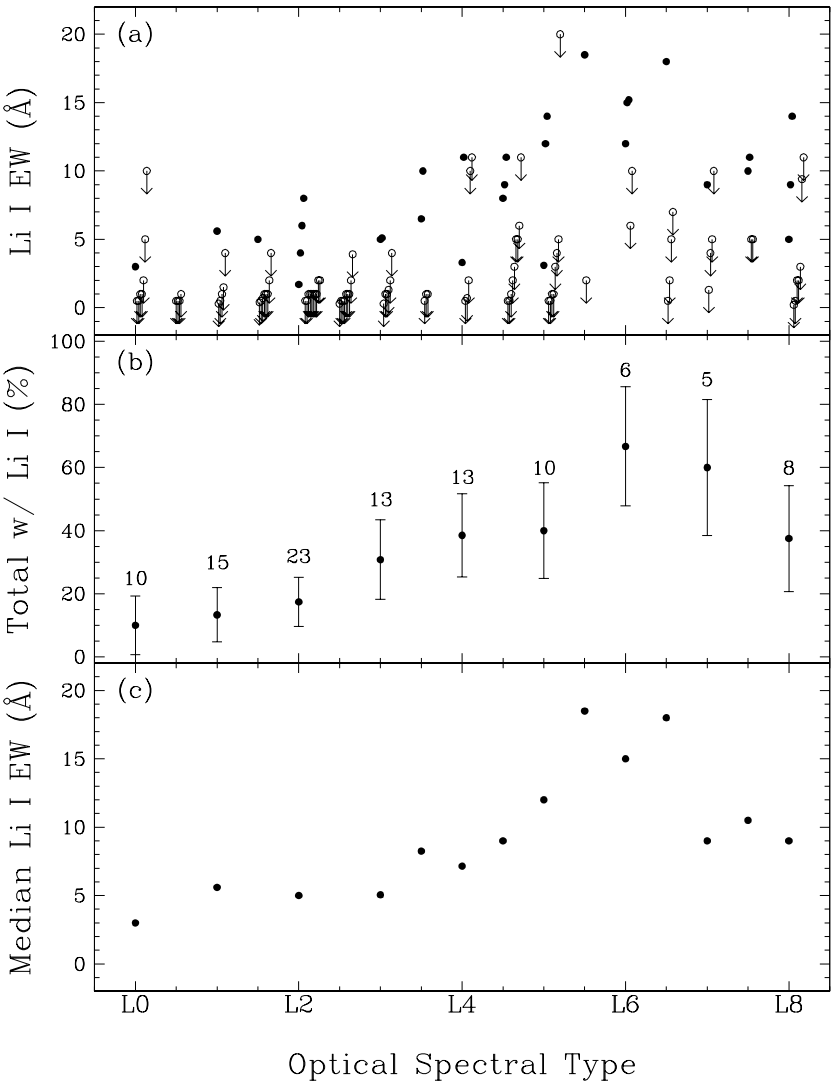

Fig. 17.— An update of Fig. 7 from Kirkpatrick et al. (2000). (a) Li I equivalent widths as a function of spectral subclass for all L dwarfs for which we have ever obtained Keck-LRIS spectra. Solid circles denote objects having a detected Li I absorption line. Open circles with downward arrows denote upper limits to the Li I EW for those objects for which no line was detected. To avoid the overlapping of data caused by the quantization of spectral types, some of the points have been given slight offsets along the x-axis. (b) Percentage of L dwarfs showing Li I absorption as a function of spectral subclass. The only objects used in this computation are those for which a Li I equivalent width of 3 Å or more would be detectable. Points have been binned into integer subtypes in which L0 and L0.5 dwarfs have been combined in the L0 bin, L1 and L1.5 dwarfs have been combined in the L1 bin, etc. The total number of objects in each bin is given above each data point. (c) Median Li strength as a function of spectral class for those objects for which lithium absorption was detected.

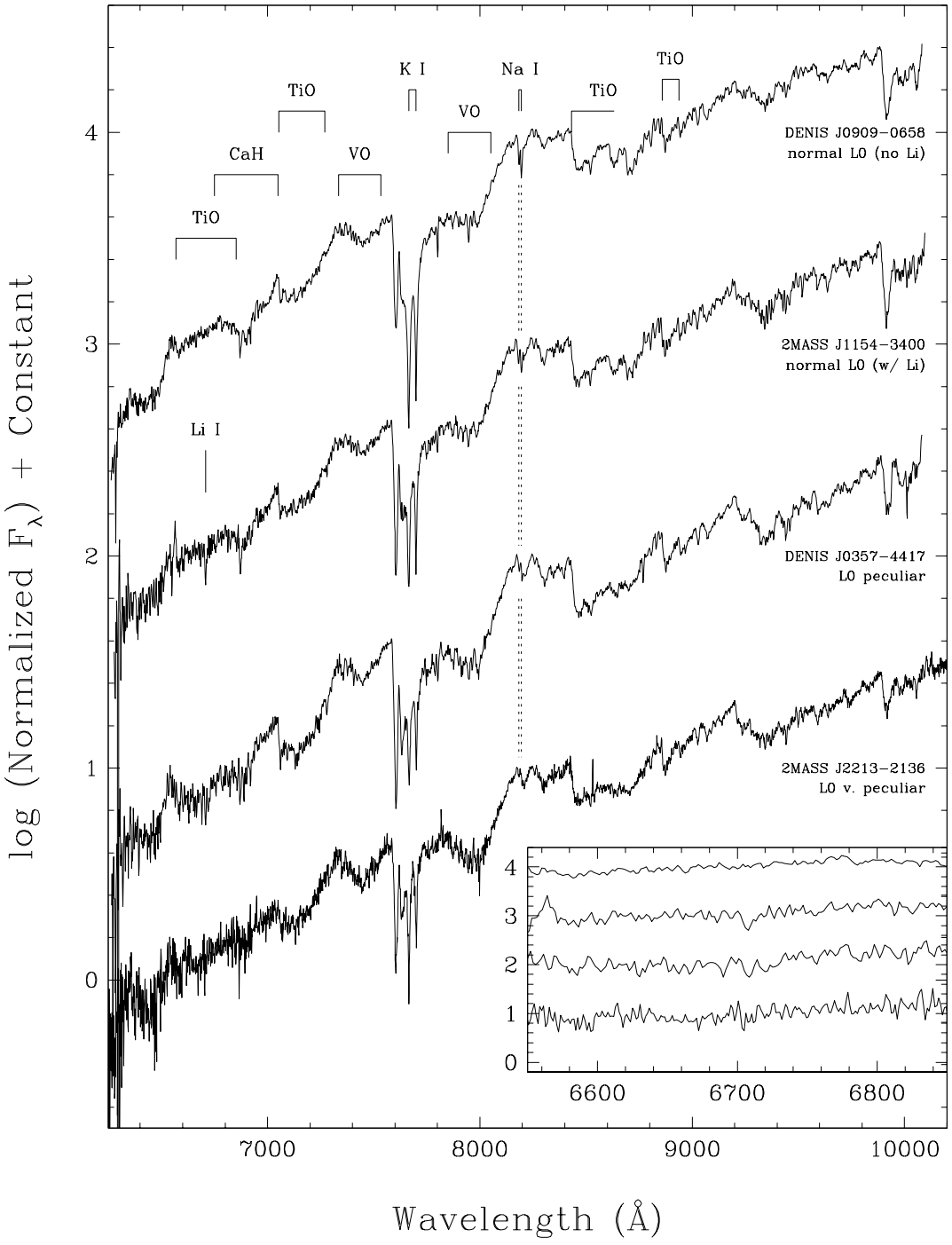

Fig. 18.— Sample spectra of optical L0 dwarfs from each of the four age bins of Table 8. These are displayed on a logarithmic scale, normalized to one at 8250 Å, with integers offsets added in the y-direction to separate spectra vertically. The spectrum with the best signal-to-noise ratio in each bin is shown. The inset shows a zoom-in around the 6708 Å Li I line for each of the four. In the inset, spectra are shown on a linear scale, normalized to one near 6750 Å, and again offset by integers.

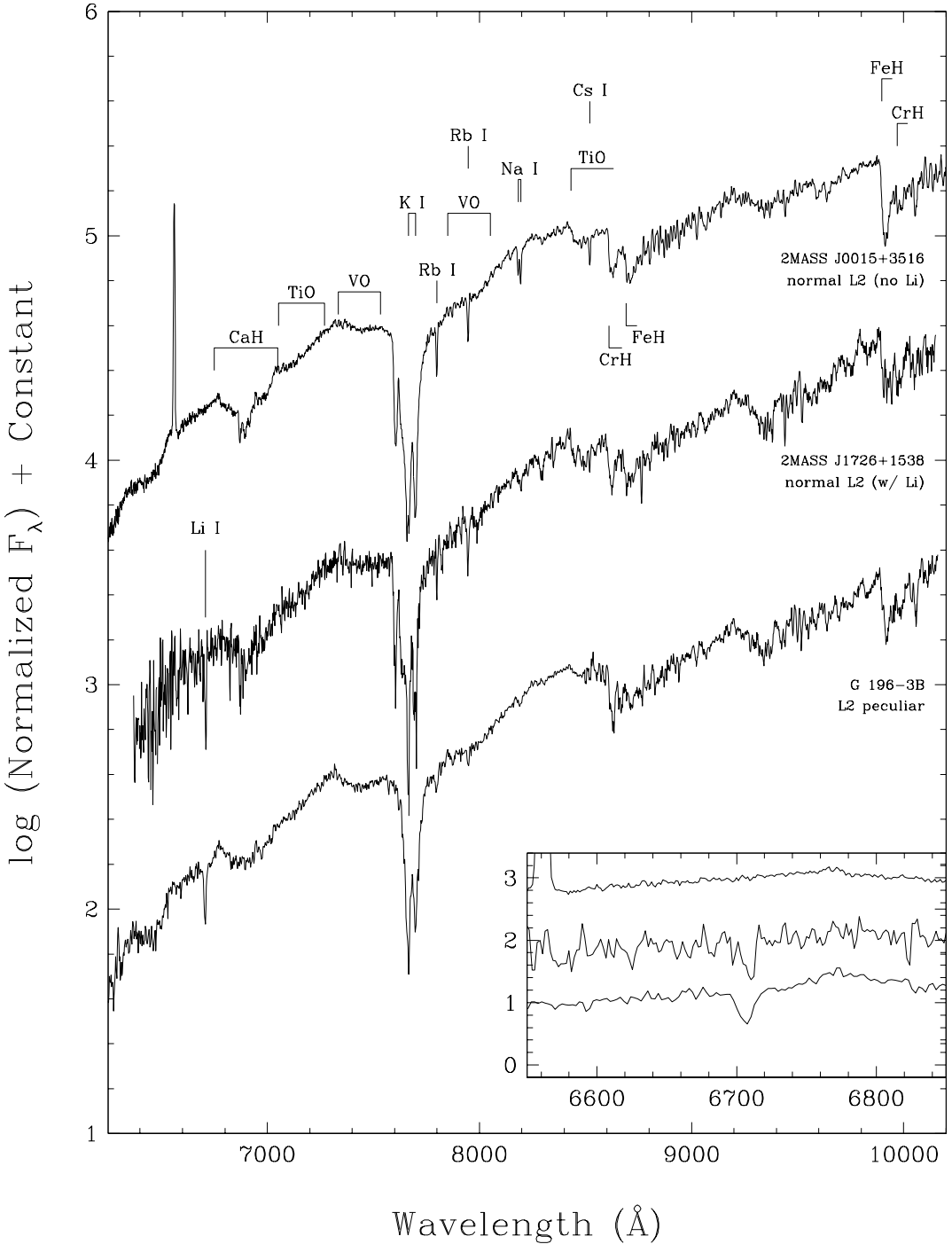

Fig. 19.— Sample spectra of optical L2 dwarfs from each of the three populated age bins of Table 8. The inset shows a zoom-in around the Li I line for each of the three. Normalizations and scalings are the same as in Figure 18.

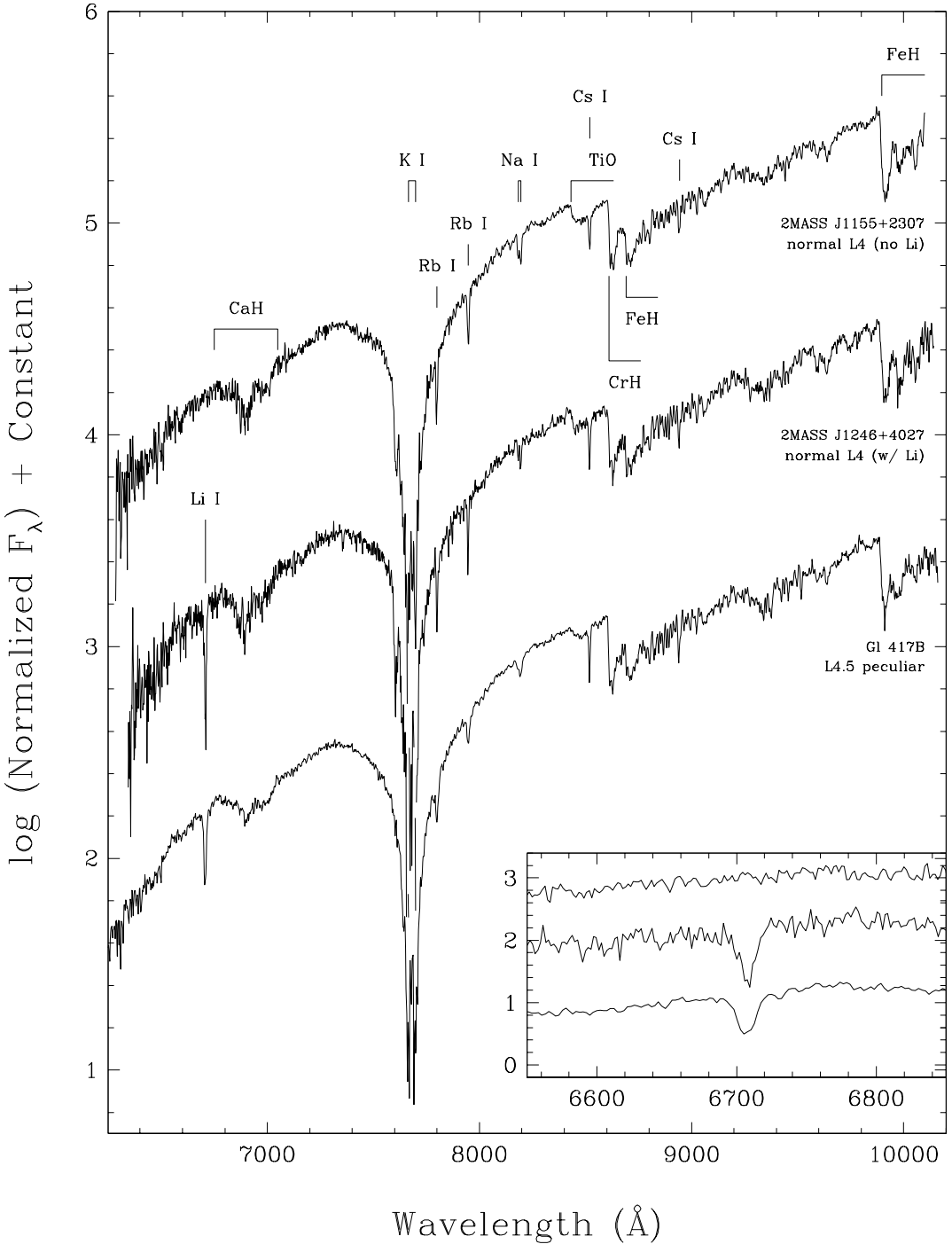

Fig. 20.— Sample spectra of optical L4 dwarfs from each of the three populated age bins of Table 8. The inset shows a zoom-in around the Li I line for each of the three. Normalizations and scalings are the same as in Figure 18.

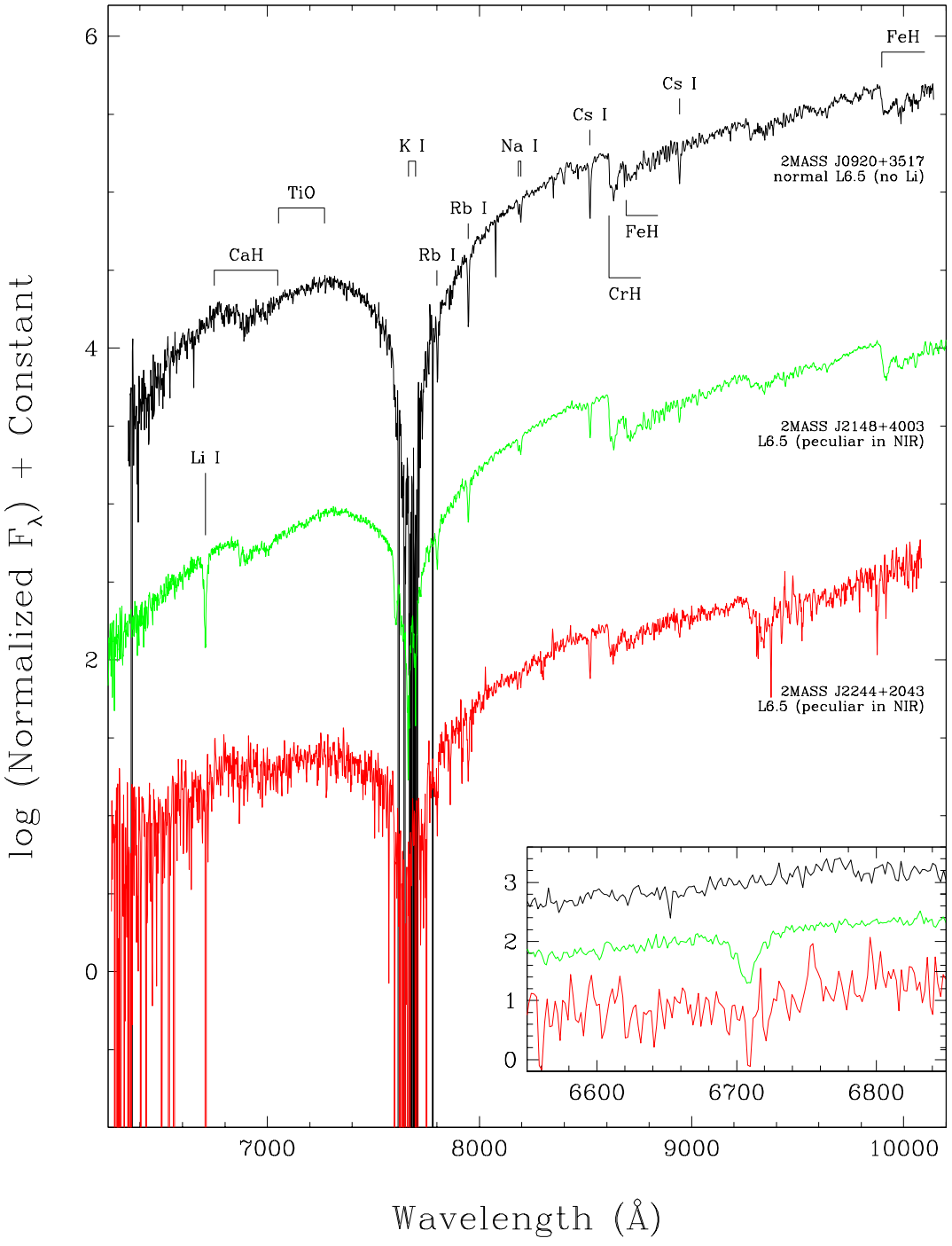

Fig. 21.— Sample spectra of optical L6.5 dwarfs from each of the three populated age bins of Table 8. The inset shows a zoom-in around the Li I line for each of the three. Normalizations and scalings are the same as in Figure 18.

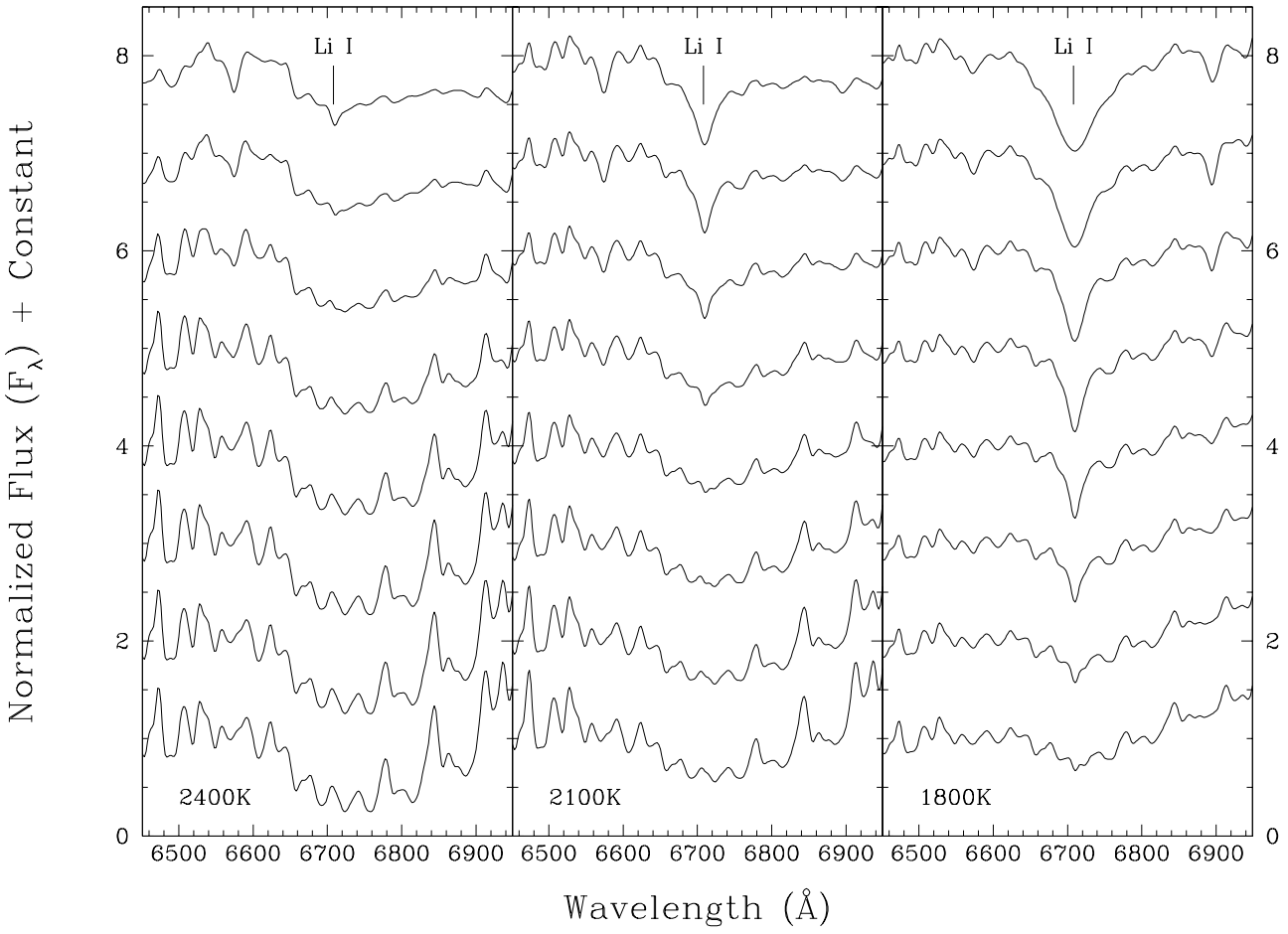

Fig. 22.— Synthetic spectral models at effective temperatures of 2400K (left panel), 2100K (middle panel), and 1800K (right panel) for objects of solar abundance. Each panel illustrates the behavior of the spectra over a range of gravities, decreasing in half-dex increments from log(g)=6.0 at the top of each panel to log(g)=2.5 at the bottom. Note the universal weakening of the Li I line as gravity is lowered. The spectra displayed here have a resolution of 10 Å, identical to that of our empirical spectra.